

MASTER

IS-T-704

REACTIONS OF SIGMA-BONDED ORGANOCHROMIUM(III) COMPLEXES

John Paul Leslie II

Ph. D. Thesis Submitted to Iowa State University

Ames Laboratory, ERDA
Iowa State University
Ames, Iowa 50011

NOTICE

This report was prepared as an account of work sponsored by the United States Government. Neither the United States nor the United States Energy Research and Development Administration, nor any of their employees, nor any of their contractors, subcontractors, or their employees, makes any warranty, express or implied, or assumes any legal liability or responsibility for the accuracy, completeness or usefulness of any information, apparatus, product or process disclosed, or represents that its use would not infringe privately owned rights.

Date Transmitted: December 1975

PREPARED FOR THE U. S. ENERGY RESEARCH AND DEVELOPMENT
ADMINISTRATION UNDER CONTRACT NO. W-7405-eng-82

DISTRIBUTION OF THIS DOCUMENT IS UNLIMITED *LB*

DISCLAIMER

This report was prepared as an account of work sponsored by an agency of the United States Government. Neither the United States Government nor any agency Thereof, nor any of their employees, makes any warranty, express or implied, or assumes any legal liability or responsibility for the accuracy, completeness, or usefulness of any information, apparatus, product, or process disclosed, or represents that its use would not infringe privately owned rights. Reference herein to any specific commercial product, process, or service by trade name, trademark, manufacturer, or otherwise does not necessarily constitute or imply its endorsement, recommendation, or favoring by the United States Government or any agency thereof. The views and opinions of authors expressed herein do not necessarily state or reflect those of the United States Government or any agency thereof.

DISCLAIMER

Portions of this document may be illegible in electronic image products. Images are produced from the best available original document.

NOTICE

This report was prepared as an account of work sponsored by the United States Government. Neither the United States nor the United States Energy Research and Development Administration, nor any of their employees, nor any of their contractors, subcontractors, or their employees, makes any warranty, express or implied, or assumes any legal liability or responsibility for the accuracy, completeness, or usefulness of any information, apparatus, product or process disclosed, or represents that its use would not infringe privately owned rights.

Available from: National Technical Information Service
U. S. Department of Commerce
P.O. Box 1553
Springfield, VA 22161

Price: Microfiche \$2.25

Reactions of sigma-bonded
organochromium(III) complexes

by

John Paul Leslie II

A Dissertation Submitted to the
Graduate Faculty in Partial Fulfillment of
The Requirements for the Degree of
DOCTOR OF PHILOSOPHY

Department: Chemistry
Major: Inorganic Chemistry

Approved:

James Hespenson
In Charge of Major Work

R.E. McCarley
For the Major Department.

OB Konas
For the Graduate College

Iowa State University
Ames, Iowa

1975

TABLE OF CONTENTS

	Page
ABSTRACT	xv
SYMBOLS AND CONVENTIONS	xiii
PART I. THE KINETICS AND MECHANISM OF REACTIONS BETWEEN DICHLOROMETHYLCHROMIUM(III) ION AND CHROMIUM(II) ION	1
INTRODUCTION	2
EXPERIMENTAL	6
Materials	6
CrCHCl_2^{2+}	6
$\text{CrCH}_2\text{Cl}^{2+}$	8
CrCl^{2+}	9
$\text{Cr}(\text{ClO}_4)_3$	10
Cr^{2+}	10
Other materials	12
Methods	12
Analyses	12
Stoichiometry	15
Kinetics	17
Computation of kinetic results	18
Mass spectrum experiments	20
Radiotracer experiments	21
RESULTS AND DISCUSSION	24
Characterization and Stoichiometry of Reaction	24
Kinetics	30
High $[\text{H}^+]$	30

Low $[H^+]$	37
Radiotracer Experiments	46
APPENDIX	53
PART II. KINETICS OF FORMATION OF PENTAAQUO-4-PYRIDINOMETHYLCHROMIUM(III) ION AND ITS EXCHANGE REACTION WITH CHROMIUM(II) ION 58	
INTRODUCTION	59
EXPERIMENTAL	63
Materials	63
$CrCH_2-\text{C}_6\text{H}_4-\text{ONH}^{3+}$	63
$BrCH_2-\text{C}_6\text{H}_4-\text{ONH}^+\text{Br}^-$	63
Cr^{2+} solutions	64
Other materials	64
Methods	65
Analyses	65
Exchange kinetics	67
Chemical kinetics	69
RESULTS AND DISCUSSION	71
Exchange Kinetics	71
Chemical Kinetics	79
APPENDIX	89
PART III. REACTIONS OF SIGMA-BONDED ORGANOCHROMIUM(III) COMPLEXES WITH MERCURY(II) ELECTROPHILES 92	
INTRODUCTION	93
EXPERIMENTAL	100

Materials	100
Aliphatic alkylchromium(III) complexes	100
Haloalkylchromium(III) complexes	103
Aralkylchromium(III) complexes	104
Organic hydroperoxides	106
Mercury compounds	109
Other materials	110
Methods	111
Analyses	111
Spectra	114
Stoichiometry	114
Kinetics	115
RESULTS	119
Characterization	119
Characterization of organochromium(III) complexes	119
Nmr spectra of organomercury(II) products	126
Characterization of reactions	131
Kinetics	134
Preliminary experiments	134
Kinetics of Hg^{2+} reactions	138
Kinetics of CH_3Hg^+ reactions	151
Activation parameters and Hammett correlations	164

DISCUSSION	174
BIBLIOGRAPHY	184
ACKNOWLEDGEMENTS	188

LIST OF FIGURES

	Page
I-1. Electronic spectrum of CrCHCl_2^{2+} and $\text{CrCH}_2\text{Cl}^{2+}$	25
I-2. Elution profile for stoichiometry experiment ST3	28
I-3. Elution profile for stoichiometry experiment ST4	28
I-4. Standard first-order rate plots for Runs 4 and 23	31
I-5. Guggenheim rate plots for Runs 10 and 11	31
I-6. Second-order rate plot for Run 32	36
I-7. Absorbance <u>vs</u> time traces for runs at low $[\text{H}^+]$ showing effect of varying $[\text{H}^+]$	38
I-8. Absorbance <u>vs</u> time traces for runs at low $[\text{H}^+]$ showing effect of varying $[\text{Cr}^{2+}]$	39
II-1. McKay plot for Run E1	73
II-2. McKay plot for Run E2	73
II-3. McKay plot for Run E3	74
II-4. McKay plot for Run E4	74
II-5. Plot of $R_{\text{ex}}/[\text{CrCH}_2\text{C}_5\text{H}_4\text{NH}^{3+}]$ <u>vs</u> $[\text{Cr}^{2+}]$ for exchange kinetic runs	76
II-6. First-order rate plots for the formation of $\text{CrCH}_2\text{C}_5\text{H}_4\text{NH}^{3+}$	80
III-1. Electronic spectrum of CrCH_3^{2+}	122
III-2. Electronic spectrum of $\text{CrCH}_2\text{CH}_3^{2+}$	122
III-3. Electronic spectrum of $\text{CrCH}_2\text{CH}_2\text{CH}_3^{2+}$	123
III-4. Electronic spectrum of $\text{CrCH}(\text{CH}_3)_2^{2+}$	123

III-5.	Electronic spectrum of $\text{CrCH}_2\text{Cl}^{2+}$	124
III-6.	Electronic spectrum of $\text{CrCH}_2\text{Br}^{2+}$	124
III-7.	Electronic spectrum of CrCF_3^{2+}	125
III-8.	Electronic spectrum of $\text{CrCH}_2\text{C}_6\text{H}_5^{2+}$	125
III-9.	Spectrophotometric titration for reaction of $\text{CrCH}_2\text{CH}_2\text{CH}_3^{2+}$ and CH_3Hg^+	132
III-10.	Spectrophotometric titration for the reaction of $\text{CrCH}_2\text{CH}_2\text{CH}_3^{2+}$ and Hg^{2+}	133
III-11.	Swinbourne rate plot for reaction of $\text{CrCH}_2\text{CH}_2\text{CH}_3^{2+}$ and Hg^{2+} , see Table III-4	139
III-12.	Swinbourne rate plot for reaction of $\text{CrCH}_2\text{C}_6\text{H}_5^{2+}$ and Hg^{2+} , see Table III-6	139
III-13.	Standard first-order rate plot for reaction of $\text{CrCH}_2\text{Br}^{2+}$ and Hg^{2+} , see Table III-5	140
III-14.	Plot showing first-order dependence on $[\text{Hg}^{2+}]$ in reaction with $\text{CrCH}_2\text{CH}_2\text{CH}_3^{2+}$	146
III-15.	Plot showing first-order dependence on $[\text{Hg}^{2+}]$ in reaction with $\text{CrCH}_2\text{Cl}^{2+}$	146
III-16.	Plot showing dependence on $[\text{Hg}^{2+}]$ in reaction with $\text{CrCH}(\text{CH}_3)_2^{2+}$, note non-zero intercept	150
III-17.	Swinbourne rate plot for reaction of CrCH_3^{2+} and CH_3Hg^+ , see Table III-8	152
III-18.	Swinbourne rate plot for reaction of $\text{CrCH}_2\text{CH}_2\text{CH}_3^{2+}$ and CH_3Hg^+ , see Table III-8	152
III-19.	Standard first-order rate plot for reaction of $\text{CrCH}_2\text{C}_6\text{H}_5^{2+}$ and CH_3Hg^+ , see Table III-9	153
III-20.	Plot showing first-order dependence on $[\text{CH}_3\text{Hg}^+]$ for reaction with $\text{CrCH}_2\text{CH}_2\text{CH}_3^{2+}$	160

III-21.	Plot showing first-order dependence on $[\text{CH}_3\text{Hg}^+]$ for reaction with $\text{CrCH}_2\text{C}_6\text{H}_5^{2+}$	160
III-22.	Plot showing dependence on $[\text{CH}_3\text{Hg}^+]$ for reaction with $\text{CrCH}_2\text{C}(\text{CH}_3)_3^{2+}$, note non-zero intercept	162
III-23.	Plot of k_{MeHg} vs $[\text{H}^+]^{-1}$ for reaction of CrCH_3^{2+} and CH_3Hg^+	165
III-24.	Eyring plot for reaction $\text{CrCH}_2\text{CH}_2\text{CH}_3^{2+}$ and Hg^{2+}	167
III-25.	Eyring plot for reaction of $\text{CrCH}_2\text{Cl}^{2+}$ and Hg^{2+}	168
III-26.	Eyring plot for reaction of $\text{CrCH}_2\text{CH}_2\text{CH}_3^{2+}$ and CH_3Hg^+	169
III-27.	Hammett plot for reactions of para-substituted benzylchromium(III) ions with Hg^{2+}	172
III-28.	Hammett plot for the reactions of para-substituted benzylchromium(III) ions with CH_3Hg^+	173

LIST OF TABLES

	Page
I-1. Spectral data for CrCHCl_2^{2+} and $\text{CrCH}_2\text{Cl}^{2+}$	24
I-2. Kinetic data for reaction of CrCHCl_2^{2+} and Cr^{2+} . Conditions: $[\text{H}^+] = 1.0 \text{ M}$, $\mu = 2.5 \text{ M}$, temp = 25.1°	32
I-3. Kinetic results of fast and slow steps in the reaction of CrCHCl_2^{2+} and Cr^{2+} at low $[\text{H}^+]$. Conditions: $[\text{CrCHCl}_2^{2+}] = 2 \times 10^{-3} \text{ M}$, $\mu = 2.50 \text{ M}$, $\lambda = 350 \text{ nm}$, $T = 25.1^\circ$	41
I-4. Mass spectral data for the experiments on exchange of protons with CrCHCl_2^{2+}	44
I-5. Expected relative activities of Cr products of the reaction of Cr^{2+} and CrCHCl for Schemes I-III	48
I-6. Specific activity, S, of Cr samples for radiotracer experiments	49
I-7. Observed and calculated specific activities of fractions in radiotracer experiments, S_x refers to the early fractions (CrCl^{2+} and CrBr^{2+}); S_{CrR} refers to middle fractions (CrCHCl_2^{2+} and $\text{CrCH}_2\text{Cl}^{2+}$); and S_y refers to later fractions (Cr^{3+}). Specific activities are given as 10^{-6} S/cmp/M	52
II-1. Specific activity (S) vs time data for exchange kinetic runs. Conditions: $[\text{H}^+] = 1.0 \text{ M}$, $\mu = 1.0 \text{ M}$, $T = 55.0^\circ$	72
II-2. Summary of results for exchange kinetic runs. Conditions: $[\text{H}^+] = 1.0 \text{ M}$, $\mu = 1.0 \text{ M}$, $T = 55.0^\circ$	75
II-3. Kinetic data for the reaction of Cr^{2+} and $\text{BrCH}_2\text{C}_5\text{H}_4\text{NH}^+$. Conditions: $[\text{H}^+] = 1.0 \text{ M}$, $\mu = 1.0 \text{ M}$, $T = 55.0^\circ$, $\lambda = 308 \text{ nm}$	81

III-1. Spectral data for aliphatic and haloaliphatic CrR ²⁺ complexes, λ given in nm, ϵ given in M ⁻¹ cm ⁻¹	120
III-2. Spectral data for aralkylchromium(III) complexes, CrCH ₂ -  -Z ²⁺ ; λ given in nm, ϵ given in M ⁻¹ cm ⁻¹	121
III-3. Nmr data for organomercury products of reactions of CrR ²⁺ with Hg(II); chemical shift (δ) referenced to TMS	127
III-4. Kinetic data for the reactions of Hg ²⁺ with aliphatic CrR ²⁺ complexes. Conditions: [H ⁺] = 0.25 M, μ = 0.50 M, T = 25.0°; runs done by stopped-flow method	141
III-5. Kinetic data for the reactions of Hg ²⁺ with haloalkyl CrR ²⁺ complexes. Conditions: [H ⁺] = 0.25 M, μ = 0.50 M, T = 25.0°; runs done on the Cary 14	143
III-6. Kinetic data for the reactions of Hg ²⁺ with para-substituted benzylchromium(III) ions, CrCH ₂ -  -Z ²⁺ . Conditions: [H ⁺] = 0.25 M, μ = 0.50 M, T = 25.0°; runs done by stopped-flow method	144
III-7. Kinetic data for the reaction of Hg ²⁺ with CrCH(CH ₃) ₂ ²⁺ . Conditions: [H ⁺] = 0.25 M, μ = 0.50 M, λ = 290 nm, T = 25.0°; runs done on Cary 14	149
III-8. Kinetic data for the reactions of CH ₃ Hg ²⁺ and aliphatic CrR ²⁺ complexes. Conditions: [H ⁺] = 0.25 M, μ = 0.50 M, T = 25.0°; runs done by stopped-flow method	154
III-9. Kinetic data for reactions of CH ₃ Hg ⁺ and para-substituted benzylchromium(III) complexes, CrCH ₂ -  -Z. Conditions: [H ⁺] = 0.25 M, μ = 0.50 M, T = 25.0°; runs done on Cary 14 unless otherwise indicated	156

III-10. Kinetic data on reaction of $\text{CrCH}_2\text{C}(\text{CH}_3)_3^{2+}$ and CH_3Hg^+ . Conditions: $[\text{H}^+] = 0.25 \text{ M}$, $\mu = 0.50 \text{ M}$, $T = 25.0^\circ$, $[\text{CrR}^{2+}] = \sim 3 \times 10^{-4} \text{ M}$	161
III-11. Summary of second-order rate constants for reaction of Hg^{2+} and CH_3Hg^+ with para-substituted benzylchromium(III) ions, $\text{CrCH}_2\text{C}_6\text{H}_5\text{-Z}$ and Hammett σ values for the various substituents	170
III-12. Summary of second-order rate constants for the reactions of CrR^{2+} with Hg^{2+} , CH_3Hg^+ , and Br_2 and for reactions of other organometallic complexes with Hg^{2+} ; k 's given in $\text{M}^{-1}\text{s}^{-1}$ at 25°	176
III-13. Rate trends for $\text{S}_{\text{E}}2$ reactions, values of $k_{\text{R}}/k_{\text{CH}_3}$ for aliphatic R groups	179
III-14. Summary of activation parameters for reactions of CrR^{2+} complexes	182

SYMBOLS AND CONVENTIONS

Certain symbols appear throughout this thesis and are defined as follows:

A	Absorbance
<u>M</u>	Molarity or moles/liter
[]	Concentration of species in solution (<u>M</u>)
μ	Ionic strength
ϵ	Extinction coefficient or molar absorptivity ($M^{-1}cm^{-1}$)
b	Pathlength of optical cell or reaction vessel (cm)
T	Temperature
t	Time
s	Second
λ	Wavelength (nm)
nm	Nanometer
cpm	Counts per minute
S	Specific activity (cpm/ <u>M</u>)
-R	Denotes an organic group sigma-bonded through a saturated carbon atom. (Also used to denote the gas constant in the Eyring equation.)
\circ (subscript)	Refers to the value of a measured quantity at $t = 0$; i.e., at the beginning of an experiment
∞ (subscript)	Refers to the value of a measured quantity at $t = \infty$; i.e., at the end of an experiment
t (subscript)	Refers to the value of a measured quantity at a specific time after $t = 0$ in an experiment

Other symbols that are used only a few times are defined as they appear in the text.

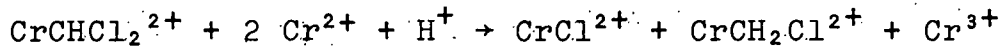
A convention used throughout this work concerns the notation for metal ions in solution. In general, the water molecules in the primary coordination sphere of metal ions are not shown. For example, Cr^{3+} refers to the hexaaquo species, $(\text{H}_2\text{O})_6\text{Cr}^{3+}$, and CrR^{2+} refers to the pentaquo organochromium(III) species, $(\text{H}_2\text{O})_5\text{CrR}^{2+}$.

Reactions of sigma-bonded
organochromium(III) complexes

John Paul Leslie II

Under the supervision of James H. Espenson
From the Department of Chemistry
Iowa State University

Three projects were carried out, each dealing with the kinetics and mechanism of reactions of sigma-bonded organochromium(III) complexes of the form $(H_2O)_5CrR^{2+}$. Part I describes the kinetics of the reaction of dichloromethylchromium(III) ion with chromium(II) ion in aqueous acid according to

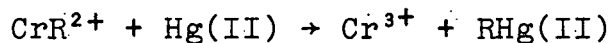


The rate law for this reaction is $-d[CrCHCl_2^{2+}]/dt = k_{Cr}[CrCHCl_2^{2+}][Cr^{2+}]$ ($k_{Cr} \approx 0.014 \text{ M}^{-1}\text{s}^{-1}$ at 25°), and radio-tracer experiments, in which one reactant was tagged with Cr-51, showed that the radioisotope is distributed into all chromium products. These results are consistent with a mechanism in which initial halogen atom abstraction by Cr^{2+} produces $CrCl^{2+}$ and a radical intermediate that reacts further with Cr^{2+} and H^+ via a dinuclear intermediate to form the other products.

USERDA Report IS-T-704. This work was performed under Contract W-7405-end-82 with the Energy Research and Development Administration.

Part II deals with the radio-exchange of 4-pyridinomethyl-chromium(III) ion with Cr^{2+} -51 and the kinetics of formation of the organochromium species at 55° in 1 M H^+ . The radio-exchange occurs with the rate law, $-\frac{d[\text{CrCH}_2\text{C}_5\text{H}_4\text{NH}^{3+}]}{dt} = k_{\text{ex}}[\text{CrCH}_2\text{C}_5\text{H}_4\text{NH}^{3+}][\text{Cr}^{2+}]$ ($k_{\text{ex}} = 0.058 \text{ M}^{-1}\text{s}^{-1}$ at 55°) indicating a bimolecular process. The rate law for the formation of $\text{CrCH}_2\text{C}_5\text{H}_4\text{NH}^{3+}$ from Cr^{2+} and $\text{BrCH}_2\text{C}_5\text{H}_4\text{NH}^+$ is $\frac{d[\text{CrCH}_2\text{C}_5\text{H}_4\text{NH}^{3+}]}{dt} = k_o[\text{Cr}^{2+}][\text{BrCH}_2\text{C}_5\text{H}_4\text{NH}^{3+}]$ ($k_o = 16.9 \text{ M}^{-1}\text{s}^{-1}$ at 55° in 1.0 M H^+). These results are compared to those of other workers on the decomposition of $\text{CrCH}_2\text{C}_5\text{H}_4\text{NH}^{3+}$.

Part III deals with the reactions of Hg^{2+} and CH_3Hg^+ with a series of $(\text{H}_2\text{O})_5\text{CrR}^{2+}$ complexes, in which R is an aliphatic alkyl group, a haloalkyl group, or an aralkyl group

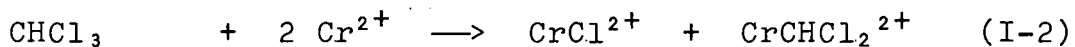
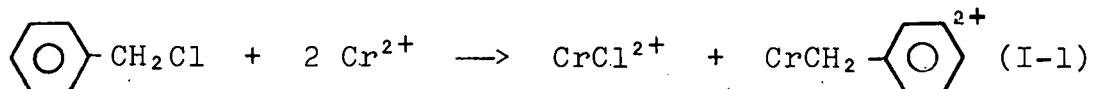


The rate law in all cases is $-\frac{d[\text{CrR}]}{dt} = k_{\text{Hg}}[\text{Hg(II)}][\text{CrR}^{2+}]$. From the trends in the rate constants, including a Hammett correlation for the aralkylchromium(III) reactions, the mechanism was concluded to be an $S_E 2$ (open) type, probably with retention of configuration about the saturated carbon undergoing substitution.

PART I. THE KINETICS AND MECHANISM OF REACTIONS BETWEEN
DICHLOROMETHYLCHROMIUM(III) ION AND CHROMIUM(II)
ION

INTRODUCTION

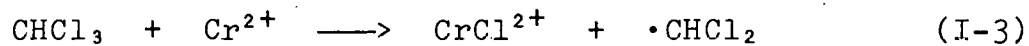
Organochromium(III) complexes of the form $(H_2O)_5CrR^{2+}$, containing metal-carbon sigma bonds, have been known since the late 1950's when Anet and LeBlanc synthesized benzyl-chromium(III) ion (1), $CrCH_2C_6H_5^{2+}$ and dichloromethyl-chromium(III) ion (2), $CrCHCl_2^{2+}$. These complexes were made quite simply according to equations I-1 and I-2 by mixing aqueous Cr^{2+} solutions with the halides, $C_6H_5CH_2Cl$ or $CHCl_3$, under heterogeneous conditions. No solid salts of these



species could be isolated, but they were shown to be quite stable in water and pure solutions could be obtained by ion exchange chromatography.

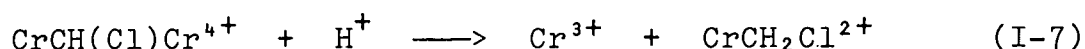
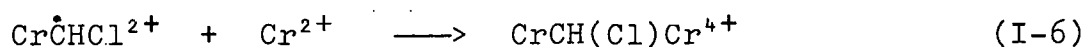
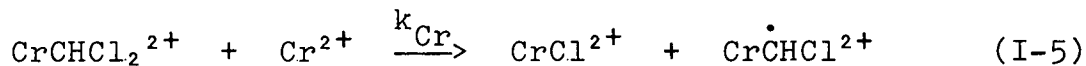
Dodd and Johnson (3) later studied further the reactions of Cr^{2+} and haloforms, CHX_3 , ($X = Cl, Br, I$) under homogeneous conditions in acetone:water solvent. They found that two different organochromium products can be made from Cr^{2+} and CHX_3 , depending on the relative amounts of the two reagents. When CHX_3 is in large excess, $CrCHX_2^{2+}$ is produced as found by Anet for $X=Cl$, but when Cr^{2+} is in large excess, monohalo-methylchromium(III) ion, $CrCH_2X^{2+}$ is the major product.

The authors proposed a mechanism for the formation of CrCHCl_2^{2+} in which initial halogen abstraction by Cr^{2+} gives CrCl^{2+} and an organic free radical which then rapidly reacts with a second Cr^{2+} to give CrCHCl_2^{2+} as shown by the following equations:



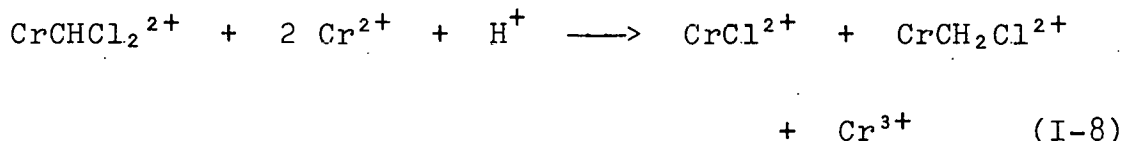
No kinetic evidence was given for this mechanism, but it is consistent with work on other reactions of Cr^{2+} with organic halides, namely the formation of benzylchromium(III) ion (1,4) and pyridinomethylchromium(III) ions (5). It is also consistent with the work of Castro and Kray (6) on the stepwise reduction of haloforms and methylene halides by Cr^{2+} in aqueous DMF solvent under conditions where no organochromium species were observed.

The formation of $\text{CrCH}_2\text{Cl}^{2+}$ was rationalized by a further reaction of CrCHCl_2^{2+} with excess Cr^{2+} according to



Again, no kinetic evidence was offered for this mechanism and no precedent for such a reaction was known at that time. The formation of the dinuclear intermediate, $\text{CrCH}(\text{Cl})\text{Cr}^{4+}$, was purely speculative. An interesting feature of this mechanism is the homolytic transfer of a sigma-bonded carbon from one chromium to another.

It seemed advisable to test this mechanism (equations I-5 - I-7) by studying directly the reaction of CrCHCl_2^{2+} with Cr^{2+} . Experiments could be done to confirm the expected stoichiometry shown by the following:

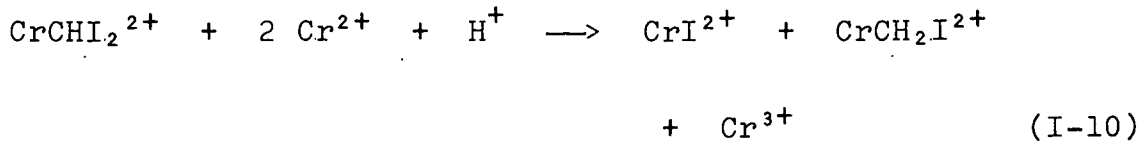


Kinetic studies might confirm the expected rate law,

$$-\frac{d[\text{CrCHCl}_2^{2+}]}{dt} = k_{\text{Cr}}[\text{CrCHCl}_2^{2+}][\text{Cr}^{2+}] \quad (\text{I-9})$$

which is consistent with equation I-5 in the mechanism being rate-determining. Such experiments, however, would not indicate anything about subsequent steps in the mechanisms, in particular the fate of the radical intermediate, CrCHCl^{2+} . It was hoped that radiotracer experiments, with one of the reactants labeled with chromium-51, might be used to determine the origin of chromium in each of the products.

In the course of this work, Nohr and Spreer (7) reported a similar study on the reaction of CrCHI_2^{2+} and Cr^{2+} shown below:



The results were the same as those expected in our study, and supported the mechanism of Dodd and Johnson (3). The stoichiometry was shown to be that of equation I-10 although in excess Cr^{2+} , the product $\text{CrCH}_2\text{I}^{2+}$ reacts further to produce Cr^{3+} and CH_4 . The rate law was found to be analogous to equation I-9. Radiotracer experiments done by Nohr and Spreer showed that radiotagged Cr-51 appeared in all chromium products, and the authors claimed that the result supported the mechanism in equations I-5 - I-7, assuming that equation I-6 is reversible.

In this project experiments as outlined above were done on the reaction of CrCHCl_2^{2+} and Cr^{2+} in order to understand the mechanism. The work reported here is somewhat redundant of that of Nohr and Spreer on a similar reaction, but this study was begun long before the other work was published.

EXPERIMENTAL

Materials

CrCHCl₂²⁺

Dichloromethylchromium(III) cation was prepared according to equation I-2 by two procedures, a variation on the method of Dodd and Johnson (3) wherein Cr²⁺ and CHCl₃ reacted under homogeneous conditions, and the method of Anet (2) in which the same reactants were stirred vigorously under heterogeneous conditions.

In the first method, a flask containing 200 ml of acetone and 10 ml of CHCl₃ was purged with nitrogen for 20 minutes, and 25 ml of 0.5 M Cr²⁺ (0.5 M in HClO₄) was added. The vessel was capped and left to react for approximately 2 hours, in which time the solution turned from light blue to a dirty brown. The acetone and excess CHCl₃ were removed by aspiration and the crude aqueous product solution was stored at -10°.

In the second procedure, CHCl₃ (10 ml) was added to 20 ml of solution that was 0.1 M in Cr²⁺ and 0.1 M in HClO₄. This mixture was allowed to react for approximately 30 minutes at room temperature with vigorous stirring under nitrogen. The unreacted CHCl₃ was removed by separatory funnel and by aspiration of the aqueous phase. The crude solution was stored at -10° until used.

The purification of CrCHCl_2^{2+} was accomplished in two ways, a simple ion exchange procedure and a more involved method in which Hg^{2+} was used to convert contaminants (CrCl^{2+} and $\text{CrCH}_2\text{Cl}^{2+}$) in the CrCHCl_2^{2+} solution to Cr^{3+} which is more easily removed by ion exchange.

In the simple ion exchange procedure, enough solution to contain 1-2 mmoles of CrCHCl_2^{2+} was placed on a column of Dowex 50W-X8 (30 x 1 cm; 50-100 mesh) cation exchange resin in the hydrogen form. The green CrCl^{2+} present in the crude solutions was eluted with 0.5 M HClO_4 , and the orange CrCHCl_2^{2+} was eluted and collected with 1.0 M HClO_4 or LiClO_4 . Some Cr^{3+} and $(\text{CrOH})_2^{4+}$ species present in the solutions remained on the column and were not collected. Since a quantitative separation of CrCHCl_2^{2+} from CrCl^{2+} or from Cr^{3+} could not be achieved by this method, only the middle cut of the CrCHCl_2^{2+} band was collected.

The second purification procedure was devised to eliminate small amounts of $\text{CrCH}_2\text{Cl}^{2+}$ that was thought to be a contaminant in the CrCHCl_2^{2+} solutions. An aliquot of the crude product solution containing 1-2 mmole of CrCHCl_2^{2+} was treated with a small excess of Hg^{2+} solution¹ and allowed to react for 10-15 minutes. A two-fold excess of HCl was then

¹Mercuric ion is known to react rapidly with CrCl^{2+} (8) and $\text{CrCH}_2\text{Cl}^{2+}$ (3) to form Cr^{3+} , but reacts only slowly with CrCHCl_2^{2+} .

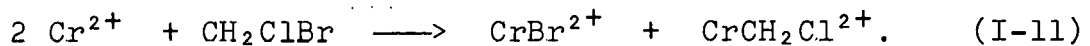
added, to complex or precipitate Hg(II) species, and the white precipitate thus produced was filtered through fine filter paper onto a column of Dowex 50W-X8 cation exchange resin (30 x 1 cm, 50-100 mesh) in the hydrogen form. The chloromercury(II) species remaining in solution were eluted with 0.1 M HCl until the eluate showed no Hg(II) test with Na₂S. The column was then washed with water until the eluate was free of Cl⁻ by testing with Ag⁺. The product was eluted with 1.0 M HClO₄ or LiClO₄.

Using either of these procedures, it was possible to obtain solutions of CrCHCl₂²⁺ that were 0.5 - 2.0 x 10⁻² M in 1.0 M H⁺ or Li⁺. These solutions could be stored for weeks if kept at -10°.

For some experiments CrCHCl₂²⁺ was concentrated by lyophilization. This was done only on low [H⁺] solutions (Li⁺ was used to elute the ion exchange columns). The CrCHCl₂²⁺ solutions were frozen in Dry Ice-acetone bath and evacuated to approximately 10⁻⁵ torr for 8-12 hours. The concentrated solutions were filtered to remove precipitated LiClO₄.

CrCH₂Cl²⁺

Monochloromethylchromium(III) cation was made by the heterogeneous reaction of Cr²⁺ with CH₂ClBr according to the equation,



An acidic solution of Cr^{2+} (50 ml, 0.1 M) and 10 ml of CH_2ClBr were mixed under nitrogen and stirred vigorously at room temperature for about 1 hour. The excess CH_2ClBr was removed by separatory funnel and by aspiration of the aqueous phase. The crude, dirty-brown solution of $\text{CrCH}_2\text{Cl}^{2+}$ could be stored at -10° for months.

The purification of $\text{CrCH}_2\text{Cl}^{2+}$ was accomplished in much the same way as for CrCHCl_2^{2+} . An aliquot of crude solution containing 1-2 mmoles of $\text{CrCH}_2\text{Cl}^{2+}$ was placed on a column of Dowex 50W-X8 cation exchange resin (30 x 1 cm, 50-100 mesh). The green CrBr^{2+} was eluted with 0.5 M HClO_4 and discarded, and the orange $\text{CrCH}_2\text{Cl}^{2+}$ was eluted and collected with 1.0 M HClO_4 . This procedure typically yielded 100 ml of $0.5 - 1.0 \times 10^{-2} \text{ M}$ $\text{CrCH}_2\text{Cl}^{2+}$ which could be stored for months at -10° .

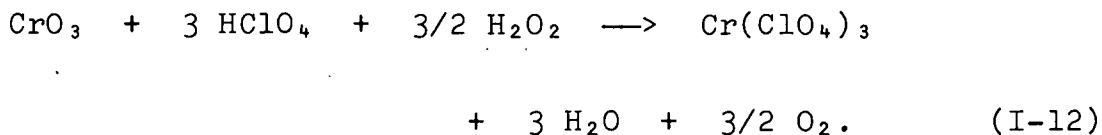
CrCl^{2+}

Monochlorochromium(III) cation was produced in solution by dissolving reagent-grade CrCl_3 in dilute acid with a catalytic amount of Cr^{2+} under air-free conditions.¹ After about 30 minutes this solution was placed on a column of Dowex 50W-X8 cation exchange resin (50-100 mesh) and eluted with 0.5 M HClO_4 to collect a pure solution of CrCl^{2+} .

¹The commercial product is actually $[\text{Cr}(\text{H}_2\text{O})_4\text{Cl}_2]\text{Cl} \cdot 2\text{H}_2\text{O}$ giving CrCl_2^+ on dissolution in H_2O . This species is catalytically aquated to CrCl^{2+} by Cr^{2+} .

Cr(ClO₄)₃

Pure chromium(III) perchlorate was prepared by reduction of CrO₃ with H₂O₂ in HClO₄ solution, according to the equation,



The trioxide (130 g, 1.3 moles) was dissolved in 70 ml of H₂O and added to 400 ml of concentrated HClO₄ (4.6 moles). This mixture was cooled to 0° and an excess of 30% H₂O₂ added slowly with constant stirring. The solution was then concentrated by evaporation, and the solid Cr(ClO₄)₃ slowly crystallized from the supersaturated solution. The product was recrystallized twice before use.

Cr²⁺

Solutions of chromium(II) ion were prepared from Cr(ClO₄)₃ by two methods, one in which Cr³⁺ is reduced by amalgamated zinc and a second one in which Cr³⁺ is electrolytically reduced at 9 volts at a mercury cathode.

The zinc reduction was carried out by simply placing an air-free acidic solution of Cr(ClO₄)₃ over freshly-prepared zinc amalgam (made by adding a solution of HgCl₂ in 2 M HCl to a few grams of reagent-grade zinc granules that had been cleaned with 2 M HCl and washed with water). The mixture was allowed to react for several hours under nitrogen. After

reduction, the solution was transferred to a rubber-capped bottle containing no zinc amalgam.

The electrolytic reduction was carried out in a three-necked round-bottom flask containing 10-20 ml of pure mercury metal (cathode). Into one neck of the flask was inserted a thin glass tube with a piece of platinum foil sealed at the end and containing a few ml of Hg; this tube served as the contact from the power supply to the mercury-pool cathode. Into the second neck of the flask was inserted a 1 cm diameter glass tube with a glass frit sealed at the end and containing about 5 ml of 4 M HClO₄. A platinum foil lead, similar to that described for the cathode, with a 1 cm² surface area was inserted into this HClO₄ solution, and served as the anode where H₂O was oxidized. The third neck of the flask was used to purge the system with nitrogen and to transfer solution in and out of the flask. An acidic solution of Cr³⁺ was placed in the electrolysis flask, and a voltage of 9 volts applied by means of a 12 volt DC power supply. After complete reduction (6-12 hours), the Cr²⁺ solution was transferred to an air-free rubber-capped bottle.

Radiotagged Cr²⁺ solutions were made using chromium-51 obtained from New England Nuclear Corporation in the form of ⁵¹CrCl₃ dissolved in HCl. A stock solution of Cr²⁺-51 was prepared by adding a small amount of this material to a serum-capped volumetric flask containing untagged Cr²⁺ over

amalgamated zinc. This solution was allowed to equilibrate for at least 24 hours.

Other materials

LiClO_4 and $\text{Ba}(\text{ClO}_4)_2$ were obtained as technical grade chemicals or made by neutralization of the carbonates with HClO_4 . Both were recrystallized twice before use.

Solid $[\text{Co}(\text{NH}_3)_5\text{Br}]\text{Br}_2$ was made earlier by standard literature preparation¹ (9).

All other materials used in Part I were reagent grade and were used without further purification.

Methods

Analyses

Concentrations of the organochromium(III) ions, CrCHCl_2^{2+} and $\text{CrCH}_2\text{Cl}^{2+}$, were determined by their visible absorption spectra. All spectral measurements were carried out on a Cary 12 or Cary 14 spectrophotometer. The extinction coefficients of the spectral peaks were determined by first measuring the spectra of freshly-prepared and purified solutions and then determining total chromium.

Total chromium was determined according to the method of Haupt (10) by oxidizing all chromium species to chromate with

¹The compound was prepared in 1969 by Diana Brooks from the procedure in reference 9.

H_2O_2 in base, boiling the solutions for 20-30 minutes to decompose excess H_2O_2 , diluting to the mark in a volumetric flask, and measuring the absorbance at λ 372 nm, $\epsilon = 4830$. When cobalt was present, a small amount of NaSCN was added to complex the cobalt and thus prevent the precipitation of cobalt(II) oxide.

Chromium(II) solutions were analyzed by the following procedure. An aliquot of Cr^{2+} solution was syringed into a volumetric flask containing 15-30% excess solution of $\text{Co}(\text{NH}_3)_5\text{Br}^{2+}$ ion that was well purged with nitrogen. The Co^{2+} released was determined spectrophotometrically as $\text{Co}(\text{NCS})_4^{2-}$ ion by adding a large excess of solid NH_4SCN and diluting to the mark with 1:1 acetone-water solution (11). From the absorbance at λ 623 nm (ϵ 1842) and the dilution factor, the concentration of Cr^{2+} was computed.

The concentrations of Li^+ and Ba^{2+} in stock solutions were determined by passing aliquots of the solutions through a column of Dowex 50W-X8 cation exchange resin in the hydrogen ion form and titrating the H^+ liberated with standard NaOH solution to the bromthymol blue end-point.

Hydrogen ion concentration in stock solutions of CrCHCl_2^{2+} and $\text{CrCH}_2\text{Cl}^{2+}$ were determined by passing through a column of Dowex 50W-X8 cation exchange resin in the H^+ form and titrating the H^+ liberated as in the Li^+ and Ba^{2+} analyses.

In some experiments at low $[H^+]$ (0.03-0.1 \underline{M}) a Beckman pH meter equipped with a combination glass vs Ag-AgCl electrode was used to determine $[H^+]$. In these measurements, the pH meter was calibrated with standard $HClO_4$ solutions that were the same ionic strength as the test solutions.

The count rate for chromium samples was measured on a wall-type NaI gamma ray scintillation counter with a 400 channel analyzer. A styrofoam block with a cylindrical hole the same size as the counting vials was mounted on the NaI crystal to ensure uniform counting geometry. Only those channels representing the energies around the peak in the Cr-51 gamma ray spectrum were tallied. Each sample was counted long enough to get at least 10^4 total counts. The background count rate was determined by counting the empty well overnight and dividing by the total time.

The activity of chromium was determined after converting to chromate with H_2O_2 and base as in the total chromium analysis. The solution was poured into a 20 ml polyethylene counting vial and counted. The chromate concentration was then determined spectrally at λ 372 nm. From the count rate and concentration the quantity, counts-per-minute/concentration, cpm/\underline{M} , was computed; this quantity is proportional to the specific activity (cpm/mole) and was used in all comparisons.

Stoichiometry

Four experiments were carried out to prove the stoichiometry of the reaction of Cr^{2+} and CrCHCl_2^{2+} , equation I-8. In two of these experiments (ST1 and ST2), the purpose was to show that two moles of Cr^{2+} were consumed per mole of CrCHCl_2^{2+} . A third experiment (ST3) was done to show that the products of the reaction consisted of two moles of dication (CrCl^{2+} and $\text{CrCH}_2\text{Cl}^{2+}$) per mole of trication (Cr^{3+}). The fourth experiment (ST4) was done to show that CrCl^{2+} and $\text{CrCH}_2\text{Cl}^{2+}$ are produced in equal amounts. The procedures of these four experiments are outlined below, and the results and implications will be discussed in a later section.

ST1 A solution $3.1 \times 10^{-2} \text{ M}$ in Cr^{2+} and $6.9 \times 10^{-3} \text{ M}$ in CrCHCl_2^{2+} ($[\text{H}^+] = 1.0 \text{ M}$) was allowed to react for 7 hours in a volumetric flask with continuous nitrogen bubbling. The $[\text{Cr}^{2+}]$ was determined at the end of the reaction to determine how much Cr^{2+} had been consumed. A blank solution containing $3.1 \times 10^{-2} \text{ M}$ Cr^{2+} in 1.0 M H^+ but no CrCHCl_2^{2+} was maintained in parallel with the test solution, and $[\text{Cr}^{2+}]$ was determined at the beginning and the end of the reaction to determine how much air-oxidation of Cr^{2+} had occurred. The final $[\text{Cr}^{2+}]$ in the test solution was corrected for air-oxidation by adding to it the difference in initial and final $[\text{Cr}^{2+}]$ from the blank.

ST2 A solution 2.6×10^{-2} M in Cr^{2+} and 0.49×10^{-2} M in CrCHCl_2^{2+} ($[\text{H}^+] = 0.03$ M, $\text{Li}^+ = 1.0$ M) was allowed to react for 9 hours in a round bottom flask with a long thin neck¹ with continuous nitrogen bubbling. The $[\text{Cr}^{2+}]$ was determined at the end of the reaction. As in ST1, a blank solution containing the same amount of Cr^{2+} but no CrCHCl_2^{2+} was maintained in parallel with the test solution, and the $[\text{Cr}^{2+}]$ was determined at the beginning and end of the reaction. The consumption of Cr^{2+} was computed in the same way as in ST1.

ST3 A 5.5 ml solution 3.8×10^{-2} M in Cr^{2+} and 1.8×10^{-2} M in CrCHCl_2^{2+} ($[\text{H}^+] = 1.0$ M) was allowed to react for two half-lives (2 hours) in a volumetric flask with continuous nitrogen bubbling. A 1.0 ml aliquot of this solution was withdrawn and syringed into a solution containing excess $\text{Co}(\text{NH}_3)_5\text{Br}^{2+}$ to oxidize unreacted Cr^{2+} to CrBr^{2+} . This solution was then placed on a column of Dowex 50W-X8 cation exchange resin (30 x 1 cm, 50-100 mesh) and eluted with 0.5 M, 1.0 M, and 2.0 M HClO_4 in 8 ml fractions to collect all chromium species. Each fraction was then converted to CrO_4^{2-} with H_2O_2 and NaOH and diluted to 25.0 ml. The absorbance of CrO_4^{2-} was measured at $\lambda 372$ nm ($\epsilon = 4830 \text{ M}^{-1}\text{cm}^{-1}$) and the mmoles of chromium computed. An elution profile (plot of

¹This vessel was designed to minimize air-oxidation of Cr^{2+} from diffusion of air to the reaction solution.

mmoles of Cr vs fraction number) was then constructed to get a qualitative idea of the distribution of di- and tripositive products.

ST4 A 10.0 ml solution 0.10 M in Cr^{2+} and 5.0×10^{-3} M in CrCHCl_2^{2+} ($[\text{H}^+] = 1.0$ M) was allowed to react to completion (one hour under these conditions). The excess Cr^{2+} was oxidized with air and the solution was placed on a column of Dowex 50W-X8 cation exchange resin (30 x 1 cm, 50-100 mesh). The column was eluted with 0.47 M NaSCN.¹ The uni- and di-positive species were collected and analyzed for total chromium as in the previous experiment. An elution profile (plot of mmoles of Cr vs fraction number) was then constructed to indicate the relative amounts of $\text{CrCH}_2\text{Cl}^{2+}$ (eluted as $\text{Cr}(\text{CH}_2\text{Cl})\text{NCS}^+$) and CrCl^{2+} produced in the reaction.

Kinetics

Most kinetic runs were monitored spectrophotometrically at wavelengths between 300 and 400 nm and were done under pseudo-first-order conditions with Cr^{2+} in excess. The reaction vessel was a quartz test tube (pathlength 2.3 cm) with a one-hole rubber stopper through which a nitrogen bubbling tube was inserted to keep the reaction solution air-free. This test tube was immersed in thermostatted water

¹The SCN⁻ ion complexes with $\text{CrCH}_2\text{Cl}^{2+}$ to form $\text{Cr}(\text{CH}_2\text{Cl})\text{NCS}^+$ but does not complex with CrCl^{2+} (12).

in the cell compartment of the spectrophotometer. The procedure was as follows: appropriate amounts of CrCHCl_2^{2+} , Li^+ , Ba^{2+} , and H^+ were placed in the test tube (solution volume 15-20 ml) and purged with nitrogen while in the cell compartment. An aliquot of Cr^{2+} stock solution was then added and the reaction solution agitated by nitrogen bubbling for a few seconds. At the end of each run, the $[\text{Cr}^{2+}]$ was determined. In all runs the ionic strength was maintained at 2.5 M, (1.0 M in monocation and 0.5 M in dication) using Li^+ and Ba^{2+} . The temperature was maintained at 25.1°.

A few runs were done under second-order conditions with $[\text{Cr}^{2+}]$ in only 50% stoichiometric excess over $[\text{CrCHCl}_2^{2+}]$. These runs were monitored spectrophotometrically or by withdrawing aliquots of the reaction solution at various times and analyzing for $[\text{Cr}^{2+}]$. The ionic strength in these reactions was higher than the pseudo-first-order runs because of the necessity to concentrate the CrCHCl_2^{2+} stock solutions. The temperature was maintained at 25.1° as before.

Computation of kinetic results

The pseudo-first-order rate constants, k_{obs} , for runs at high $[\text{Cr}^{2+}]$ were initially determined either by standard $\ln |A_t - A_\infty|$ vs time plots according to the equation,

$$\ln |A_t - A_\infty| = \ln |A_0 - A_\infty| - k_{\text{obs}} t \quad (\text{I-13})$$

where the k_{obs} = -slope, or by the Guggenheim method with plots of $\ln |A_t - A_{t+\tau}|$ vs time according to the equation,

$$\ln |A_t - A_{t+\tau}| = \ln \{|A_0 - A_\infty|(1 - \exp(-kt))\} - k_{obs}t \quad (I-14)$$

where τ is a time interval corresponding to about two or three half-lives and k_{obs} = - slope. The second-order rate constants, k_{Cr} , were then computed as $k_{obs}/[Cr^{2+}]_{av}$.¹ Later, the k_{Cr} values for all runs were recalculated using a non-linear least-squares computer program, NEW-I,² which fit values of A_0 , A_∞ , and k_{Cr} from the absorbance-time data for each run.

For the runs done under second-order conditions, k_{Cr} values were calculated from the slope of a plot of $\ln [CrCHCl_2^{2+}]/[Cr^{2+}]$ vs time, according to the equation,

$$\ln \left\{ \frac{[CrCHCl_2^{2+}]_t}{[Cr^{2+}]_t} \right\} = \ln \left\{ \frac{[CrCHCl_2^{2+}]_0}{[Cr^{2+}]_0} \right\} - \{ [Cr^{2+}]_0 - 2[CrCHCl_2^{2+}]_0 \} k_{Cr} t \quad (I-15)$$

¹This is the average concentration in the run, for this reaction $[Cr^{2+}]_{av} = [Cr^{2+}]_\infty + [CrCHCl_2^{2+}]_0$.

²The computer program was a revision of one supplied by Drs. T. Newton and R. Moore based on a report from Los Alamos Scientific Laboratory: LA2367 plus addenda.

For spectrophotometric runs, $[Cr^{2+}]_t$ and $[CrCHCl_2^{2+}]_t$ were determined from the absorbance values at various times from equations I-16 and I-17. For runs where $[Cr^{2+}]$ was monitored,

$$[CrCHCl_2^{2+}]_t = [CrCHCl_2^{2+}]_0 \times \frac{A_t - A_\infty}{A_0 - A_\infty} \quad (I-16)$$

$$[Cr^{2+}]_t = [Cr^{2+}]_0 - 2 [CrCHCl_2^{2+}]_0 + 2 [CrCHCl_2^{2+}]_t \quad (I-17)$$

$[CrCHCl_2^{2+}]$ values were determined from the directly-read values of $[Cr^{2+}]$ and equation I-17.

Mass spectrum experiments

Two experiments were done to determine if $CrCHCl_2^{2+}$ or any intermediate in its reaction with Cr^{2+} exchanges protons with the solvent. The basic idea was to make $CrCDCl_2^{2+}$, carry out a reaction with excess Cr^{2+} in H_2O to completion, treat the product $CrCHDCl^{2+}$ (or $CrCH_2Cl^{2+}$) with Br_2 to form $CHDClBr$ (or CH_2ClBr), and measure the mass spectrum of the organic product to see if deuterium was retained. The mass spectrum of $CHDClBr$ can be easily distinguished from the fully-protonated compound.

Deuterated dichloromethylchromium(III) ion was made in exactly the same way as the protonated species except that $CDCl_3$ was used instead of $CHCl_3$; the Hg^{2+} treatment was used to ensure that no $CrCHDCl^{2+}$ would be present in the $CrCDCl_2^{2+}$ solution. A sample of $CrCDCl_2^{2+}$ (10 ml of $4.5 \times 10^{-3} \text{ M}$) was treated with 1.5 ml of 0.9 M Cr^{2+} in a glass test tube with a

sidearm compartment and a vacuum stopcock assembly. After about one hour (complete reaction) the stopcock assembly was attached to a mass spectrometer and the sidearm compartment charged with about 3 ml of 1.8×10^{-2} M Br₂ solution. Both reaction and bromine solutions were frozen with liquid nitrogen and evacuated. The solutions were then thawed, the bromine added to the reaction solution, and the reaction allowed to proceed for about 10 minutes. The mass spectrum of the volatile organic products was then determined.¹

Radiotracer experiments

In order to determine the origin of chromium in each of the product species in the reaction of Cr²⁺ and CrCHCl₂²⁺ three radiotracer experiments were done in which one of the reactants was tagged with chromium-51. The basic idea behind these experiments was to carry out a reaction under approximately stoichiometric conditions to one or two half-lives, oxidize any excess Cr²⁺ to CrBr²⁺, and separate the reaction mixture by ion exchange. Fractions were collected from the column and the specific activity of each fraction measured and compared to the activity of the tagged reagent. The radiotracer experiments are designated RT1-3, and each is described below.

¹The mass spectrum experiments were carried out with the help of Jerry Flesch of Dr. Svec's group.

RT1 A solution 1.7×10^{-2} M in CrCHCl_2^{2+} and 3.8×10^{-2} M in tagged Cr^{2+} -51 was allowed to react for two half-lives (2 hours), and the remaining Cr^{2+} -51 was oxidized with excess $\text{Co}(\text{NH}_3)_5\text{Br}^{2+}$ to form CrBr^{2+} . The solution was placed on a column of Dowex 50W-X2 cation exchange resin and eluted with 0.5, 1.0, and 2.0 M HClO_4 solutions to collect all chromium species in 8 ml fractions. The activity of each fraction was determined as described above. The activity of the tagged Cr^{2+} stock solution was determined also for comparison.

RT2 The conditions of RT1 were duplicated except that the reaction proceeded for only one half-life (1 hour) and only the dipositive species were eluted from the column with 0.5 and 1.0 M HClO_4 .

RT3 This experiment was carried out just as in RT1 except that CrCHCl_2^{2+} was the tagged reagent. A solution 0.029 M in tagged CrCHCl_2^{2+} and 0.061 M in untagged Cr^{2+} was allowed to react for two half-lives (2 hours). Again in this experiment only the dipositive chromium species were collected and analyzed.

In addition to the above ratiotracer experiments, two experiments were done to show that Cr^{2+} -51 does not exchange with $\text{CrCH}_2\text{Cl}^{2+}$ or CrCHCl_2^{2+} under the same conditions.

RT4 A solution 2.4×10^{-3} M in $\text{CrCH}_2\text{Cl}^{2+}$ and 2.4×10^{-2} M in Cr^{2+} -51 was allowed to react for 1.5 hours and the excess Cr^{2+} -51 oxidized with air. No chemical

reaction occurs between these two species. The solution was placed on a column of Dowex 50W-X8 cation exchange resin and eluted with 0.5 M NaSCN. Only the $\text{Cr}(\text{CH}_2\text{Cl})\text{NCS}^+$ was collected and analyzed for activity.

RT5 In this experiment the possibility of exchange between Cr^{2+} -51 and CrCHCl_2^{2+} was investigated. To take account of the chemical reaction between these reagents, the $\text{CrCH}_2\text{Cl}^{2+}$ and CrCl^{2+} produced were converted to Cr^{3+} with Hg^{2+} as in the purification of CrCHCl_2^{2+} . A 21 ml solution 5×10^{-3} M in CrCHCl_2^{2+} and 1.3×10^{-2} M in Cr^{2+} -51 was allowed to react for one half-life (1.5 hours), and the unreacted Cr^{2+} -51 oxidized with air. Excess Hg^{2+} (2 mmoles) was then added, followed by 8 mmoles of HCl. The pure unreacted CrCHCl_2^{2+} was then retrieved by the ion exchange procedure described for the synthesis, and its activity measured in the usual way.

RESULTS AND DISCUSSION

Characterization and Stoichiometry of Reaction

The electronic spectra of CrCHCl_2^{2+} and $\text{CrCH}_2\text{Cl}^{2+}$ are shown in Figure I-1. The spectrum of CrCHCl_2^{2+} was determined using a sample purified by the mercury treatment to ensure that no $\text{CrCH}_2\text{Cl}^{2+}$ was present. A summary of the wavelength maxima and extinction coefficients is shown in Table I-1 along with the corresponding values measured by Dodd and Johnson (3). The discrepancies in ϵ values are most likely due to the presence of chromium-containing impurities, such as Cr^{3+} and CrCl^{2+} which absorb less than the organo-chromium(III) species. The total chromium analyses for samples with such impurities would lead to low ϵ values. The

Table I-1. Spectral data for CrCHCl_2^{2+} and $\text{CrCH}_2\text{Cl}^{2+}$

CrR^{2+}	λ_1 (ϵ)	λ_2 (ϵ)	λ_3 (ϵ)	Reference
CrCHCl_2^{2+}	515 (38)	397 (156)	265 (4000)	- ^a
	514 (23)	396 (115)	265 (2460)	(3)
$\text{CrCH}_2\text{Cl}^{2+}$	517 (23)	391 (225)	256 (3620)	- ^a
	517 (20)	391 (204)	262 (3630)	(3)

^aThis work.

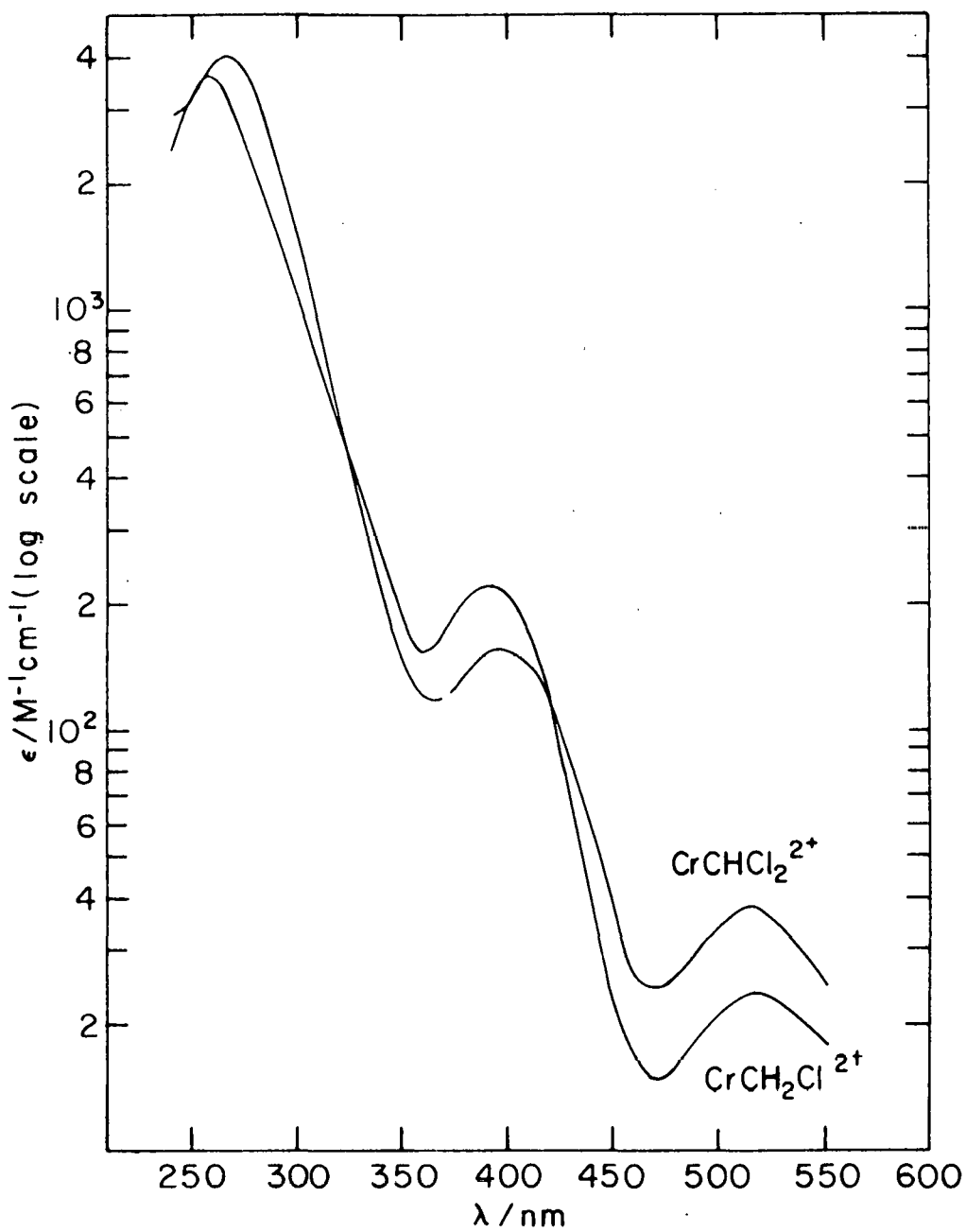


Figure I-1. Electronic spectrum of CrCHCl_2^{2+} and $\text{CrCH}_2\text{Cl}^{2+}$

ϵ values measured in this work are consistently higher than those of Dodd and Johnson and are undoubtedly closer to the actual values. For CrCHCl_2^{2+} this claim is supported by the fact that consecutive fractions in the ion exchange purification gave the same values of ϵ .¹

When an air-free solution of CrCHCl_2^{2+} was mixed with excess Cr^{2+} , the visible spectrum of the solution changed over a period of about one hour with the absorbance in the λ 510-520 nm region decreasing and that in the λ 390-400 nm region increasing. Cation exchange chromatography of this solution, after air-oxidation of excess Cr^{2+} , separated three bands on the ion exchange column: first a green band, eluted with 0.5 M HClO_4 and identified as CrCl^{2+} by its visible absorption spectrum (λ 609 and λ 428 nm), then an orange band, eluted with 1.0 M HClO_4 likewise identified as $\text{CrCH}_2\text{Cl}^{2+}$, and finally a blue band, partially eluted with 2.0 M HClO_4 shown to be Cr^{3+} by its visible spectrum (λ 575 and λ 408 nm). A green species, undoubtedly the tetrapositive chromium(III) dimer, Cr_2O^{4+} , resulting from air-oxidation of Cr^{2+} , remained on the column. These results show that the expected reaction between CrCHCl_2^{2+} and Cr^{2+} (equation I-8) does occur.

¹If chromium-containing impurities were present, the relative amounts would vary from one fraction to another and the observed ϵ values would therefore vary.

Four experiments were done to show that the stoichiometry of the reaction is as shown in equation I-8. The detailed procedure of the experiments, denoted ST1-ST4, are described in the Experimental section, and the results of the individual experiments are detailed below.

ST1 The initial and final $[Cr^{2+}]$ in the blank solution of the experiment were $3.1 \times 10^{-2} \text{ M}$ and $2.7 \times 10^{-2} \text{ M}$, respectively, indicating that $0.4 \times 10^{-2} \text{ M}$ of Cr^{2+} was lost to air oxidation. The final $[Cr^{2+}]$ for the test solution was $1.3 \times 10^{-2} \text{ M}$ and the corrected value was then $1.7 \times 10^{-2} \text{ M}$. The theoretical $[Cr^{2+}]$ at complete reaction based on $[CrCHCl_2^{2+}]$ of $6.9 \times 10^{-3} \text{ M}$ and a 2:1 stoichiometry is $1.7 \times 10^{-2} \text{ M}$, which agrees with the observed $[Cr^{2+}]_\infty$ at complete reaction.

ST2 In this experiment the initial and final values of $[Cr^{2+}]$ in the test solution were $2.6 \times 10^{-3} \text{ M}$ and $1.7 \times 10^{-3} \text{ M}$, respectively. The $[Cr^{2+}]$ in the blank solution remained at $2.6 \times 10^{-2} \text{ M}$ so no correction was needed for air oxidation. The theoretical $[Cr^{2+}]$ at complete reaction based on a $[CrCHCl_2^{2+}]$ of $0.49 \times 10^{-3} \text{ M}$ and a 2:1 stoichiometry is $1.6 \times 10^{-3} \text{ M}$, in good agreement with the $[Cr^{2+}]_\infty$ observed.

ST3 The elution profile for this experiment is shown in Figure I-2 where the amount of chromium in each fraction is plotted against fraction number. The total amount of chromium represented in the large peak in Figure I-2 (early

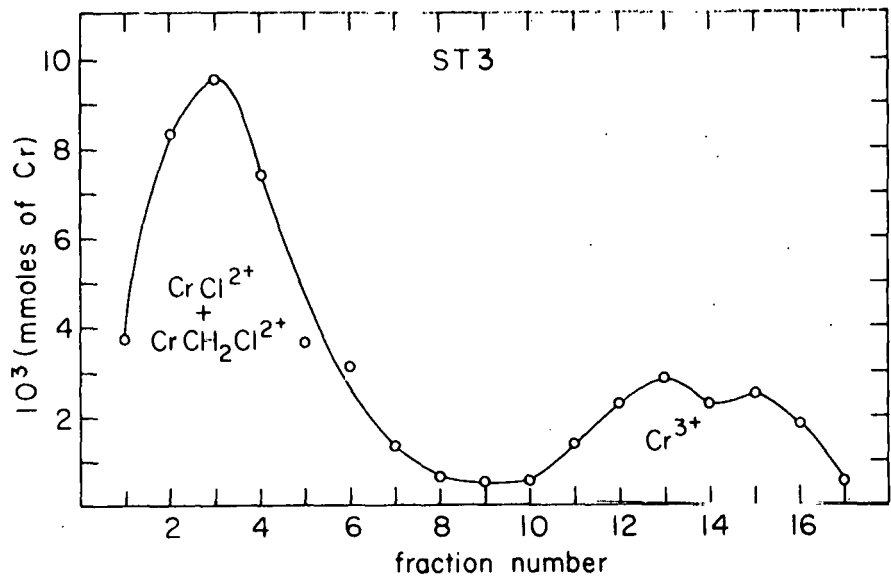


Figure I-2. Elution profile for stoichiometry experiment ST3

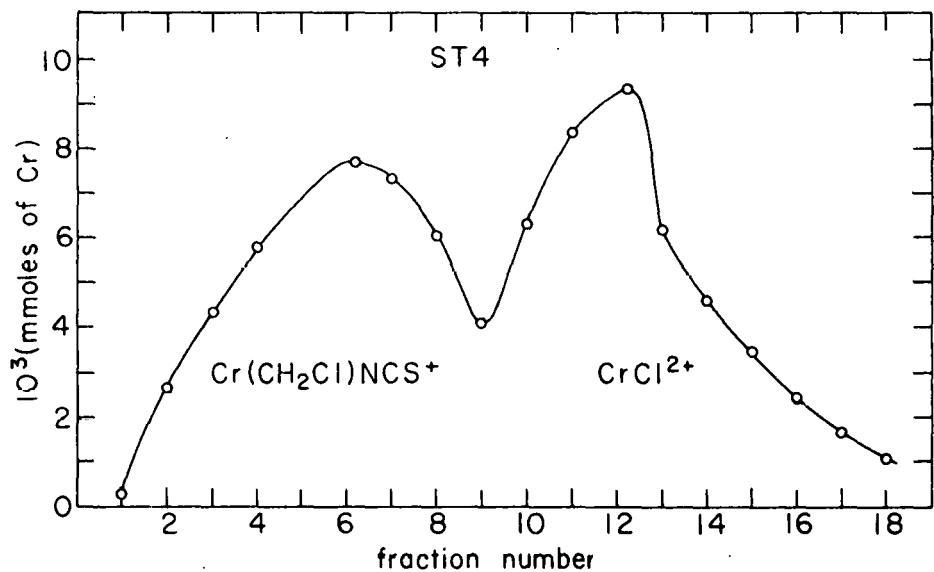


Figure I-3. Elution profile for stoichiometry experiment ST4

fractions, CrCl^{2+} and $\text{CrCH}_2\text{Cl}^{2+}$) is 3.9×10^{-2} mmoles, and that represented by the smaller peak (later fractions, Cr^{3+}) is 1.4×10^{-2} mmoles, giving a ratio of dipositive to tri-positive cations of 2.8:1. This is higher than the expected ratio of 2.0:1 based on the stoichiometry of equation I-8. This high value is consistent, however, with the fact that the reactions were allowed to proceed for only 80% completion and that the unreacted Cr^{2+} was oxidized to the dication, CrBr^{2+} .

ST4 The elution profile for this experiment is shown in Figure I-3. A quantitative separation of $\text{CrCH}_2\text{Cl}^{2+}$ (actually $\text{Cr}(\text{CH}_2\text{Cl})\text{NCS}^+$) and CrCl^{2+} was not achieved, but the areas under the two peaks in the elution profile are about equal indicating that these two products are produced in equal amounts. The total amount of chromium represented in Figure I-3 is 9.1×10^{-2} mmoles compared to 10.0×10^{-2} mmoles expected for 5.0×10^{-2} mmoles of CrCHCl_2^{2+} used in the experiment based on the stoichiometry of equation I-8.

These four experiments clearly show that the stoichiometry of the reaction between CrCHCl_2^{2+} and Cr^{2+} is as shown in equation I-8. From experiments ST1 and ST2 two moles of Cr^{2+} are consumed per mole of CrCHCl_2^{2+} as expected in both high $[\text{H}^+]$ (1.0 M) and low $[\text{H}^+]$ (0.03 M). The results of experiment ST3 show that 2 moles of dipositive cation and 1 mole of tri-positive cation are produced per mole of CrCHCl_2^{2+} . Experiment ST4 shows that one mole each of $\text{CrCH}_2\text{Cl}^{2+}$ and CrCl^{2+} are produced from one mole of CrCHCl_2^{2+} .

Kinetics

High $[H^+]$

A large number of kinetic runs was carried out on the reaction of $CrCHCl_2^{2+}$ and Cr^{2+} at $[H^+] = 1.0 \text{ M}$ with $[Cr^{2+}] \geq 10 [CrCHCl_2^{2+}]$. Pseudo-first-order plots for these runs were nicely linear indicating a first-order dependence on $[CrCHCl_2^{2+}]$. Some typical pseudo-first-order rate plots are shown in Figures I-4 and I-5. A first-order dependence on $[Cr^{2+}]$ was demonstrated by the approximate constancy of the second-order rate constant, k_{Cr} , obtained by dividing the pseudo-first-order rate constant by $[Cr^{2+}]_{av}$. The rate law for the reaction is therefore that expected (equation I-9).

The values of k_{Cr} obtained from hand plots were not accurately reproducible, varying between 1.0 and $2.0 \times 10^{-2} \text{ M}^{-1}\text{s}^{-1}$, and the absorbance values at the end of the runs, A_∞ , were not constant. A nonlinear least-squares computer program was therefore used to fit values of k_{Cr} , A_∞ , and A_0 to the absorbance-time data for each run. The computer fit k_{Cr} 's are shown in Table I-2. The precision of the computer fit data is markedly improved from that obtained by hand plots, but there is still more scatter than expected, considering that $[Cr^{2+}]$ was accurately determined for each run and that the absorbance changes were quite large (0.5 to 1.5 absorbance units).

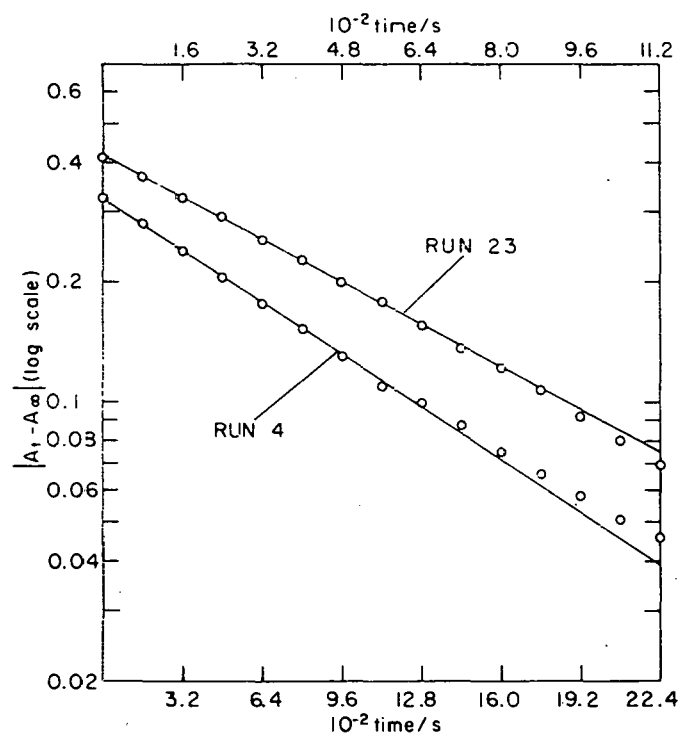


Figure I-4. Standard first-order rate plots for Runs 4 and 23

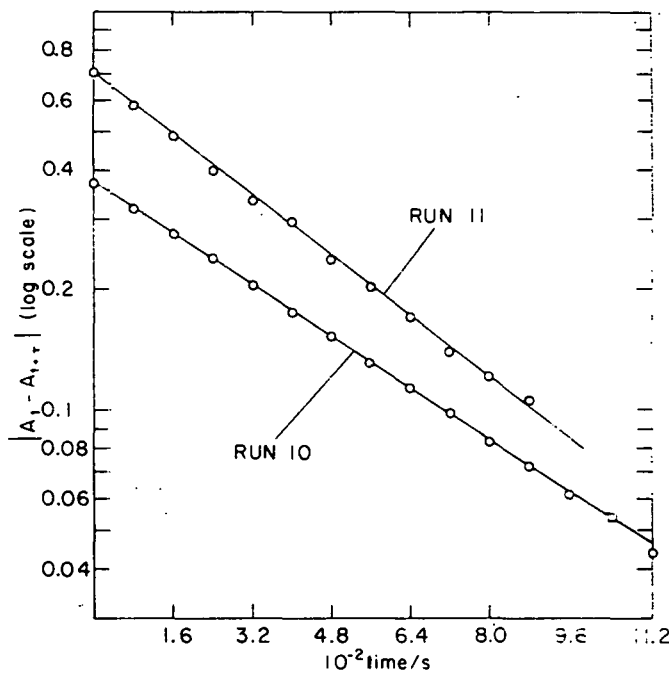


Figure I-5. Guggenheim rate plots for Runs 10 and 11

Table I-2. Kinetic data for reaction of CrCHCl_2^{2+} and Cr^{2+} .
 Conditions: $[\text{H}^+] = 1.0 \text{ M}$, $\mu = 2.5 \text{ M}$, temp = 25.1°

Expt	$10^3[\text{CrCHCl}_2^{2+}] / \text{M}$	$10^2[\text{Cr}^{2+}] / \text{M}$	λ / mm	$10^2 k_{\text{Cr}} / \text{M}^{-1} \text{s}^{-1}$
1	0.50	12.2	295	1.44
2	0.50	8.90	300	1.09
3	0.74	12.7	300	1.31
4	0.5	8.70	310	1.11
5	0.6	8.08	310	1.42
6	0.6	7.77	310	1.42
7	0.6	7.58	310	1.50
8	0.6	7.72	310	1.44
9	0.6	13.5	310	1.41
10	0.6	13.3	310	1.41
11	1.2	7.60	310	1.53
12	1.2	7.50	310	1.54
13	1.2	7.50	310	1.49
14	1.2	7.74	310	1.42
15	1.2	7.65	310	1.66 ^a
16	1.2	7.65	310	1.49
17	1.0	9.42	320	0.99
18	2.0	11.7	325	1.30
19	5.0	9.21	370	1.70
20	5.3	14.2	370	1.79
21	5.3	14.2	370	1.80
22	3.0	9.17	380	1.75
23	3.0	9.11	391	1.72
24	2.5	11.4	391	1.57
25	2.5	11.4	391	1.74
26	3.4	7.06	391	1.76

^a $[\text{Cl}^-] = 0.80 \text{ M}$.

Table I-2. (Continued)

Expt	$10^3 [\text{CrCHCl}_2^{2+}] / \text{M}$	$10^2 [\text{Cr}^{2+}] / \text{M}$	λ / mm	$10^2 k_{\text{Cr}} / \text{M}^{-1} \text{s}^{-1}$
27	1.2	10.1	392	1.41
28	2.5	10.1	392	1.42
29	9.9	2.74	391	1.59
30	9.6	3.47	---	2 ^b
31	9.58	2.84	---	1.33 ^{b,c}
32	10.4	2.90	---	1.58 ^{b,c}
33	10	2.97	---	1.25 ^{b,c}

^bReaction monitored by $[\text{Cr}^{2+}]$.

^c $[\text{H}^+] \approx 0.05 \text{ M}$.

There appears to be a wavelength dependence of k_{Cr} ; at λ 370-400 nm, the values of k_{Cr} are systematically higher ($1.6 - 1.8 \times 10^{-2} \text{ M}^{-1}\text{s}^{-1}$) than those at λ 300-320 nm ($1.1 - 1.4 \times 10^{-2} \text{ M}^{-1}\text{s}^{-1}$). This wavelength dependence is probably related to the inconstancy of A_∞ in the runs. If some slow side reaction were occurring during or after the main reaction, producing or destroying an absorbing species, the absorbance of the reaction solution, and therefore the observed rate, would be affected. The magnitude of the effect would depend on how strongly the species involved in the side reaction absorb, which would be a function of the wavelength where the reaction is monitored.

Independent experiments showed that Cr^{2+} does not react with the product, $\text{CrCH}_2\text{Cl}^{2+}$. Also, the catalytic aquation of CrCl^{2+} by Cr^{2+} could not account for the instability of A_∞ since the absorbance change involved in this reaction would be too small to be detected at the $[\text{CrCHCl}_2^{2+}]$ used. Further evidence that some side reaction occurs was seen in a run, carried out under the same conditions as the other runs, at λ 350 nm where the overall absorbance change for the main reaction is approximately zero. In this experiment the absorbance was found to increase slightly and then decrease to approximately the original value. It is therefore quite certain that some side reaction does take place, but its identity could not be determined. This point is discussed later with regard to the kinetics at low $[\text{H}^+]$.

A relevant question at this point concerns the true value of k_{Cr} . Which of the values in Table I-2 represents the true rate constant for the reaction of $CrCHCl_2^{2+}$ and Cr^{2+} , those measured at λ 370-391 nm or those at λ 300-320 nm? One experiment at high $[H^+]$ (1.0 M) and three at lower $[H^+]$ (0.05 M) were done under second-order conditions by following the disappearance of Cr^{2+} (as described in the Experimental section). These runs are included at the end of Table I-2. Since these runs were monitored by following $[Cr^{2+}]$ directly instead of the absorbance of the reaction solution, side reactions involving absorbing species should not interfere, and, theoretically, the true value of k_{Cr} can be obtained. Unfortunately, the technique itself is less accurate than the spectrophotometric method such that there is a lot of scatter in the second-order rate plots themselves. A typical plot of $\ln ([CrCHCl_2^{2+}]_t/[Cr^{2+}]_t)$ vs time is shown in Figure I-6. The values of k_{Cr} obtained by this method are within the range of those obtained spectrophotometrically.

The true value of k_{Cr} for the reaction of $CrCHCl_2^{2+}$ and Cr^{2+} is not accurately known, but it is most probably between 1.0 and $1.8 \times 10^{-2} \text{ M}^{-1}\text{s}^{-1}$. This uncertainty in k_{Cr} , however, does not affect the conclusion that the rate law is as written in equation I-9 over a 20-fold variation in $[CrCHCl_2^{2+}]$ and a four-fold variation in $[Cr^{2+}]$, at least at $[H^+] = 1.0 \text{ M}$, and this rate law is consistent with the mechanism proposed

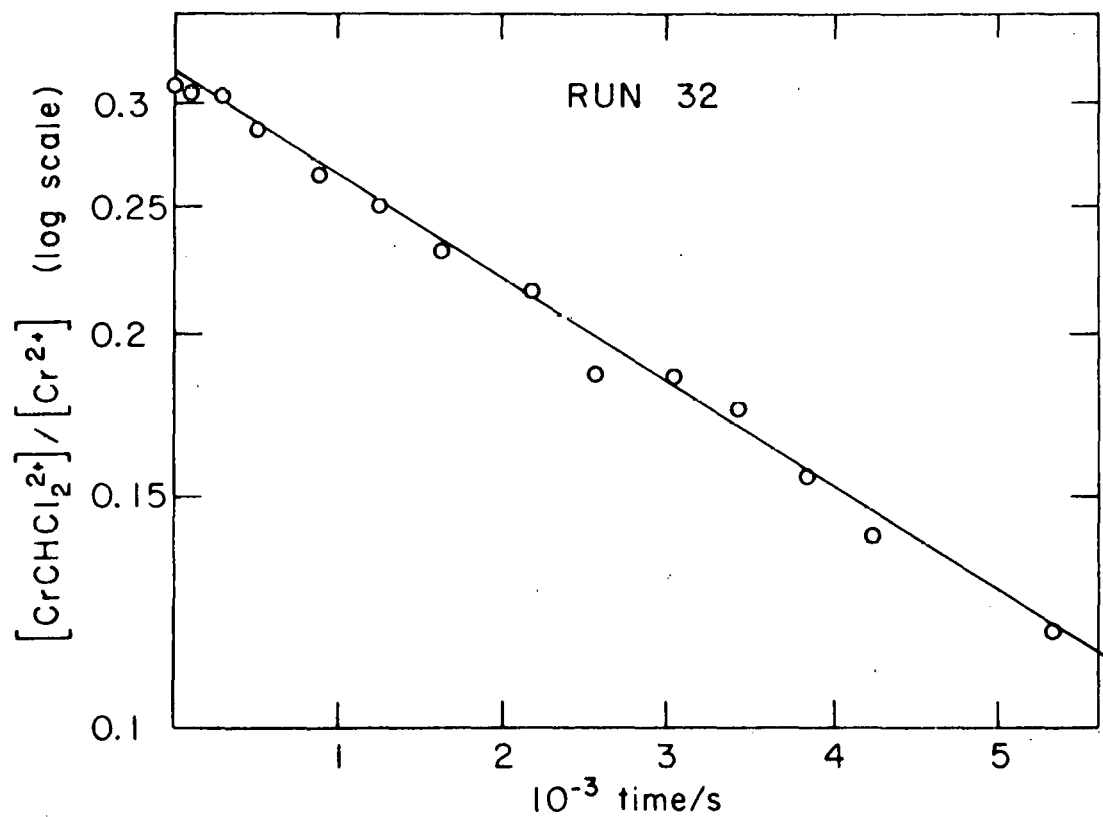


Figure I-6. Second-order rate plot for Run 32

by Dodd and Johnson (3) (equations I-5 - I-7). That the initial, rate-determining step in this mechanism is halogen abstraction from CrCHCl_2^{2+} as written in equation I-5 is hardly in doubt considering the precedent mentioned in the Introduction (1,4-5).

Low $[\text{H}^+]$

When pseudo-first-order kinetic runs were carried out at hydrogen ion concentrations below 0.10 M , some puzzling behavior was observed. Instead of the simple one-step, first-order change in absorbance seen at $[\text{H}^+] = 1.0 \text{ M}$, a two-step reaction was observed: a rapid increase in absorbance was followed by a smaller, slower decrease (at $\lambda 391 \text{ nm}$). It was found that at $\lambda 350 \text{ nm}$, where the reactants and products absorb to about the same extent, this effect is much more pronounced and could be studied conveniently. Figures I-7 and I-8 show some typical absorbance vs time traces at low $[\text{H}^+]$ that illustrate this effect at $\lambda 350 \text{ nm}$.

It is clear that an absorbing species, quite possibly a reaction intermediate, builds up in concentration under these conditions and then slowly disappears. The kinetic experiment at 1.0 M H^+ and $\lambda 350 \text{ nm}$ (see above) shows evidence for the same effect, but it is much less pronounced. Figure I-7 shows that the maximum concentration of intermediate, $[\text{Int}]_{\text{max}}$, increases with decreasing $[\text{H}^+]$,

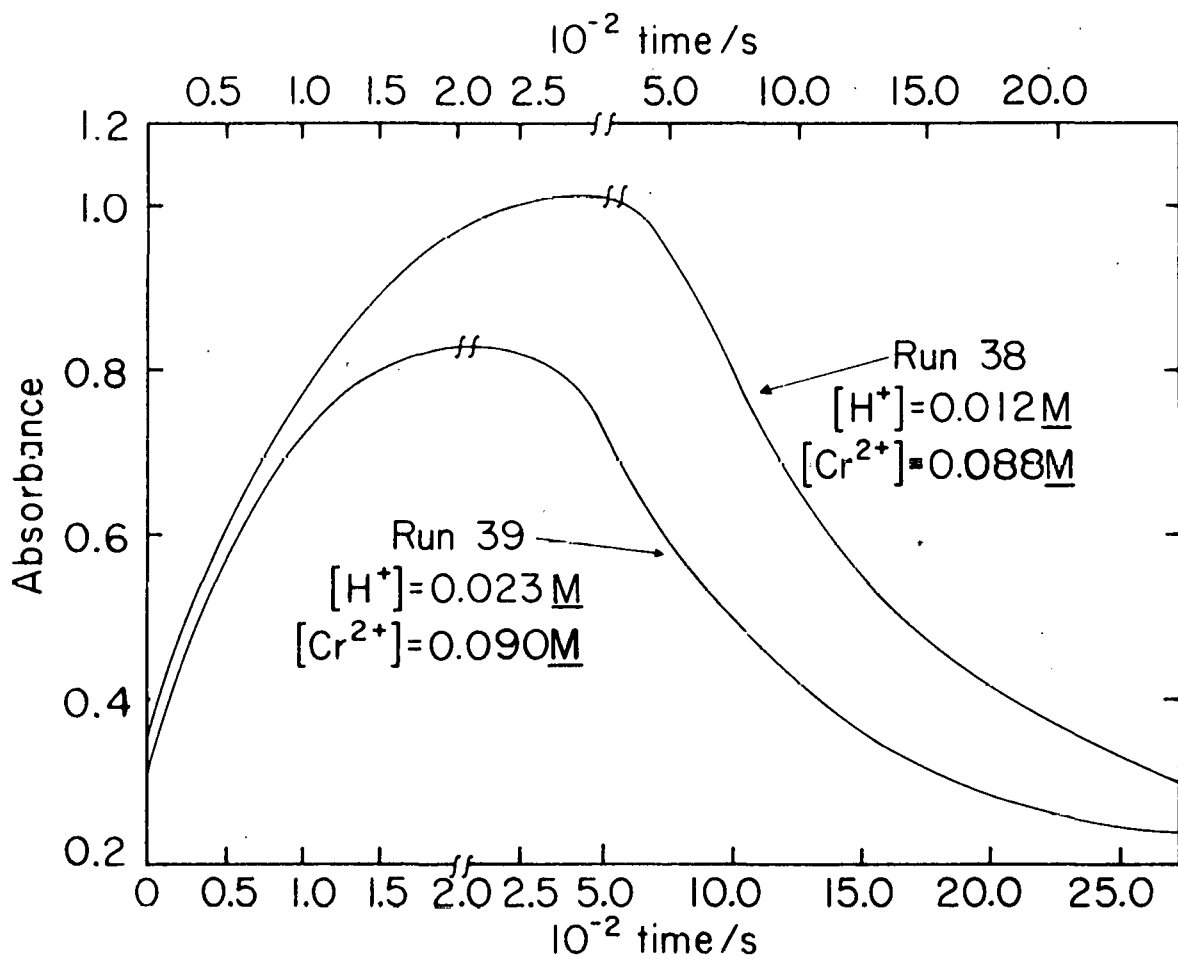


Figure I-7. Absorbance vs. time traces for runs at low $[H^+]$ showing effect of varying $[H^+]$

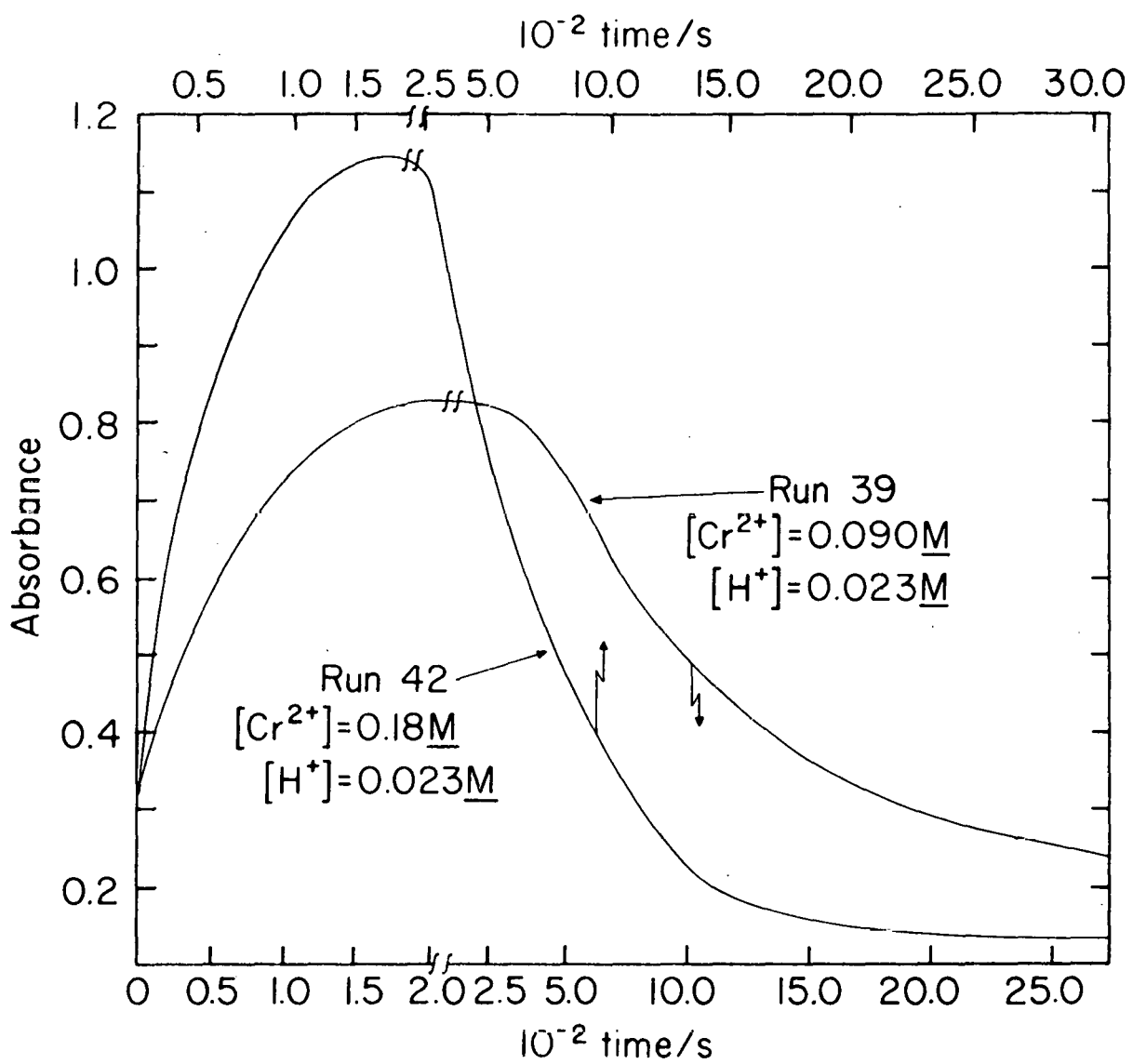


Figure I-8. Absorbance vs. time traces for runs at low $[\text{H}^+]$ showing effect of varying $[\text{Cr}^{2+}]$

and Figure I-8 shows that $[Int]_{max}$ increases with increasing $[Cr^{2+}]$. Data from other similar runs bear this out.

Guggenheim plots of the data for the rapid first step were found to be linear, indicating that the build up of intermediate is first-order in $[CrCHCl_2^{2+}]$,

$$d [Int]/dt = k_I [CrCHCl_2^{2+}] \quad (I-18)$$

Values of k_I obtained from these plots are shown in Table I-3. It can be seen that k_I is independent of $[Cr^{2+}]$ but mildly dependent on $[H^+]$ such that k_I increases with $[H^+]$. A precise order with respect to hydrogen ion could not be determined since $[H^+]$ could not be measured very accurately in these experiments.

Guggenheim plots of the slower second step of the reaction were also linear, indicating that the decay of the intermediate is first-order in $[Int]$, that is,

$$-d [Int]/dt = k_{II} [Int] \quad (I-19)$$

Values of the second-stage first-order rate constant, k_{II} , are also shown in Table I-3. The rate of this second step is independent of $[H^+]$ but first-order in $[Cr^{2+}]$ as demonstrated by the constancy of the quotient $k_{II}/[Cr^{2+}]$, also shown in Table I-3. Interestingly enough, this quotient has nearly the same value as the second-order rate constant, k_{Cr} , for the one-step reaction observed at high $[H^+]$. Whether

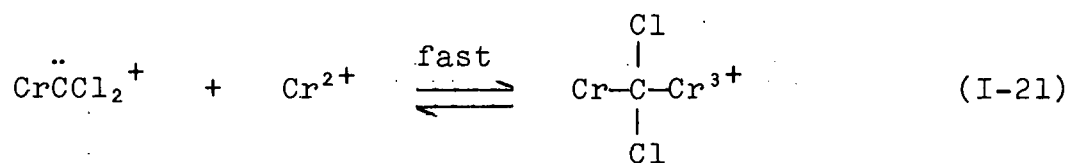
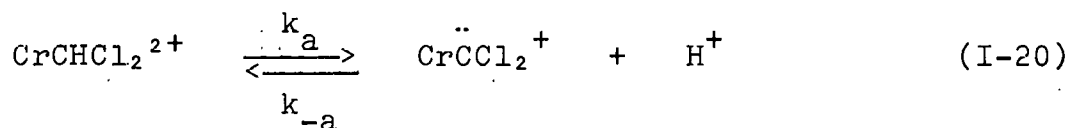
Table I-3. Kinetic results of fast and slow steps in the reaction of CrCHCl_2^{2+} and Cr^{2+} at low $[\text{H}^+]$. Conditions: $[\text{CrCHCl}_2^{2+}] = 2 \times 10^{-3} \text{ M}$, $\mu = 2.50 \text{ M}$, $\lambda = 350 \text{ nm}$, $T = 25.1^\circ$

Expt	$10^2 [\text{Cr}^{2+}] / \text{M}$	$10^2 [\text{H}^+] / \text{M}$	First Step		Second Step	
			$10^2 k_I / \text{s}^{-1}$	$10^3 k_{II} / \text{s}^{-1}$	$10^2 k_{II} [\text{Cr}^{2+}]^{-1} / \text{M}^{-1} \text{s}^{-1}$	L
34	8.31	- ^a	1.49	1.06	1.28	
35	3.95	- ^a	1.37	0.489	1.24	
36	3.64	- ^a	0.88	0.416	1.14	
37	5.12	2.1	1.11	0.606	1.18	
38	8.99	1.2	1.08	1.12	1.25	
39	8.82	2.3	1.35	1.01	1.15	
40	9.34	3.1	1.77	1.15	1.23	
41	9.97	3.4	2.05	1.36	1.36	
42	17.9	2.3	1.74	2.35	1.31	
43	18.0	2.5	1.63	2.40	1.33	

^a $[\text{H}^+]$ not measured directly, approximately $0.01 - 0.05 \text{ M}$.

or not this coincidence is a genuine mechanistic effect, will be considered later. The rapid first step is 7-30 times faster than the second step depending on $[Cr^{2+}]$ and $[H^+]$.

It is instructive at this point to consider one mechanism which might explain these results:



According to this proposal, the dinuclear chromium species, $Cr_2CCl_2^{3+}$, is the substance whose absorption is seen at $\lambda 350$ nm. Note that this dichromium cation lies off the main reaction pathway; that is, its formation does not lead to products. Rather, it is formed at high $[Cr^{2+}]$ and low $[H^+]$ but reverts to $CrCHCl_2^{2+}$ as the main reaction with Cr^{2+} proceeds. The predicted increase with $[Cr^{2+}]$ and decrease with $[H^+]$ are consistent with our experiments. The rate of formation of $Cr_2CCl_2^{3+}$ would be independent of $[Cr^{2+}]$ assuming k_a in equation I-20 is rate-determining. Since the rate of disappearance of the intermediate is roughly the same as that of the simple bimolecular reaction at 1.0 M $[H^+]$, equations I-20 and I-21 could lie off the main reaction pathway and provide a nonreacting storage place for $CrCHCl_2^{2+}$.

The obvious way to test this rationale is to determine whether CrCHCl_2^{2+} exchanges protons with the solvent during the course of reaction with Cr^{2+} . Two experiments were done, as described in the Experimental section, at high and low $[\text{H}^+]$ (denoted MS1 and MS2, respectively). The results of these experiments are shown in Table I-4 along with those of a similar experiment (MS3) in which authentic nondeuterated $\text{CrCH}_2\text{Cl}^{2+}$ reacted with Br_2 under conditions similar to the other experiments. The data in Table I-4 shows only the relative intensities for the mass peaks characteristic for the CH_2ClBr product of the reaction.

It is clear from Table I-4 that when the deuterated complex, CrCDCl_2^{2+} , reacts with Cr^{2+} , the product is the deuterated CrCHDCl^{2+} since the subsequent reaction of this complex with Br_2 gives only CHDClBr . The mass peaks for the molecular ions CHDCl^+ , CHDBr^+ , and CHDClBr^+ are very strong whereas those of CH_2Cl^+ , CH_2Br^+ , and CH_2ClBr are essentially negligible.

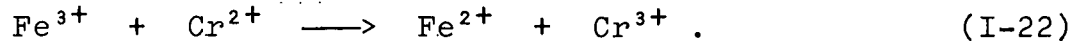
These results show that the reactions in equations I-20 and I-21 do not occur either at high or low $[\text{H}^+]$, and the rationale that could have explained the results of the experiments at low $[\text{H}^+]$ must therefore be abandoned.

Several more experiments were done to shed light on the nature and identity of this intermediate, but the results did not prove particularly helpful. These experiments

Table I-4. Mass spectral data for the experiments on exchange of protons with CrCHCl_2^{2+}

Mass Peak	Relative Intensity			Molecular Ion
	MS1	MS2	MS3	
49	17	5	141	$\text{CH}_2^{35}\text{Cl}^+$
50	>250	88	5	$\text{CDH}^{35}\text{Cl}^+$
51	7	2	50	$\text{CH}_2^{37}\text{Cl}^+$
52	9.0	2.8	15	$\text{CHD}^{37}\text{Cl}^+$
93	14	46	24	$\text{CH}_2^{79}\text{Br}^+$
94	37	120	2	$\text{CHD}^{79}\text{Br}^+$
95	6	14	18	$\text{CH}_2^{81}\text{Br}^+$
96	4.0	148	7	$\text{CHD}^{81}\text{Br}^+$
128	6	6	29	$\text{CH}_2^{35}\text{Cl}^{79}\text{Br}^+$
129	178	153	7	$\text{CHD}^{35}\text{Cl}^{79}\text{Br}^+$
130	9	8	111	$\text{CH}_2^{35}\text{Cl}^{81}\text{Br}^+$
				$\text{CH}_2^{37}\text{Cl}^{79}\text{Br}^+$
131	228	187	5	$\text{CHD}^{35}\text{Cl}^{81}\text{Br}^+$
				$\text{CHD}^{37}\text{Cl}^{79}\text{Br}^+$
132	5	3	30	$\text{CH}_2^{37}\text{Cl}^{81}\text{Br}^+$
133	55	50	--	$\text{CHD}^{37}\text{Cl}^{81}\text{Br}^+$

involved carrying out kinetic runs at λ 350 nm in low $[H^+]$ in the usual way except that when the maximum absorbance, A_{max} , was reached (i.e., at $[Int]_{max}$) various reagents were added to see what effect they had on the intermediate. When hydrogen ion was added at A_{max} , the intermediate was destroyed essentially instantaneously, a rather confusing result considering that the rate of decay of $[Int]$ proved independent of $[H^+]$ at low $[H^+]$. When oxygen was bubbled into the reaction solution at A_{max} to oxidize Cr^{2+} , the intermediate was destroyed more rapidly than when Cr^{2+} was allowed to remain. This constitutes a second confusing result considering that the decay of $[Int]$ is first-order in $[Cr^{2+}]$. Other experiments were done in which excess Cr^{2+} was oxidized with Fe^{3+} after A_{max} was reached; this reaction is



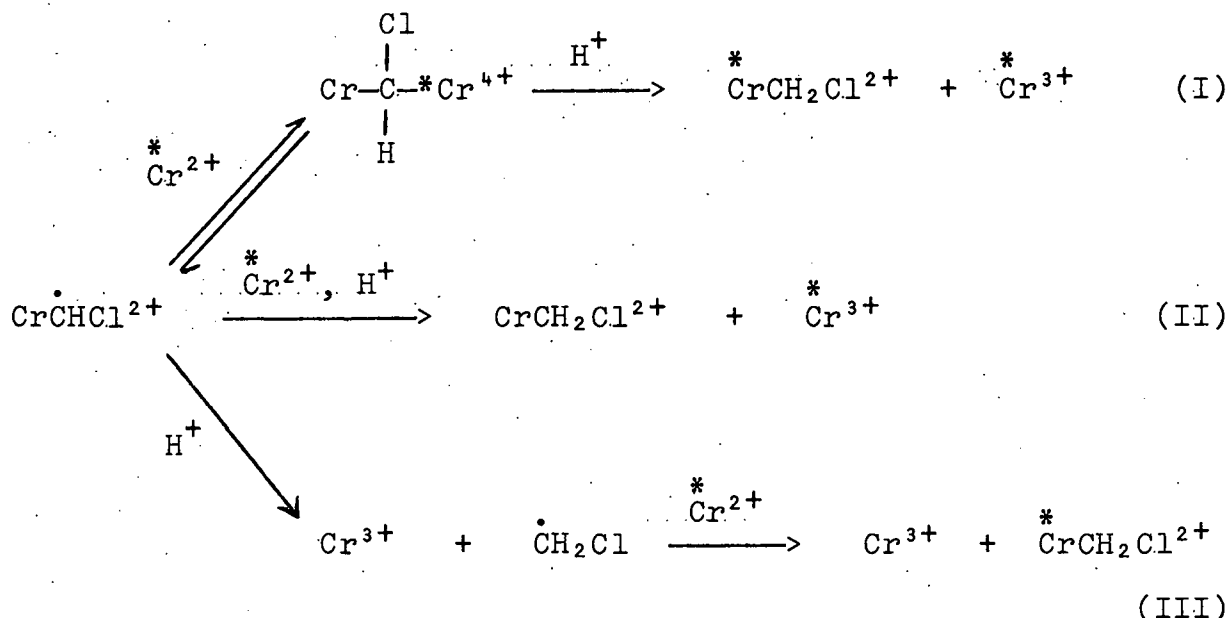
When the amount of added Fe^{3+} was less than that of Cr^{2+} , the rate of decay of $[Int]$ was slower than when no Fe^{3+} was added, consistent with the observed first-order dependence on $[Cr^{2+}]$. When enough Fe^{3+} was added to oxidize all of the Cr^{2+} , however, the rate of decay of intermediate was faster than when oxygen was used to oxidize excess Cr^{2+} . We are unable to explain the results of these experiments with added H^+ , O_2 , or Fe^{3+} .

No further work on this problem was done, and the complicated behavior of the reaction at low $[H^+]$ remains unexplained. It should be noted from the last three entries in Table I-2 that when the reaction was monitored by the consumption of $[Cr^{2+}]$ at low $[H^+]$ under second-order conditions, the aberrant behavior seen in the pseudo-first-order spectrophotometric runs was not observed, but rather straightforward second-order behavior. The major conclusion from the kinetic results of this study is still considered valid, that the reaction is first-order in both $[CrCHCl_2^{2+}]$ and $[Cr^{2+}]$ and that equation I-5 is the rate-determining first step in the reaction.

Radiotracer Experiments

The results of the stoichiometry and kinetics experiments discussed so far are consistent with the mechanism proposed by Dodd and Johnson (3), shown in equations I-5 - I-7. The kinetic results in particular indicate that the first and rate determining step in the mechanism is halogen abstraction from $CrCHCl_2^{2+}$, leaving the radical species, $Cr\dot{C}HCl^{2+}$, which then goes on to react with Cr^{2+} to form products. It was of interest to learn the mechanism of this latter reaction.

Three likely mechanisms were considered for the reaction of $Cr\dot{C}HCl^{2+}$ with Cr^{2+} as represented below in schemes I-III:



Scheme I is essentially the mechanism proposed by Dodd and Johnson (equations I-5 - I-7) which consists of an inner-sphere type reaction of CrCHCl^{2+} and Cr^{2+} forming a dinuclear intermediate which then may react with a proton to form products. Scheme II can be considered an outer-sphere type reaction wherein simple electron-transfer and protonation occur either simultaneously or consecutively. Scheme III involves prior scission of the Cr-C bond, possibly by a proton, to give an organic radical which reacts with Cr^{2+} to form products.

The distribution of tagged chromium (denoted by $\overset{*}{\text{Cr}}$) in these mechanisms suggests a way of discriminating among them. Table I-5 shows the expected relative activity of the chromium products of the reaction compared to that of $\overset{*}{\text{Cr}}{}^{2+}$ for each mechanism.

Table I-5. Expected relative activities of Cr products of the reaction of Cr^{2+} and CrCHCl for Schemes I-III

Scheme	Cr^{2+}	CrCl^{2+}	$\text{CrCH}_2\text{Cl}^{2+}$	Cr^{3+}
I	1	1	1/2	1/2
II	1	1	0	1
III	1	1	1	0

Five experiments, as described in the Experimental section, were carried out to determine which, if any, of the isotopic distributions shown in Table I-5 occurs. The results of three of these experiments (RT1-RT3) are given in Table I-6 which shows the specific activities (cpm/ M) of the consecutive fractions of chromatographed reaction solutions along with the predominant species occurring in the fractions. The last entry for each experiment is the activity of the tagged reagent before the experiment was started.

At first glance, the results do not seem to correspond to any of the isotopic distributions shown in Table I-5. The most glaring apparent discrepancy is that in RT1 and RT2, the activities of the earliest fractions, which contain only CrCl^{2+} and CrBr^{2+} ,¹ are considerably lower than that of Cr^{2+} .

¹This complex comes from the oxidation of unreacted Cr^{2+} with $\text{Co}(\text{NH}_3)_5\text{Br}^{2+}$

Table I-6. Specific activity, S, of Cr samples for radiotracer experiments.

	RT1		RT2		RT3		
Frac-	Frac-		Frac-		Frac-		
tion $10^{-6} \text{S}/\text{cpmM}^{-1}$	Species		tion $10^{-6} \text{S}/\text{cpmM}^{-1}$	Species	tion $10^{-6} \text{S}/\text{cpmM}^{-1}$	Species	
1	4.1	CrCl^{2+}	1	3.7	CrCl^{2+}	1	CrCl^{2+}
2	4.0	+	2	3.9	+	2	2.2
3	5.0	CrBr^{2+}	3	3.8	CrBr^{2+}	3	2.2
4	4.1		4	3.8		4	2.1
5	3.7		5	3.7		5	2.1
6	3.5		6	2.9		6	2.1
7	3.5		7	2.4	CrCHCl_2^{2+}	7	2.1
8	3.7	CrCHCl_2^{2+}	8	2.2	+	8	2.1
9	3.5	+	9	1.7	$\text{CrCH}_2\text{Cl}^{2+}$	9	2.1
10	3.4	$\text{CrCH}_2\text{Cl}^{2+}$	10	2.1		10	2.4
11	3.3					11	2.4
12	4.9		Cr^{2+}	5.1 ^a		CrCHCl_2^{2+}	6.2 ^a
19	4.6						
20	4.1						
21	4.4	Cr^{3+}					
22	4.6						
23	4.7						
Cr^{2+}	5.3 ^a						

^aSpecific activity of tagged reagent before adding to the untagged reagent.

All three mechanisms from Table I-5 indicate that CrCl^{2+} should have the same activity as Cr^{2+} , and so should CrBr^{2+} since it is derived solely from unreacted Cr^{2+} . The same discrepancy is apparent in RT3 where CrCHCl_2^{2+} was the tagged reagent, since in this experiment the CrCl^{2+} and CrBr^{2+} fractions should not be tagged at all according to schemes I-III.

These results imply that Cr^{2+} must exchange with some species in the system to account for dilution of the radiotag in products derived from tagged Cr^{2+} in RT1 and RT2 and to account for the presence of any radiotag in products derived from originally untagged Cr^{2+} in RT3. It is known that CrCl^{2+} and CrBr^{2+} exchange chromium rapidly with Cr^{2+} (13), but this cannot explain the radiotracer results since these species are derived from the Cr^{2+} in the first place. The product Cr^{3+} is known to exchange with Cr^{2+} only very slowly with a half-life of days (14); so Cr^{3+} could not be responsible for the dilution of activity in Cr^{2+} .

Experiments RT4 and RT5, described in the Experimental section, were designed to determine if Cr^{2+} exchanges chromium with either the product $\text{CrCH}_2\text{Cl}^{2+}$ or the reactant CrCHCl_2^{2+} , respectively. In RT4, no exchange between $\text{CrCH}_2\text{Cl}^{2+}$ and tagged Cr^{2+} was observed after 1.5 hours; that is, $\text{CrCH}_2\text{Cl}^{2+}$ recovered from the reaction mixture showed no activity. Likewise, in RT5 no activity was found in unreacted CrCHCl_2^{2+} after it had been in the presence of tagged Cr^{2+} for 1.5 hours.

It is clear, therefore, that none of the stable chromium(III) species present during the reaction can be responsible for the dilution of the Cr^{2+} radiotag in RT1 and RT2 or the presence of radiotagged Cr^{2+} in RT3. The only possibility left is that some intermediate in the reaction, one derived from CrCHCl_2^{2+} , must exchange with Cr^{2+} . The only mechanism of the three suggested that involves such an intermediate is Scheme I. If the reaction forming the dinuclear intermediate in Scheme I is rapidly reversible, it would provide a pathway for the chromium originally present in CrCHCl_2^{2+} or Cr^{2+} to be distributed into all the products.

Using the mechanism in equations I-5 - I-7 (Scheme I), the theoretical specific activities of the fractions in the radiotracer experiments can be computed for comparison with those observed. The details of these computations are given in the Appendix and the results are shown in Table I-7. The agreement between observed and calculated values of S is quite good, a result that lends strong support for Scheme I as the mechanism for reaction of the radical intermediate, $\cdot\text{CrCHCl}$, with Cr^{2+} .

The radiotracer experiments, then, support the mechanism proposed by Dodd and Johnson (3), as do the kinetics and stoichiometry experiments. These same results were found by Nohr and Spreer (7) for reaction CrCH_2^{2+} and Cr^{2+} . The

essential features of this mechanism are as shown in equations I-5 - I-7.

Table I-7. Observed^a and calculated^b specific activities of fractions in radiotracer experiments. S_x refers to the early fractions (CrCl^{2+} and CrBr^{2+}); S_{CrR} refers to middle fractions (CrCHCl_2^{2+} and $\text{CrCH}_2\text{Cl}^{2+}$); and S_y refers to later fractions (Cr^{3+}). Specific activities are given as $10^{-6}\text{S}/\text{cmp}/\underline{\text{M}}$

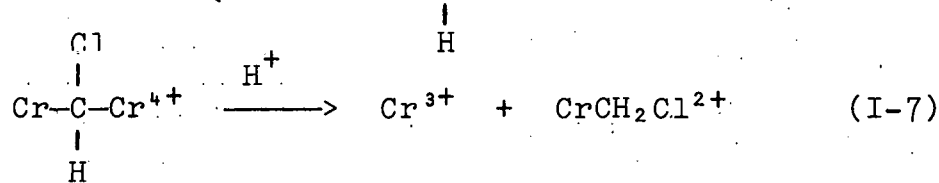
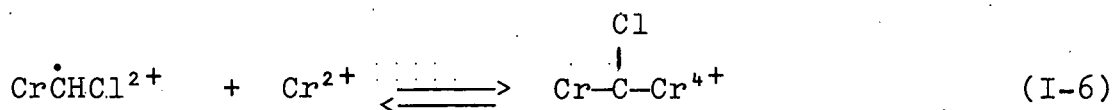
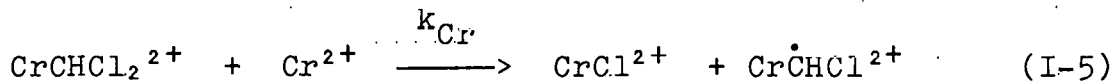
Experiment	S_x		S_{CrR}		S_y	
	obs.	calc.	obs.	calc.	obs.	calc.
RT1	4.3 ± 0.4	3.5	3.5 ± 0.1	3.3	4.5 ± 0.2	4.4
RT2	3.8 ± 0.1	4.0	2.3 ± 0.2	2.3	---	4.5
RT3	2.2 ± 0.025	2.2	2.2 ± 0.15	2.4	---	1.1

^aObserved values taken from Table I-6.

^bProcedure for calculations given in the Appendix.

APPENDIX

This section outlines the computation of specific activities of the various ion exchange fractions for the radiotracer experiments RT1-3, based on the proposed mechanism (equations I-5 - I-7) reiterated below.



The following definitions will be used in the derivations:

$$x = [\text{Cr}^{2+}] + [\text{CrCl}^{2+}] = [\text{Cr}^{2+} \text{ fraction}].$$

$$y = [\text{Cr}^{3+}] = [\text{CrCH}_2\text{Cl}^{2+}] = [\text{CrCl}^{2+}].$$

u = Activity of the Cr^{2+} fraction (in cpm).

v = Activity of Cr^{3+} and $\text{CrCH}_2\text{Cl}^{2+}$ (in cpm).

$S_x = u/x$ = specific activity of the Cr^{2+} fraction
(in cpm/M).

$S_y = v/y$ = specific activity of Cr^{3+} and $\text{CrCH}_2\text{Cl}^{2+}$
(in cpm/M).

S_o = Specific activity of CrCHCl_2^{2+} (in cpm/M).

Rate = $k_{\text{Cr}}[\text{Cr}^{2+}][\text{CrCHCl}_2^{2+}]$.

The rate of change of $[Cr^{2+}$ fraction] is given by

$$\frac{dx}{dt} = - \text{Rate} \quad (I-23)$$

and the rate of change of activity of the Cr^{2+} fraction is given by

$$\frac{dv}{dt} = -2 \frac{u}{x} \text{Rate} + S_o \text{Rate} \quad (I-24)$$

Combining these two equations gives

$$\frac{dv}{dx} = S_o - 2 \frac{u}{x} \quad (I-25)$$

Integration of equation I-25 by using the integrating factor, $1/x^2$ gives

$$\frac{u}{x} = S_o + Cx = S_x \quad (I-26)$$

where C is the constant of integration.

To get S_y we can write

$$\frac{dy}{dt} = + \text{Rate} \quad (I-27)$$

$$\frac{dv}{dt} = + S_x \text{Rate} \quad (I-28)$$

and dividing gives

$$\frac{dv}{dy} = S_x = S_o + Cx \quad (I-29)$$

From the stoichiometry of the reaction (equation I-8),

$[Cr^{2+}] = [Cr^{2+}]_0 - 2y$, and from the definition of x and y given above, $x = [Cr^{2+}]_0 - y$. Substituting this into equation I-29 gives

$$\frac{dy}{dx} = S_0 + C[Cr^{2+}]_0 - Cy \quad (I-30)$$

and integration yields

$$\frac{y}{x} = S_0 + C[Cr^{2+}]_0 - \frac{1}{2} Cy = S_y \quad (I-31)$$

For the radiotracer experiments in which Cr^{2+} is the tagged reagent (RT1 and RT2) S_0 is 0 so that equation I-26 reduces to

$$S_x = Cx = \frac{S_{x0}}{[Cr^{2+}]} x \quad (I-32)$$

(C , in this case, evaluated at t_0 where x_0 is $[Cr^{2+}]_0$ and S_{x0} is the specific activity of the tagged Cr^{2+}).

Likewise, equation I-31 reduces to

$$S_y = C[Cr^{2+}]_0 - \frac{1}{2} Cy = S_{x0} \left(1 - \frac{y}{2[Cr^{2+}]_0}\right) \quad (I-33)$$

For experiment RT3, where $CrCHCl_2^{2+}$ is the tagged reagent, S_0 is finite and constant (since $CrCHCl_2^{2+}$ does not exchange with anything in the reaction mixture). In this case C can be evaluated from equation I-26 by realizing that at t_0 , S_x is 0 and $C = -S_0/[Cr^{2+}]_0$; thus

$$S_x = S_o \left(1 - \frac{x}{[Cr^{2+}]_o}\right) \quad (I-34)$$

Equation I-31 becomes

$$S_y = S_o - \frac{S_o}{[Cr^{2+}]_o} [Cr^{2+}]_o - \frac{1}{2} Cy = \frac{1}{2} \left(\frac{S_o}{[Cr^{2+}]_o}\right) y \quad (I-35)$$

In the radiotracer experiments, the specific activity of the fractions containing $CrCl^{2+}$ and $CrBr^{2+}$ is S_x ; that of the fractions containing $CrCHCl_2^{2+}$ and $CrCH_2Cl^{2+}$, S_{CrR} , is given by

$$S_{CrR} = \frac{S_y \cdot y + S_o [CrCHCl_2^{2+}]}{y + [CrCHCl_2^{2+}]} ; \quad (I-36)$$

and that of the Cr^{3+} fractions is, of course, S_y .

For RT1, $[CrCHCl_2^{2+}]_o = 1.7 \times 10^{-2} \text{ M}$, $[Cr^{2+}]_o = 3.8 \times 10^{-2} \text{ M}$, and $S_{xo} = 5.3 \times 10^6 \text{ cpm/M}$. At 75% reaction (2 half-lives), $[Cr^{2+}] = 1.25 \times 10^{-2} \text{ M}$, $[CrCHCl_2^{2+}] = 0.44 \times 10^{-2} \text{ M}$, and $y = 1.28 \times 10^{-2} \text{ M}$. The values of S_x , S_{CrR} , and S_y for RT1 are thus 3.5, 3.3, and $4.4 \times 10^6 \text{ cpm/M}$, respectively.

For RT2, the initial reactant concentrations are the same as in RT1, and $S_{xo} = 5.1 \times 10^6 \text{ cpm/M}$. At 50% reaction (1 half-life), $[Cr^{2+}] = 2.10 \times 10^{-2} \text{ M}$ and $[CrCHCl_2^{2+}] = y = 0.85 \times 10^{-2} \text{ M}$. The values of S_x , S_{CrR} , and S_y are thus 4.0, 2.3 and $4.5 \times 10^6 \text{ cpm/M}$, respectively.

Finally, for RT3, $[CrCHCl_2^{2+}]_o = 2.9 \times 10^{-2} \text{ M}$, $[Cr^{2+}] = 6.1 \times 10^{-2} \text{ M}$, and $S_o = 6.2 \times 10^6 \text{ cpm/M}$. At 75%

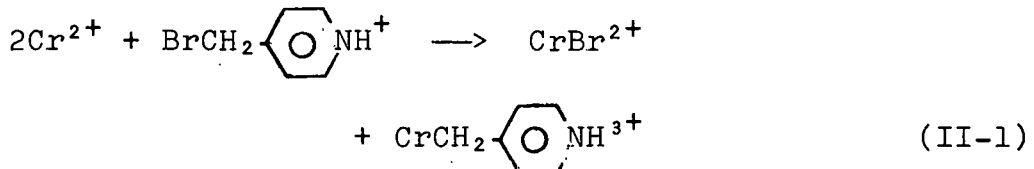
reaction, $[Cr^{2+}] = 1.74 \times 10^{-2} \text{ M}$, $[CrCHCl_2^{2+}] = 0.73 \times 10^{-2} \text{ M}$, and $y = 2.18 \times 10^{-2} \text{ M}$. The values of S_x , S_{CrR} , and S_y are thus 2.2, 2.4, and $1.1 \times 10^6 \text{ cpm/M}$, respectively.

PART II. KINETICS OF FORMATION OF PENTAAQUO-4-PYRIDINOMETHYL-
CHROMIUM(III) ION AND ITS EXCHANGE REACTION WITH
CHROMIUM(II) ION

INTRODUCTION

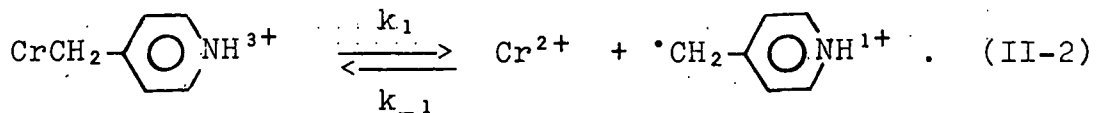
Complexes of Cr(III) of the general type $[\text{CrL}_5\text{X}]^{(3-n)+}$ hydrolyze slowly in aqueous solution and this process usually occurs by heterolytic cleavage of the Cr-X bond (15). There is evidence, however, that the organo-chromium(III) complex, pentaaquo-4-pyridinomethylchromium(III) cation (hereafter designated as $\text{CrCH}_2\text{C}_5\text{H}_4\text{NH}^{3+}$) decomposes in aqueous acidic solutions by homolytic cleavage of the Cr-C bond (16,17).

This complex was first prepared by Coombes, *et al.* by the reaction of Cr^{2+} with 4-bromomethylpyridinium bromide, $\text{BrCH}_2\text{C}_5\text{H}_4\text{NH}^+\text{Br}^-$, in aqueous acid solution (5),



The complex was confirmed to contain a metal-carbon sigma bond by comparison of its electronic spectrum with those of known chromium complexes of this type and by the products of decomposition in aqueous solution. In a detailed study of the decomposition process (16), Coombes and Johnson found that the major organic products are those expected from a radical precursor (*i.e.*, 1,2 di-4-pyridylethane and pyridine-4-aldehyde). The kinetics showed that in the presence of oxygen the reaction is first-order in Cr(III) complex, but when air is excluded, the kinetics are complicated, showing

an order with respect to $[\text{CrCH}_2\text{C}_5\text{H}_4\text{NH}^{3+}]$ less than one. Moreover, the activation energy is higher than expected for the heterolytic dissociation of a Cr(III) complex. The conclusion from these findings was that $\text{CrCH}_2\text{C}_5\text{H}_4\text{NH}^{3+}$ decomposes in acid solution by a homolytic rather than heterolytic scission of the Cr-C bond as in the following:



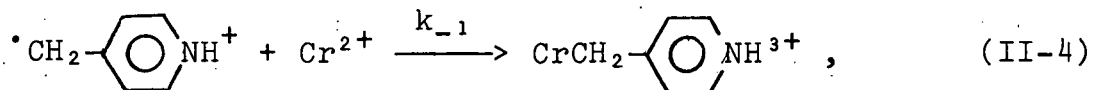
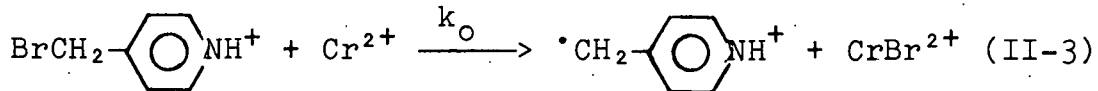
Schmidt and Swaddle did a more detailed kinetic study of the decomposition in the absence of oxygen, concluding that homolysis is the first step in the mechanism (17). When air was rigorously excluded, the reaction was much slower and under certain concentration conditions showed a half-order dependence on $[\text{CrCH}_2\text{C}_5\text{H}_4\text{NH}^{3+}]$. When Cr^{2+} was added, the rate was retarded and became first order in complex and inverse-first-order in added $[\text{Cr}^{2+}]$. These workers were able to write a detailed mechanism for decomposition accounting for these observations that included equation II-2 as the first step. By measuring the rate in the presence and absence of oxygen and with added Cr^{2+} , they were able to assign values to the various rate constants in the mechanism including k_1 and k_{-1} in equation II-2.

$k_1 = 5.2 \times 10^{-5} \text{ s}^{-1}$ and $k_{-1} = 1.0 \times 10^{-2} \text{ M}^{-1} \text{ s}^{-1}$ in 1.0 M HClO_4 at 55°C.

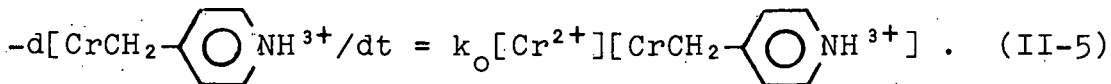
It appeared that these values of k_1 and k_{-1} as well as certain aspects of the assigned mechanism could be readily checked by independent experiments. This seemed advisable since it would be the only confirmed case of homolytic cleavage of a Cr-C bond. Also, the value k_{-1} from the work of Schmidt and Swaddle seems quite small compared to known rates of other reactions between Cr^{2+} and alkyl radicals which generally have second-order rate constants of 10^6 - $10^8 \text{ M}^{-1} \text{ s}^{-1}$ (18). Moreover, were the value of k_{-1} really as low as assigned by these workers, the synthetic process from Cr^{2+} and the organic bromide (equation II-1) could not proceed as indicated. This is so because the synthetic process has as its second and presumably rapid step (equation II-4) the same reaction as the reverse of homolysis (equation II-2). At a specific rate of $10^{-2} \text{ M}^{-1} \text{ s}^{-1}$, it could not account for the rate of the synthetic reaction.

If the reaction in equation II-2 does in fact occur, it should provide a pathway for chromium exchange between $\text{CrCH}_2\text{C}_5\text{H}_4\text{NH}^{3+}$ and free Cr^{2+} . The rate of exchange could be easily studied with radiotracer techniques by tagging one of the reactants with ^{51}Cr , a weak gamma emitter. According to the proposed mechanism, unless other pathways for exchange exist, the rate of exchange should be first-order in $[\text{CrCH}_2\text{C}_5\text{H}_4\text{NH}^{3+}]$ and independent of $[\text{Cr}^{2+}]$ with a rate constant identical to k_1 .

The value of k_{-1} could also be checked. The assumed mechanism for formation of $\text{CrCH}_2\text{C}_5\text{H}_4\text{NH}^{3+}$ is shown below



where the first step is rate determining. This mechanism is almost certainly operative in light of many known reactions of alkyl halides with Cr^{2+} (3,4,6). The expected rate law for this reaction is

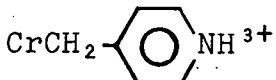


By a quantitative study of the rate of this reaction over a wide range of concentration variation, a lower limit of the fast, second step can be made based on the rate of the slow first step.

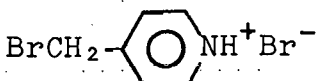
Kinetic experiments have been done on the chromium exchange between $\text{CrCH}_2\text{C}_5\text{H}_4\text{NH}^{3+}$ and Cr^{2+} and on the synthetic reaction (equation II-1) in order to check the mechanism of Schmidt and Swaddle and their values of k_1 and k_{-1} , and to determine the mechanism of chromium exchange.

EXPERIMENTAL

Materials



The complex was prepared by the literature method (5) from chromous perchlorate and 4-bromomethylpyridinium bromide. The synthetic reaction is shown in equation II-1. A 20 ml solution containing 0.25 g $\text{BrCH}_2\text{C}_5\text{H}_4\text{NHBr}$ (1 mmol) was purged with nitrogen for 30 minutes and 2 mmol of Cr^{2+} added by syringe. (It was important to have $\text{BrCH}_2\text{O}_5\text{H}_4\text{N}^+$ in slight excess to avoid the need to oxidize excess Cr^{2+} and risk contamination with Cr^{3+} .) The solution, which immediately turned a dirty-brown, was placed on a 35 x 1½ cm column of Dowex 50W-X2 cation exchange resin where two bands were observed; the bright green band of CrBr^{2+} followed by the orange band of $\text{CrCH}_2\text{C}_5\text{H}_4\text{NH}^3+$. The CrBr^{2+} was eluted with 0.5 and 1.0 M HClO_4 and discarded, and the product $\text{CrCH}_2\text{C}_5\text{H}_4\text{NH}^3+$ was eluted with 2.0 M HClO_4 . Only the middle fraction of the orange band was kept. The solutions could be stored for weeks if kept frozen at -10°.



This compound was synthesized by the method of Bixler and Niemann (19) from 4-pyridinomethylcarbinol, $\text{HOCH}_2\text{C}_5\text{H}_4\text{N}$ and HBr . A 20 g sample of the carbinol (0.18 mole) was

dissolved in 180 ml of 48% HBr and refluxed for five hours. The solvent was evaporated under vacuum to yield a thick, yellow-white paste which was washed twice with 100 ml portions of cold absolute ethanol and dried under vacuum. A 42% yield (19.6 g) of fluffy white product was obtained (M.P. 188-192, lit. 185-187 (19)).

Cr²⁺ solutions

Solid Cr(ClO₄)₃ (prepared by reduction of CrO₃ with H₂O₂ in HClO₄ and recrystallized twice) was dissolved in dilute HClO₄ (0.1 - 1.0 M) and reduced to Cr²⁺ with amalgamated zinc. The reduction was carried out under nitrogen in a rubber-capped bottle with stirring for at least 24 hours to ensure complete reaction. In most cases the solution was transferred for storage to another rubber-capped bottle not containing amalgamated zinc.

Radiotagged ⁵¹Cr²⁺ solutions were made from Chromium 51 obtained from New England Nuclear Corporation in the form of ⁵¹CrCl₃ dissolved in HCl. A stock solution of ⁵¹Cr²⁺ was prepared by adding a small amount of this material to a serum-capped volumetric flask containing untagged Cr²⁺ over amalgamated zinc. This solution was allowed to equilibrate for at least 24 hours.

Other materials

The complex [Co(NH₃)₅Br]Br₂ was prepared earlier as described in Part I (footnote, page 12). All other materials

mentioned in Part II were reagent grade and were used without further purification.

Methods

Analyses

The concentration of the complex $\text{CrCH}_2\text{C}_5\text{H}_4\text{NH}^{3+}$ was estimated by the electronic spectrum of solutions and the published extinction coefficients at its spectral peaks (λ 225, ϵ 6750; λ 308 nm, ϵ 15,600; λ 550, ϵ 92 (5)). The peak at 550 nm was usually used, and the purity of solutions was assessed by comparing the concentration obtained spectrophotometrically and the total chromium concentration.

The total chromium was determined by oxidizing all chromium species to chromate with H_2O_2 in base, boiling the solutions for 20-30 minutes to decompose excess H_2O_2 , diluting to the mark in a volumetric flask, and measuring the absorbance at λ 372 nm, ϵ = 4830 (10). When cobalt was present, a small amount of NaSCN was added to complex the cobalt and thus prevent the precipitation of cobalt(II) oxide.

The concentrations of Cr^{2+} solutions were determined by two methods as described below.

Method I For concentrations $>10^{-2}$ M, an aliquot of Cr^{2+} solution was syringed into a volumetric flask containing 15-30% excess solution of $\text{Co}(\text{NH}_3)_5\text{Br}^{2+}$ ion that was well purged with nitrogen. The Co^{2+} released was determined

spectrophotometrically as $\text{Co}(\text{NCS})_4^{2-}$ ion by adding a large excess of solid NH_4SCN and diluting to the mark with 1:1 acetone-water solution. From the absorbance at λ 623 nm, ϵ 1842, and the dilution factor, the concentration of Cr^{2+} was computed (11).

Method II For $[\text{Cr}^{2+}] < 10^{-2}$ M a more sensitive method was used. Into separate volumetric flasks identical volumes of a $\text{Co}(\text{NH}_3)_5\text{Br}^{2+}$ solution was pipetted and one of these was deaerated. An aliquot of Cr^{2+} solution was then syringed into the air-free solution, the amount corresponding to about 50% of the $\text{Co}(\text{III})$. The concentration of $\text{Co}(\text{NH}_3)_5\text{Br}^{2+}$ in each flask was determined spectrally at λ 253 nm, ϵ 16,700 (20). From the difference in $[\text{Co}(\text{NH}_3)_5\text{Br}^{2+}]$ the $[\text{Cr}^{2+}]$ was computed.

The hydrogen ion concentrations of $\text{CrCH}_2\text{C}_5\text{H}_4\text{NH}^{3+}$ solutions were determined by passing an aliquot through a short column of Dowex 50W - X8 resin in the hydrogen form. The acid liberated was titrated with standard NaOH to the bromothymol blue end point.

The specific activity of chromium samples was determined after converting to chromate with H_2O_2 and base as in the total chromium analysis. The solution was poured into a 20 ml counting vial and counted. The chromate concentration was then determined spectrally at λ 372 nm. From the count rate and concentration the specific activity, S in cpm/M , was computed.

The count rate was measured on a well-type NaI gamma ray scintillation counter with a 400 channel analyzer. A styrofoam block with a cylindrical hole the same size as the counting vials was mounted on the NaI crystal to ensure uniform counting geometry. Only those channels representing the energies around the peak in the ^{51}Cr gamma ray spectrum were tallied. Each sample was counted long enough to get at least 10^4 total counts. The background count rate was determined by counting the empty well overnight and dividing by the total time.

All spectral data for kinetic runs and analyses were obtained on a Cary 14 spectrophotometer equipped with a thermostatted cell compartment and high-intensity tungsten lamp.

Exchange kinetics

The exchange kinetic runs were carried out in a ground-glass Erlenmeyer flask fitted with a condensor (to prevent evaporation) and monitored by the following procedure. Approximately 100 ml of $\text{CrCH}_2\text{C}_5\text{H}_4\text{NH}^{3+}$ solution was placed in the reaction vessel, deaerated with nitrogen, and thermostatted at 55°C in a water bath. A small volume of radio-tagged Cr^{2+} solution was then syringed into the vessel and the timer started. Aliquots were withdrawn by syringe at various times (every 10-20 minutes) and immediately put into a volumetric flask containing a 20-30% excess of $\text{Co}(\text{NH}_3)_5\text{Br}^{2+}$

solution to oxidize the Cr^{2+} to CrBr^{2+} . The time of each point was recorded when the aliquot was syringed into the flask. The volumetric flasks were stored in an ice bath until they were analyzed. From each such solution a small sample of the $\text{CrCH}_2\text{C}_5\text{H}_4\text{NH}^{3+}$ was isolated by an ion exchange procedure similar to that used in the synthesis. The activity of $\text{CrCH}_2\text{C}_5\text{H}_4\text{NH}^{3+}$ was then determined as described above.

The activity of $\text{CrCH}_2\text{C}_5\text{H}_4\text{NH}^{3+}$ at complete exchange was determined by removing a small aliquot of reaction solution and measuring the chromium activity without the ion exchange procedure, since the activity of both chromium species should be the same when exchange equilibrium has been attained.

The concentration of Cr^{2+} was measured by Method II above at various times during each run to assure its constancy. In no run did $[\text{Cr}^{2+}]$ change by more than 15%.

The rate of exchange was determined by plotting $\ln (1-f)$ vs time according the McKay equation, (21)

$$\ln (1-f) = - R_{\text{ex}} \left(\frac{a+b}{ab} \right) t \quad (\text{II-6})$$

where f is the fraction of exchange (activity at t /activity at t_∞), R_{ex} is the exchange rate, and a and b are the concentrations of the two reactants. This equation holds for any exchange process regardless of the mechanism.

A linear least-squares computer program¹ was used to plot the data in the McKay equation. Values of activity and time were entered, and the program computed $\ln(1-f)$ values and the least-squares line of the McKay plot, along with a graphical representation of the activity vs time data and the McKay plots themselves for visual inspection. R_{ex} was calculated from the slope and the known concentrations of $\text{CrCH}_2\text{C}_5\text{H}_4\text{NH}^{3+}$ and Cr^{2+} according to equation II-6.

Chemical kinetics

The rate of formation of $\text{CrCH}_2\text{C}_5\text{H}_4\text{NH}^{3+}$ from Cr^{2+} and $\text{BrCH}_2\text{C}_5\text{H}_4\text{NH}^+$ was determined spectrophotometrically at $\lambda 308$ nm, a peak for the Cr(III) complex. A solution of $\text{BrCH}_2\text{C}_5\text{H}_4\text{NH}^+$ was placed in a quartz test tube (path length 2.3 cm) capped by a one-hole rubber stopper, deaerated, and thermostatted 55°C in the cell compartment of the spectrophotometer. A small volume of Cr^{2+} solution was then added, the solution was stirred with the nitrogen bubbling for a few seconds, and the spectrophotometer turned on to obtain a trace of absorbance vs time. All experiments were carried out air-free under pseudo-first-order conditions with either reactant in excess. In all runs $[\text{H}^+]$ was maintained at 1.0 M and the ionic strength was 1.0 M.

¹The computer program was provided by Dr. D. S. Martin.

The pseudo-first-order rate constant, k_{obs} , for each run was determined as the slope of a standard plot of $\ln(A_\infty - A_t)$ vs time according to equation I-13 (page 18). The second-order rate constant, k_o , was computed from k_{obs} and the concentration of limiting reagent. For runs in which $[Cr^{2+}]$ was limiting, $k_o = k_{obs}/2[BrCH_2C_5H_4NH^+]$, and when $[BrCH_2C_5H_4NH^+]$ was limiting, $k_o = k_{obs}/[Cr^{2+}]$. This point is discussed further in the next section and in the Appendix.

RESULTS AND DISCUSSION

Exchange Kinetics

Four experiments were done on the exchange reaction of Cr^{2+} and $\text{CrCH}_2\text{C}_5\text{H}_4\text{NH}^{3+}$; the activity vs time data for these runs are shown in Table II-1. The McKay plots for all runs are shown in Figures II-1 through II-4 and a summary of the kinetic data are shown in Table II-2.

The k_{ex} values in Table II-2 were calculated by dividing R_{ex} by the product of $[\text{Cr}^{2+}]$ and $[\text{CrCH}_2\text{C}_5\text{H}_4\text{NH}^{3+}]$. The constancy of the k_{ex} shows that equation II-7 is the rate law for the exchange reaction. The first-order dependence on



$[\text{Cr}^{2+}]$ is an important point and is further demonstrated by a plot of $R_{\text{ex}}/[\text{CrCH}_2\text{C}_5\text{H}_4\text{NH}^{3+}]$ vs $[\text{Cr}^{2+}]$ shown in Figure II-5.

Some points concerning the accuracy of these measurements should be noted. There is a great deal of scatter in the McKay plots giving rise to standard deviations of up to 12% in R_{ex} . This scatter is reflected in the error bars in Figure II-5. In addition, the McKay plot is very sensitive to the value of the activity at infinite time, S_{∞} , and this is subject to the same uncertainty as the other points in a given experiment. (The computer program treats S_{∞} as a constant and fits the other points to it.) Therefore, the

Table II-1. Specific activity (S) vs time data for exchange kinetic runs. Conditions: $[H^+] = 1.0 \text{ M}$, $\mu = 1.0 \text{ M}$, $T = 55.0^\circ$

<u>Run E1</u>		<u>Run E2</u>	
$[Cr^{2+}] = 2.7 \times 10^{-3} \text{ M}$	$[Cr^{2+}] = 4.3 \times 10^{-3} \text{ M}$	$[CrCH_2C_5H_4NH^{3+}] = 1.3 \times 10^{-3} \text{ M}$	$[CrCH_2C_5H_4NH^{3+}] = 1.0 \times 10^{-3} \text{ M}$
<u>Time/min</u>	$10^{-6} \text{ S/cpm M}^{-1}$	<u>Time/min</u>	$10^{-6} \text{ S/cpm M}^{-1}$
1.5	1.64	2	3.02
2.1	3.74	11	4.04
41.5	4.91	23	4.89
60	6.38	35	4.82
81	6.30	46	5.38
100	6.60	60	5.57
121	7.19	75	5.95
141	7.39	∞	6.75
∞	8.33		

<u>Run E3</u>		<u>Run E4</u>	
$[Cr^{2+}] = 2.3 \times 10^{-3} \text{ M}$	$[Cr^{2+}] = 9.5 \times 10^{-3} \text{ M}$	$[CrCH_2C_5H_4NH^{3+}] = 1.0 \times 10^{-3} \text{ M}$	$[CrCH_2C_5H_4NH^{3+}] = 3.05 \times 10^{-3} \text{ M}$
<u>Time/min</u>	$10^6 \text{ S/cpm M}^{-1}$	<u>Time/min</u>	$10^{-6} \text{ S/cpm M}^{-1}$
2	4.46	2	4.95
14	6.63	8.5	6.17
27	8.17	12.2	8.16
40	9.89	17.7	11.7
52	10.3	23.5	11.9
65	12.0	31.4	13.6
76.5	11.0	44.0	14.1
96	15.6	∞	16.2
∞	21.2		

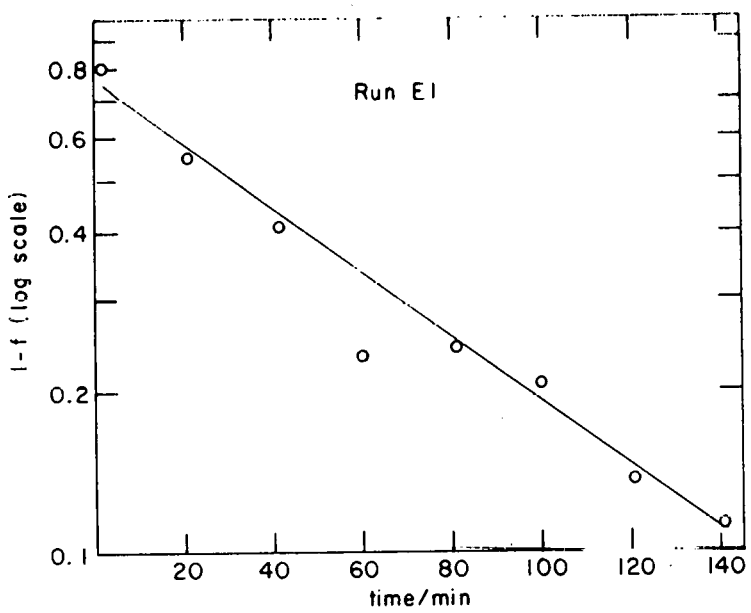


Figure II-1. McKay plot for Run E1

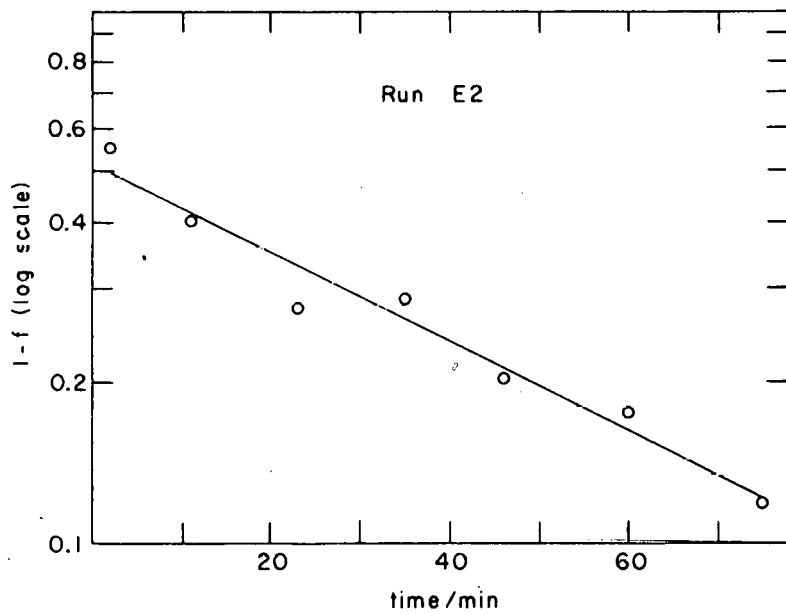


Figure II-2. McKay plot for Run E2

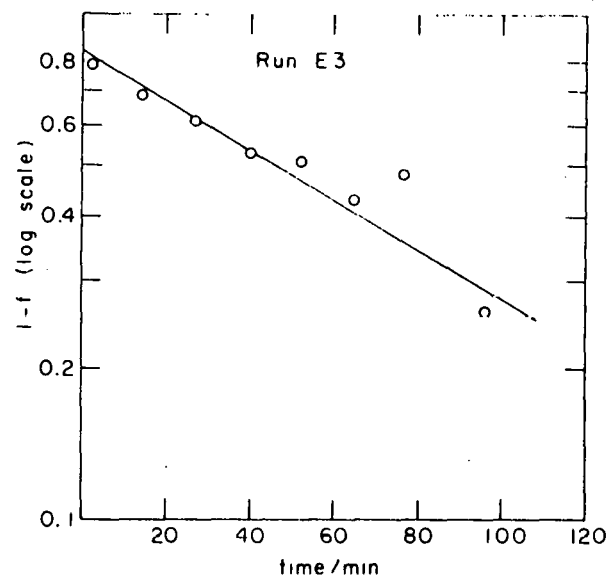


Figure II-3. McKay plot for Run E3

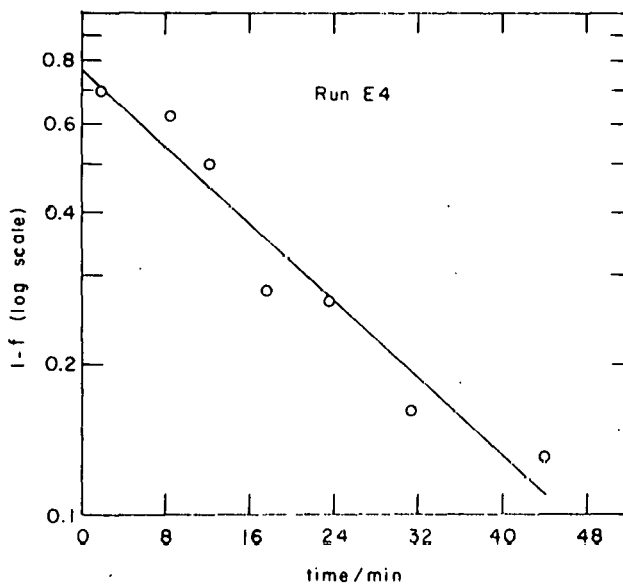


Figure II-4. McKay Plot for Run E4

Table II-2. Summary of results for exchange kinetic runs.
 Conditions: $[H^+] = 1.0 \text{ M}$, $\mu = 1.0 \text{ M}$, $T = 55.0^\circ$

Expt	$10^3 [Cr^{2+}] / M$	$10^3 [CrCH_2C_5H_4NH^{3+}] / M$	$10^7 R_{ex} / M s^{-1} \pm \delta^a$	$10^2 k_{ex} / M^{-1}s^{-1} \pm \delta^a$
E1	2.7	1.3	2.0 ± 0.1	5.7 ± 0.2
E2	4.3	1.0	2.6 ± 0.2	6.0 ± 0.5
E3	2.3	1.0	1.3 ± 0.1	5.7 ± 0.7
E4	9.5	3.05	17 ± 2	5.9 ± 0.7
			av k_{ex}	5.8 ± 0.5

^a δ = standard deviation determined from that of slope of the McKay plots.

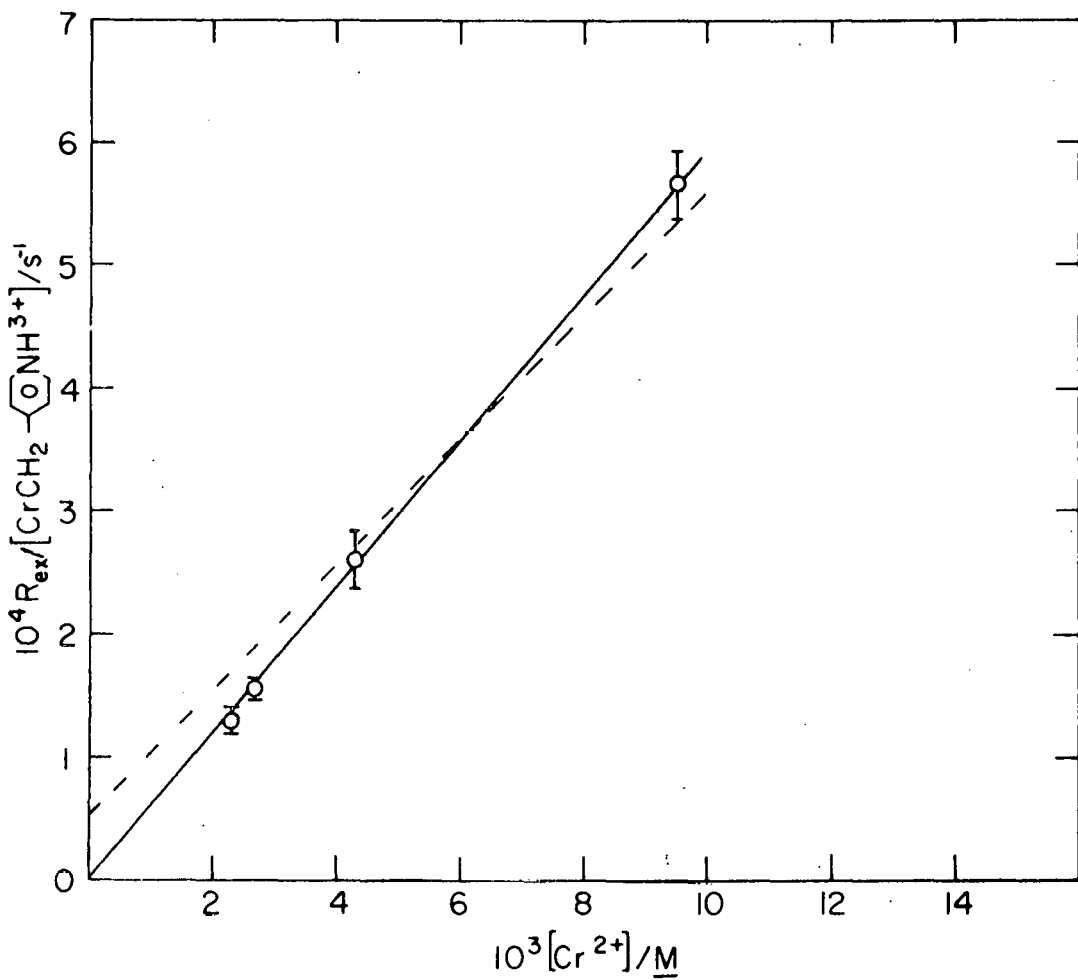


Figure II-5. Plot of $R_{ex} / [\text{CrCH}_2\text{C}_5\text{H}_4\text{NH}^{3+}]$ vs $[\text{Cr}^{2+}]$ for exchange kinetic runs

standard deviation of the slopes in the McKay plots do not reflect the absolute error inherent in these measurements, so that the constancy of k_{ex} in Table II-2 and the linearity of the graph in Figure II-5 are perhaps misleading. The importance of this point will become apparent in later discussion.

The intercepts at zero-time in the McKay plots imply that a significant amount of exchange occurs at the time of mixing. Ideally, these intercepts should be unity on the semi-log plots in Figures II-1 to II-4; the values for experiments E1-E4 are 0.78, 0.52, 0.83, and 0.78, respectively. There are two possible explanations for this observation: (a) an equilibrium such as in equation II-2 might be shifted rapidly to the left as Cr^{2+} is added thus carrying Cr-51 into the complex at the time of mixing, or (b) some exchange is induced by the separation technique employed. To test the former possibility, experiment E4 was done by adding the Cr^{2+} in two stages; about 75% was added untagged and allowed to equilibrate for several minutes, and 25% was added later as tagged Cr^{2+} . The zero-time intercept for this experiment is not significantly different from the others, so possibility (a) above is ruled out. The nonunity intercepts of the McKay plots are therefore ascribed to separation-induced exchange. This seems to be a common problem in radiotracer kinetics (21), and considering the scatter in the data such behavior is not surprising.

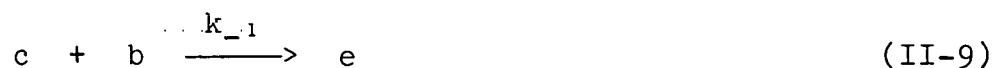
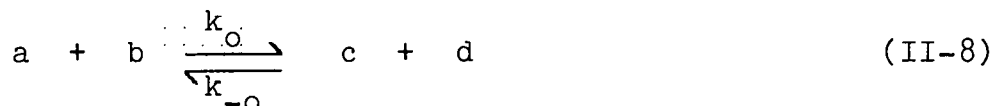
Attempts were made to do more kinetic runs at lower $[Cr^{2+}]$ ($< 10^{-3} \text{ M}$) but failed owing to the apparent oxidation of Cr^{2+} at low concentration under these conditions. Chloride ion was found in solutions containing $10^{-3} \text{ M} Cr^{2+}$ and $1.0 \text{ M} HClO_4$ at 55°C , so it is assumed that ClO_4^- ion is the oxidant.

The rate law in equation II-7 is contrary to that suggested by equation II-2. Instead of being independent of $[Cr^{2+}]$, the exchange is first-order in this reactant and this implies a bimolecular pathway for exchange. If the unimolecular pathway implied by equation II-2 were operative as well, Figure II-5 would show a positive intercept corresponding to the amount of reaction occurring by the unimolecular path. The dashed line in Figure II-5 shows the expected intercept if Swaddle's k_1 value of $5.2 \times 10^{-5} \text{ s}^{-1}$ were correct. The zero intercept would suggest, then, that the unimolecular path does not occur or that the proposed value of k_1 is too large. However, considering the possible errors associated with the four points as discussed earlier, a positive intercept of the magnitude corresponding to the published value of k_1 and therefore the unimolecular path cannot be ruled out unequivocally. The main importance of the present result is that there exists a more efficient pathway for exchange, a bimolecular substitution process.

Chemical Kinetics

Eleven kinetic runs were carried out on the formation of $\text{CrCH}_2\text{C}_5\text{H}_4\text{NH}^{3+}$ from $\text{BrCH}_2\text{C}_5\text{H}_4\text{NH}^+$ and Cr^{2+} (equation II-1). Typical pseudo-first-order rate plots are shown in Figure II-6 for Runs 3 and 10. For all experiments, these plots were linear to at least 3 half-lives. The results of the eleven experiments are shown in Table II-3, which shows the k_o values computed as described in the Experimental section (also see Appendix). The agreement of the second-order rate constant as the reactant concentrations are varied over a wide range and with either reagent in excess confirms the rate law shown in equation II-5 which is consistent with the assumed mechanism (equations II-3 and II-4). The average values of k_o from Table II-3 are 16.9 ± 0.7 and $12.9 \pm 0.6 \text{ M}^{-1} \text{ s}^{-1}$ for 1.0 M and 0.1 M H^+ , respectively.

From the rate data above, it is possible to compute a lower limit on the value of k_{-1} for equation II-4. The assumed mechanism in equations II-3 and II-4 can be rewritten schematically as follows:



where the symbols a, b, etc., represent the species as they appear in equations II-3 and II-4. The procedure involves

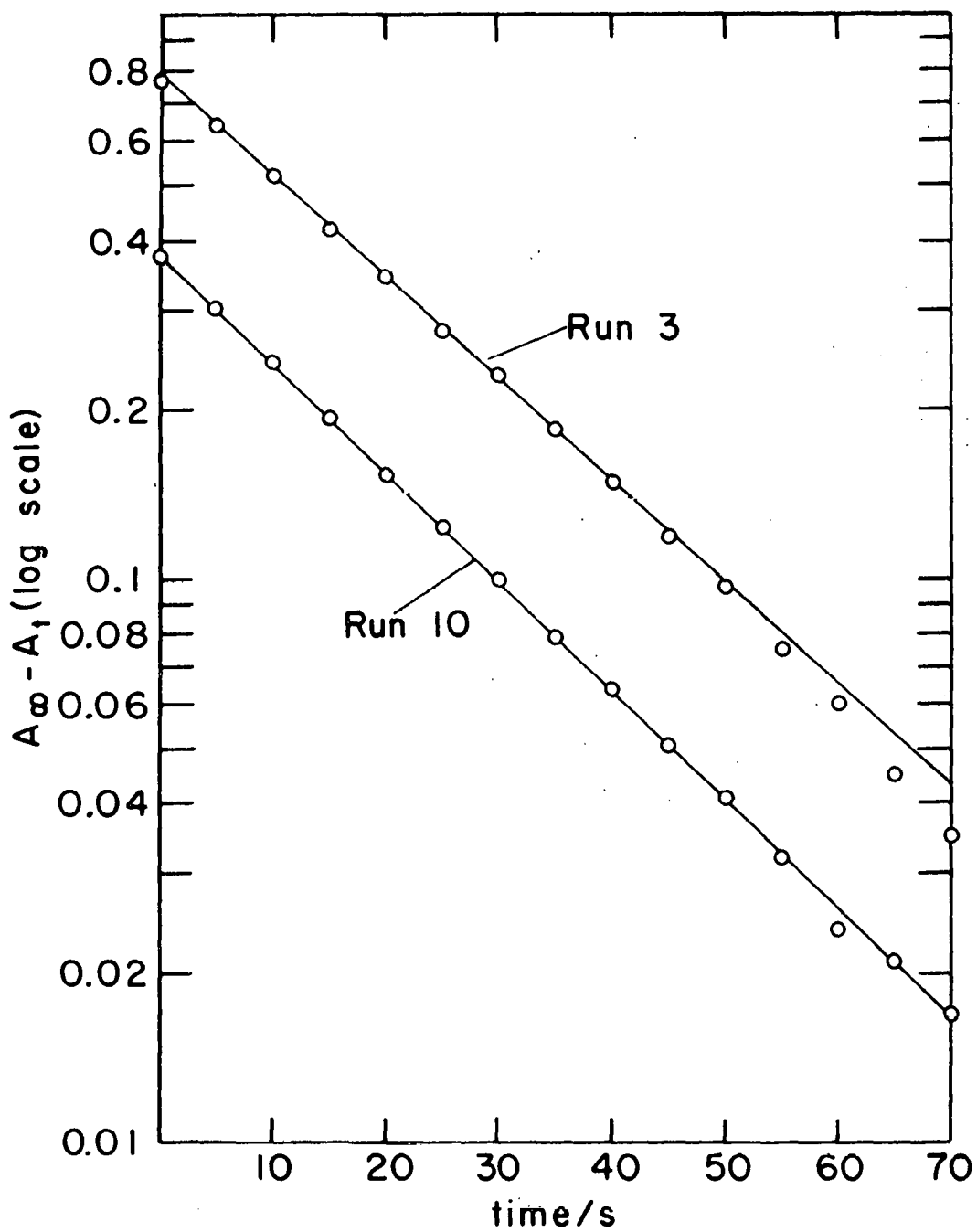


Figure II-6. First-order rate plots for the formation of $\text{CrCH}_2\text{C}_5\text{H}_4\text{NH}^{3+}$

Table II-3. Kinetic data for the reaction of Cr^{2+} and $\text{BrCH}_2\text{C}_5\text{H}_4\text{NH}^+$. Conditions: $[\text{H}^+] = 1.0 \text{ M}$, $\mu = 1.0 \text{ M}$, $T = 55.0^\circ$, $\lambda = 308 \text{ nm}$

Run	$10^4 [\text{BrCH}_2\text{C}_6\text{H}_4\text{NH}^+]/\text{M}$	$10^4 [\text{Cr}^{2+}]/\text{M}$	$k_o/\text{M}^{-1}\text{s}^{-1}$	$10^2 k_{\text{obs}}/\text{s}^{-1}$
1	15.5	0.6	16.9	5.23
2	15.7	0.5	18.7	5.86
3	12.5	0.9	16.2	4.06
4	13.4	0.3	16.9	4.54
5	6.84	0.6	18.1	2.48
6	0.15	11.7	16.9	1.98
7	0.15	21.8	16.1	3.52
8	0.13	49.8	15.6	6.21
9 ^a	11.6	0.7	12.8 ^a	2.96
10 ^a	0.16	15.3	13.8 ^a	2.11
11 ^a	0.14	36.9	12.0 ^a	4.42

^a $[\text{H}^+] = 0.10 \text{ M}$, $\mu = 0.10 \text{ M}$.

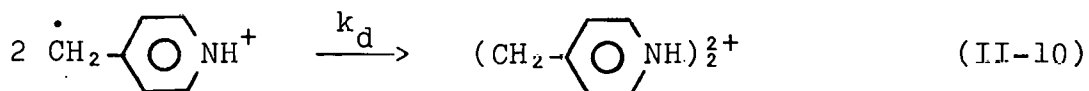
solving the differential equations for this scheme numerically, without using the steady-state assumption for $[c]$ ($[\text{CH}_2\text{C}_5\text{H}_4\text{NH}^+]$). This was done by a computer program which employed the Runge-Kutta method.¹ The input for the program were initial concentrations of a and b and values of k_o , k_{-o} , and k_{-1} , and the output consisted of the concentrations of all species, a through e , at various times during the run. From the concentrations of $e([\text{CrCH}_2\text{C}_5\text{H}_4\text{NH}^{3+}])$ obtained in this way, a first-order kinetic plot was constructed, and the rate constant was computed for comparison with that observed experimentally for the run. This computation was carried out using the known value of k_o , an arbitrarily low value for k_{-o} (since the back reaction is assumed to be unimportant), and varying values of k_{-1} . The point of this is to see for what values of k_{-1} the calculated rate plot varies from that observed experimentally for the particular run.

By applying this method to several of the runs in Table II-3, it was found that when the entered value of k_{-1} exceeds $10^3 \text{ M}^{-1}\text{s}^{-1}$, the first-order plots are linear and the calculated rate constants agree well with those observed, but when k_{-1} is lower than this value, the rate plots are

¹The computer program was devised by O. J. Parker and modified by J. H. Espenson.

curved, indicating that these low k_{-1} values are inconsistent with the observed kinetics. Therefore, based on the observed value of k_o and the fact that clean first-order behavior is observed for the reaction, a lower limit on k_{-1} can be set of $10^3 \text{ M}^{-1}\text{s}^{-1}$. This varies considerably from the value of Schmidt and Swaddle for k_{-1} of $10^{-2} \text{ M}^{-1}\text{s}^{-1}$ (17).

Another way to set a lower limit on k_{-1} from the data in Table II-3 is suggested by the fact that the same value of k_o is obtained whether $\text{BrCH}_2\text{C}_5\text{H}_4\text{NH}^+$ or Cr^{2+} is the limiting reagent. Another possible reaction for the organic radical, $\cdot\text{CH}_2\text{C}_5\text{H}_4\text{NH}^+$ in equation II-1 and II-4 (c in equations II-8 and II-9) is dimerization as in the following:



This reaction is expected to be rapid based on high dimerization rate constants, k_d , of many other organic radicals, (10^6 - 10^9) (22). If such a reaction were competitive with equation II-4 such that significant amounts of organic radical went on to dimerize instead of reacting with Cr^{2+} , then the observed value of k_o should be lower for runs in which Cr^{2+} is the limiting reagent (see Appendix); that is, less than 2 moles of Cr^{2+} would be consumed per mole of $\text{BrCH}_2\text{C}_5\text{H}_4\text{NH}^+$, and the observed value of k_o would then be lower than the true value and would vary with $[\text{Cr}^{2+}]$. The value of k_o measured when Cr^{2+} is in large excess can be

considered the true value (that is, unaffected by the possible occurrence of the dimerization process) since in that case the fate of the organic radical makes no difference to the observed k_o value. This argument is explained further in the Appendix.

The values of k_o given in Table II-3 exhibit no systematic trend at low $[Cr^{2+}]$, the observed k_o being the same regardless of whether Cr^{2+} or $BrCH_2C_5H_4NH^+$ is the limiting reagent. This implies that the radical intermediate, $\dot{CH}_2C_5H_4NH^+$, reacts exclusively to form $CrCH_2C_5H_4NH^{3+}$ and no dimer is formed. Using this fact and a value of the dimerization rate constant, k_d , estimated as $10^9 \text{ M}^{-1}\text{s}^{-1}$ from the k_d values for similar organic radicals (22), a lower limit of k_{-1} can be set.

The procedure for this computation is described in the Appendix. From the value of k_{obs} from Run 3 and the value of k_o from Run 6, the percentage of $\dot{CH}_2C_5H_4NH^+$ that dimerizes, was calculated to be 8%; this is the maximum amount, optimistically estimated, of dimerization that can be accommodated by the data in Table II-3. From this value the lower limit on k_{-1} is $2 \times 10^6 \text{ M}^{-1}\text{s}^{-1}$. This lower limit is larger than the value of $10^3 \text{ M}^{-1}\text{s}^{-1}$ obtained from the procedure described earlier and is much larger than the value of $10^{-2} \text{ M}^{-1}\text{s}^{-1}$ estimated by Schmidt and Swaddle. The lower limit on k_{-1} of $2 \times 10^6 \text{ M}^{-1}\text{s}^{-1}$ is consistent with studies

for similar reactions of Cr^{2+} with organic radicals done by Cohen and Meyerstein (18), who studied the kinetics of these reactions directly using radicals generated by pulse radiolysis and found second-order rate constants in the range 10^6 - 10^8 $\text{M}^{-1}\text{s}^{-1}$.

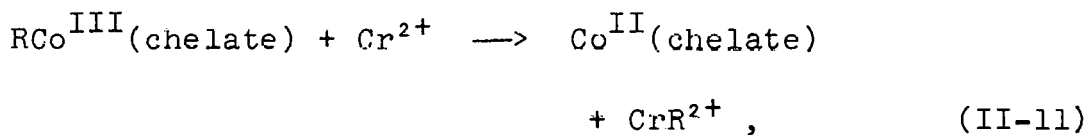
It is concluded, from the kinetic results on the reaction of Cr^{2+} and $\text{BrCH}_2\text{C}_5\text{H}_4\text{NH}^+$ and from the work of Cohen and Meyerstein (18) on the direct reaction of Cr^{2+} and organic radicals, that the values of 10^{-2} $\text{M}^{-1}\text{s}^{-1}$ for k_1 in equation II-2 proposed by Schmidt and Swaddle is incorrect by at least a factor of 10^8 . In addition to the discrepancies between these results and those of Schmidt and Swaddle, there are some severe internal inconsistencies in their results.

The present results also show that little if any of the exchange between Cr^{2+} and $\text{CrCH}_2\text{C}_5\text{H}_4\text{NH}^{3+}$ occurs by a unimolecular pathway. The reported value for k_1 in equation II-2 of $5.2 \times 10^{-5} \text{ s}^{-1}$ proposed by the other workers is not necessarily too large, however, since the homolysis is evidently supplemented as a major pathway for chromium exchange by a bimolecular mechanism which clearly involves a different and unrelated reaction. Thus we are unable, from the exchange experiments, to confirm or refute the value for k_1 .

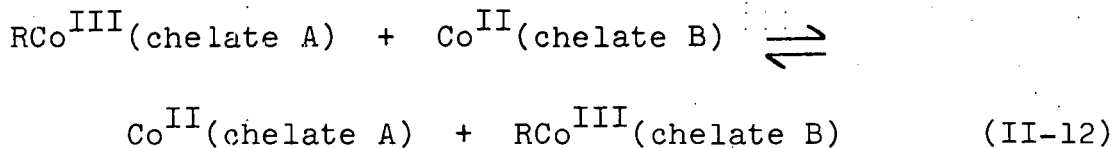
The question of whether homolytic scission of the Cr-C bond (equation II-2) is involved in the decomposition of

$\text{CrCH}_2\text{C}_5\text{H}_4\text{NH}^{3+}$ remains open. The results of Coombes and Johnson (16), that the organic products of the reaction are those derived from a radical precursor and that the kinetic behavior of the reaction depends on the presence or absence of oxygen, indicate that some homolytic process occurs. This is consistent with the results of other studies (23,24) on reactions of the analogous benzylchromium(III) cation, $\text{CrCH}_2\text{C}_6\text{H}_5^{2+}$. In particular, the results of Nohr and Espenson (24) on the oxidation of $\text{CrCH}_2\text{C}_6\text{H}_5^{2+}$ by a variety of oxidants show conclusively that a unimolecular homolysis of the Cr-C bond does occur in this compound. If such a reaction as equation II-2 occurs in the decomposition of $\text{CrCH}_2\text{C}_5\text{H}_4\text{NH}^{3+}$, then k_1 is probably smaller than $5.2 \times 10^{-5} \text{ s}^{-1}$ and k_{-1} is certainly much larger than $10^{-2} \text{ M}^{-1}\text{s}^{-1}$ and indeed must be greater than 10^6 based on the present results.

The finding that the exchange between Cr^{2+} and $\text{CrCH}_2\text{C}_5\text{H}_4\text{NH}^{3+}$ is predominantly a bimolecular rather than a unimolecular process is an important result. Examples of such a radical transfer process, though rare, are found in the reactions of alkylcobalt(III) complexes with Cr^{2+} (25-27), as shown below,



and with Co(II) derivatives (28, 29),



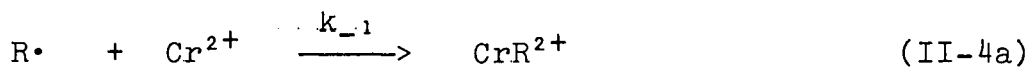
The mechanism can be described in three possible ways:

(a) outer-sphere electron transfer with concurrent or subsequent transfer of the alkyl radical, (b) inner-sphere electron transfer via an electron-deficient, saturated carbon bridge, and (c) homolytic substitution at the saturated carbon, or an $S_{\text{H}}2$ mechanism (30). Recent studies on the reactions in equation II-11 (27) and equation II-12 (29) indicate that possibility (a) is not operative in these cases. Since the present reaction is quite similar to those above, it is unlikely that the outer-sphere electron transfer process is operative in this case. The inner-sphere, group transfer mechanism, (b), is analogous to those well-known for many inorganic redox reactions (15, ch. 6). The difference between the present case and those involving other bridging ligands (e.g., Cl^- or SCN^-) is that the saturated carbon has no lone pair to coordinate with the incoming group so that the precursor complex for alkyl transfer is electron-deficient. The $S_{\text{H}}2$ mechanism, (c), is one that has never been conclusively demonstrated for a substrate involving a saturated carbon (30), but has been claimed for reactions

II-11 and II-12. Actually, inner-sphere group transfer and bimolecular homolytic substitution are two names for the same mechanism, and both could be used to describe the exchange between $\text{CrCH}_2\text{C}_5\text{H}_4\text{NH}^{3+}$ and Cr^{2+} .

APPENDIX

The mechanism for the reaction of $\text{BrCH}_2\text{C}_5\text{H}_4\text{NH}^+$ and Cr^{2+} is restated below in abbreviated form from equations II-3 and II-4



The rate law for this mechanism is

$$\text{Rate} = - \frac{d[\text{RBr}]}{dt} = - \frac{1}{2} \frac{d[\text{Cr}^{2+}]}{dt} = k_o [\text{RBr}][\text{Cr}^{2+}] \quad (\text{II-13})$$

so that for runs in which RBr is the limiting reagent, the first-order rate constant, k_{obs} , is $k_o [\text{Cr}^{2+}]$ whereas when $[\text{Cr}^{2+}]$ is limiting, k_{obs} is $2k_o [\text{RBr}]$.

If we allow for the dimerization of R^{\cdot} , the following step (abbreviated from equation II-10) is added to the above



mechanism. When RBr is the limiting reagent, the expression for $d[\text{RBr}]/dt$ is again given by equation II-13 since the further reactions of R^{\cdot} does not affect the rate of consumption of RBr. When Cr^{2+} is the limiting reagent, however, the expression for $d[\text{Cr}^{2+}]/dt$ changes to

$$-\frac{d[\text{Cr}^{2+}]}{dt} = k_o [\text{Cr}^{2+}][\text{RBr}] \left\{ 1 + \frac{k_{-1}[\text{Cr}^{2+}]}{k_{-1}[\text{Cr}^{2+}] + k_d[\text{R}^{\cdot}]} \right\} \quad (\text{II-14})$$

Therefore, the k_{obs} should be less than $2 k_o [RBr]$, depending upon how much reaction II-10 occurs.

We define a term α as the percentage of $R\cdot$ that reacts to form dimer,

$$\alpha = \frac{k_d[R\cdot]}{k_{-1}[Cr^{2+}] + k_d[R\cdot]} \quad (II-15)$$

Rearranging gives

$$k_d[R\cdot] = \frac{\alpha}{1 - \alpha} k_{-1}[Cr^{2+}] \quad (II-16)$$

and so the expression for k_{obs} for equation II-14 becomes

$$k_{obs} = (2 - \alpha) k_o [RBr] \quad (II-17)$$

To obtain the highest possible value of α that could be accommodated by the data in Table II-3, we chose the run with limiting $[RBr]$ with the highest value of k_o , Run 6, $k_o = 16.9 \text{ M}^{-1}\text{s}^{-1}$; and we chose the run with limiting $[Cr^{2+}]$ with the lowest value of $k_{obs}/[RBr]$, Run 3, $k_{obs} = 4.06 \times 10^{-2} \text{ s}^{-1}$. Substituting these values into equation II-17 using $[RBr] = 1.25 \times 10^{-3} \text{ M}$ from Run 3, we get a value for α of 0.08 or 8%.

To obtain the lower limit on k_{-1} , we use equation II-15 (dropping the term $k_d[R\cdot]$ from the denominator since α is small) and the steady-state concentration of $R\cdot$,

$$[R\cdot]_{ss} = \frac{k_o}{k_{-1}} [RBr] \quad (II-18)$$

Combining II-15 and II-18 and rearranging gives

$$k_{-1} = \left(\frac{k_o k_d [RBr]}{\alpha [Cr^{2+}]_{av}} \right)^{\frac{1}{2}} \quad (II-19)$$

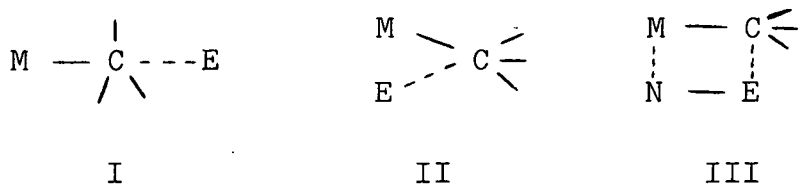
Using the following values: $k_o = 16.9 \text{ M}^{-1}\text{s}^{-1}$, $k_d = 10^9 \text{ M}^{-1}\text{s}^{-1}$ (see text), $[RBr] = 1.25 \times 10^{-3} \text{ M}$, $\alpha = 0.08$, and $[Cr^{2+}] = 4.5 \times 10^{-6} \text{ M}$ (the average $[Cr^{2+}]$ in Run 3), equation II-19 gives a lower limit on k_{-1} of $2 \times 10^6 \text{ M}^{-1}\text{s}^{-1}$.

PART III. REACTIONS OF SIGMA-BONDED ORGANOCHROMIUM(III)
COMPLEXES WITH MERCURY(II) ELECTROPHILES

INTRODUCTION

In the previous two projects it was found that the alkyl group in the organochromium complex is transferred homolytically from one chromium to another. It is also known that the chromium-carbon bond can be cleaved heterolytically resulting in the transfer of a carbanion from chromium to another atom. These are said to be electrophilic reactions and the atom to which the carbon is transferred is called an electrophile. The detailed mechanism of electrophilic attack on saturated carbon has been of considerable interest for many years, and the subject has been discussed in great detail by Abraham (31) and by Jensen and Rickborn (32).

Three basic mechanisms have been observed for electrophilic reactions, denoted $S_E 1$, $S_E 2$ (open), and $S_E 2$ (cyclic). The $S_E 1$ mechanism is simple unimolecular dissociation of the M-C bond (where M is a metal or other electropositive atom attached to the carbon undergoing substitution) producing a carbanion which reacts with the electrophile. The $S_E 2$ (open) mechanism is a bimolecular reaction with a two-centered or open transition state in which the electrophile, E, attacks directly at the carbon as shown in I and II below. Finally, the $S_E 2$ (cyclic) mechanism is a bimolecular reaction involving the four-centered or cyclic transition state III where a group, N, attached to the electrophile assists in cleaving the M-C bond by coordinating to M.



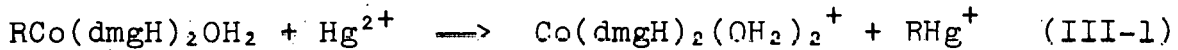
The basic features of electrophilic reactions that are of interest are (a) the electronic effects resulting from attaching electron-withdrawing groups to the carbon atom undergoing substitution; (b) the effects of increasing the steric bulk of groups on the reacting carbon atoms; and (c) the stereochemistry at the reacting carbon. These features are interrelated and are important in elucidating the mechanism of electrophilic cleavage of M-C bonds, particularly with regard to which of the above transition states is operative in a given reaction. The direction and magnitude of the electronic effect (as determined quantitatively by a linear free energy relationship) may indicate whether a cyclic or open transition state is operative in the mechanism; or the sensitivity of the reaction to steric effects may shed light on whether retention or inversion occurs, by correlating the mode of reaction with observed rate trends for a series of alkyl groups.

There are many studies reported in the literature on reactions of organometallic compounds with Hg(II) and other electrophiles. The work reported before 1973 is discussed by Abraham (31) and by Jensen and Rickborn (32). The vast

majority of these studies have concerned substrates containing nontransition metals (31) (e.g., R_2Zn , R_3Tl , and R_4Sn) or complexes of transition metals in low oxidation states stabilized by electron-denoting ligands (e.g., $RAu[P(C_6H_5)_3]$ (31) and $\eta^5-C_5H_5Fe(CO)_2R$ (33)). A particularly large amount of work has been done on R_2Hg and $RHgX$ substrates using a variety of electrophiles (e.g., H^+ , X_2 , and $Hg(II)$ species) in different media (32).

Electrophilic reactions involving transition metal complexes where the metal is in a high oxidation state have been studied only recently with a large amount of work being done on macrocyclic complexes of $Co(III)$ (34-42) including alkylcobalamins (43).

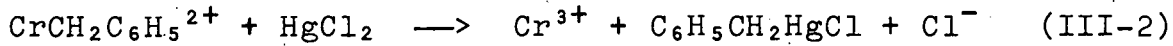
Of particular interest to this work are the studies in references 34 and 35 on the reactions of mercury(II) ion with alkylcobaloximes, $RCo(dmgh)_2H_2O$, in aqueous acid, as shown below. The relevant results of these studies are as follows:



(a) the first-order dependence on both Hg^{2+} and on $RCo(dmgh)_2H_2O$ and the trend in second-order rate constants with varying R group show that an S_E^2 (open) mechanism is operative; (b) a profound decrease in reactivity of $RCo(dmgh)_2H_2O$ was observed when an electron-withdrawing substituent, CF_3 , was attached to R; (c) for the reactions

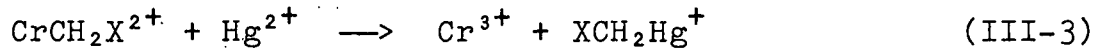
where $R = p\text{-CH}_2\text{C}_6\text{H}_4\text{Z}$, the variation in rate with Z gave a Hammett ρ value of -1.2, typical of the S_E^2 (open) mechanism. (an even more profound effect was observed for $R = p\text{-C}_6\text{H}_5\text{Z}$ where ρ was found to be -6.3); (d) finally, no evidence was found for the formation of R_2Hg , presumably owing to the lower electrophilicity of RHg^+ , the product of the first step. In a stereochemical determination, Fritz, et al. (36) also established that the reaction of Hg^{2+} with $\text{RCO}(\text{dmgh})_2\text{OH}_2$, $R = \text{CH}_2\text{CH}_2\text{C}(\text{CH}_3)_3$, proceeds with inversion of configuration at the α -carbon atom, using an nmr method. Tada and Ogawa (37) also found inversion in the reaction of Hg^{2+} with $\text{RCO}(\text{dmgh})_2\text{OH}_2$ ($R = \text{cis-}$ and trans-4-tert-butylcyclohexyl), by the change from cis to trans in reactant to RHg(II) product.

Organochromium complexes have been known to react with mercury(II) electrophiles since the first example of the former was synthesized in the late 1950's. Anet and LeBlanc (1) found that benzylmercuric chloride was produced on reaction of $\text{CrCH}_2\text{C}_6\text{H}_5^{2+}$ with HgCl_2 :

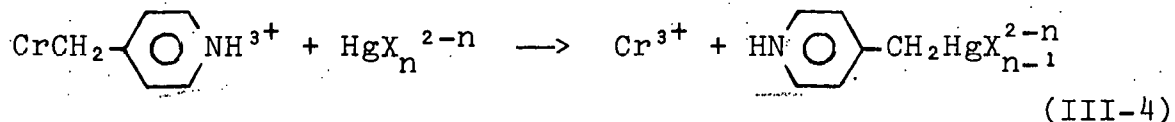


This reaction was used as evidence for the identity of the organochromium species. Later Dodd and Johnson (3) found that monochloro- and monobromomethylchromium ions react with mercuric nitrate to produce the corresponding organo-mercurials and hexaquochromium(III) ion (equation III-3);

CrCH_2I and $\text{CrCH}_2\text{X}^{2+}$, on the other hand, were found to react differently, producing some Hg_2^{2+} . The latter class of reaction is excluded from those considered here.



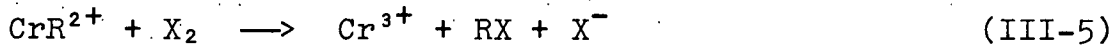
Other workers (44-46) carried out a detailed kinetic study on the reactions of 2-, 3-, and 4-pyridinomethyl-chromium ions with chloro- and bromo-complexes of mercury(II) and thallium(III) (i.e., HgX_n^{2-n} and TiX_n^{3-n} where $n = 0-4$) in aqueous acid solution;



The relevant findings of these studies are as follows: (a) the reactions are all first-order in organochromium species and in electrophile and independent of hydrogen ion concentration, consistent with the $S_E 2$ mechanism; (b) the reactivity of the electrophile decreases as n increases or as the electrophilicity decreases; (c) a cyclic mechanism was ruled out by the absence of significant amounts of halochromium products; (d) the reactivity of the organochromium decreases as the pyridinium nitrogen gets closer to the reaction site (i.e., 4 > 3 > 2) indicating that greater positive charge on the reacting carbon retards the reaction; (e) mercury-carbon bond-making is the important rate process in the transition

state, and not chromium-carbon bond-breaking. All these results indicate that electrophilic cleavage of the pyridino-methylchromium(III) complex by Hg(II) and Tl(III) proceeds by an S_E^2 (open) mechanism.

Other studies involving electrophilic attack on alkyl-chromium(III) complexes were done by Espenson and Williams (47) and Chang and Espenson (48) on the electrophilic halogenation of a series of CrR^{2+} complexes using Br_2 and I_2 ,



The important results of these studies were as follows:

(a) the reactions were all first-order in both dihalogen and organochromium, ruling out an S_E^1 mechanism; (b) a profound electronic effect was observed in which a halogen atom attached to the reacting carbon ($\text{R} = \text{CH}_2\text{X}$) decreased the rate tremendously; (c) as shown in equation III-5 above, the products of the reaction do not include CrX^{2+} complexes, ruling out an S_E^2 (cyclic) mechanism; (d) the Hammett ρ values for the reactions of para-substituted benzylchromium(III) ions with Br_2 and I_2 were found to be -0.82 and -1.29, respectively, typical of an S_E^2 (open) mechanism. A more detailed consideration of these aspects will appear in the Discussion section in comparison to the results of the present work.

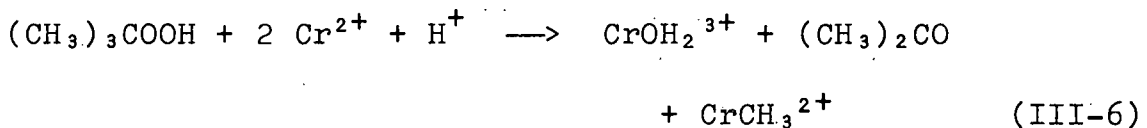
In this project, the reactions of a series of organo-chromium complexes with Hg^{2+} and CH_3Hg^+ have been studied. The substrates investigated were CrR^{2+} species in which $R = CH_3, CH_2CH_3, CH_2CH_2CH_3, CH_2C(CH_3)_3, CH(CH_3)_2, CH_2Cl, CH_2Br$, and CF_3 . Also included in the series were five para-substituted benzylchromium(III) ions, $CrCH_2C_6H_5Z^{2+}$, where $Z = H, Me, Br, CF_3$, and CN . The rates of most of the reactions have been measured to determine the values of rate constants for the different substituents R . A Hammett correlation has been carried out on the benzylchromium(III) series. In a few cases, the rates of reaction have been measured as a function of temperature in order to compute activation parameters. In the course of the work, three new CrR^{2+} complexes have been synthesized, in which $R = CH(CH_3)_2, CH(CH_3)CH_2CH_3$, and $C(CH_3)_3$.

EXPERIMENTAL

Materials

Aliphatic alkylchromium(III) complexes

All the CrR^{2+} complexes where R is of the form $\text{C}_n\text{H}_{2n+1}$ were synthesized by the method devised by Ardon *et al.* (49) and by Schmidt *et al.* (50) for the preparation of CrCH_3^{2+} wherein tert-butylhydroperoxide reacts with Cr^{2+} ,



The detailed procedure used in this work for the preparation of CrCH_3^{2+} is as follows: A 50 ml aqueous solution 0.01 M in H^+ was purged with nitrogen and cooled to 0° , and 1.0 mmole of $(\text{CH}_3)_3\text{COOH}$ (0.1 ml of 6.1 M) was added. To this was added 3.2 mmoles of Cr^{2+} (8.0 ml of 0.4 M in 0.05 M H^+). The reaction was complete in seconds, giving a dirty brown solution, and the excess Cr^{2+} was oxidized with oxygen. The reaction solution was placed on a column of Dowex 50W-X8 cation exchange resin (15 x 1 cm, 100-200 mesh) in the lithium ion form that had been cooled to 0° . The reaction solution and eluent solutions were forced through the column with about 1 psi of nitrogen pressure. The column was washed with about 50 ml of cold H_2O and the yellow product was eluted with 0.5 M LiClO_4 leaving the blue Cr^{3+} and green $(\text{CrOH})_2^{4+}$ on the column.

The other aliphatic CrR^{2+} complexes were prepared by analogous procedures, several of which were previously used by Espenson and Williams (47, 51), but conditions were not optimally adjusted. In this work, a 2.5 to 3-fold molar excess of Cr^{2+} over hydroperoxide, $\text{RC}(\text{CH}_3)_2\text{OOH}$, was used in each case, and the conditions for the syntheses and ion exchange purifications were essentially the same as those for CrCH_3^{2+} , with exceptions as noted below. In most cases, including that of CrCH_3^{2+} , the procedures typically yielded 50 ml of 3×10^{-3} M CrR^{2+} . These solutions were kept at 0° or -10° and were used within 8 hours of preparation.

For ethylchromium(III) and *n*-propylchromium(III) cations, some chromium(VI) was detected in the eluate from the ion exchange column. The origin of this contaminant was not investigated, but it is presumably a side product of the synthetic reaction. It was removed by simply washing the ion exchange column with a larger volume of H_2O (200 ml) before elution of the CrR^{2+} species with 0.5 M LiClO_4 .

The secondary alkyl complexes, isopropyl- and sec-butyl-chromium(III) cations, were found to be mildly oxygen-sensitive. In the case of the isopropyl complex, $\text{CrCH}(\text{CH}_3)_2^{2+}$, the rate of hydrolysis was about ten times faster in the presence of air than when air was excluded. (This point is discussed further in the Results section.) The reaction solutions for the preparations of these two compounds were

therefore purged with nitrogen after the O_2 -oxidation of excess Cr^{2+} , and the ion exchange columns were kept air-free by pre-washing with air-free H_2O and by purging the eluent solutions with nitrogen.

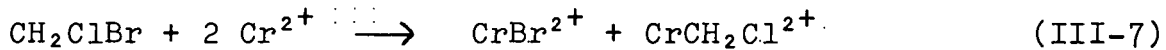
Neopentylchromium(III) ion, $CrCH_2C(CH_3)_3^{2+}$, was found to decompose too readily to allow ion exchange purification as in the other CrR^{2+} complexes.¹ Therefore, the crude reaction solutions were used in all kinetics experiments under the assumption that Cr^{3+} , $Cr_2O_4^{4+}$, and the organic by-products were innocuous in the reactions studied. This point was shown independently as described in the Results section. Small amounts of crude $CrCH_2C(CH_3)_3^{2+}$ were prepared by placing a few drops of the hydroperoxide into about 15 ml of air-free 0.01 M $HClO_4$ at 0° and then adding 0.25 to 1.0 mmoles of Cr^{2+} solution. The excess Cr^{2+} was oxidized as before and the dirty-green solutions were used immediately.

The tert-butylchromium(III) cation, $CrC(CH_3)_3^{2+}$, was made in the same way as $CrCH_3^{2+}$. No ion exchange purification of this complex was attempted, although there is no reason that such a procedure should not work.

¹This result is contrary to those of Williams (51) who found that $CrCH_2C(CH_3)_3^{2+}$ could be purified by ion exchange.

Haloalkylchromium(III) complexes

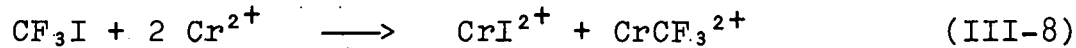
Chloromethylchromium(III), $\text{CrCH}_2\text{Cl}^{2+}$, cation was prepared in a two-phase reaction of Cr^{2+} with excess CH_2ClBr according to



A volumetric flask containing 50 ml of 0.01 M HClO_4 and 10 ml of CH_2ClBr was purged with nitrogen and 10 ml of 0.5 M Cr^{2+} was added. This heterogeneous mixture was stirred under nitrogen for one hour at room temperature. The unreacted CH_2ClBr was discarded, and approximately 10 ml of the aqueous layer was placed on a column of Dowex 50W-X8 cation exchange resin (10 x 1 cm, 100-200 mesh) in the hydrogen ion form. The green CrBr^{2+} was eluted with 0.5 M HClO_4 , and the red $\text{CrCH}_2\text{Cl}^{2+}$ was eluted and collected with 1.0 M HClO_4 . Typically, 50 ml of 1×10^{-2} M $\text{CrCH}_2\text{Cl}^{2+}$ was obtained which could be stored at -10° for several weeks without appreciable decomposition.

Bromomethylchromium(III) cation, $\text{CrCH}_2\text{Br}^{2+}$, was made in the same way as $\text{CrCH}_2\text{Cl}^{2+}$ except that CH_2Br_2 (5-10 ml) was substituted for CH_2ClBr , and reaction time was only 30 minutes. The CH_2Br_2 was purified before use by washing with concentrated H_2SO_4 and H_2O . Typically, this procedure yielded 50 ml of 2×10^{-2} M $\text{CrCH}_2\text{Br}^{2+}$.

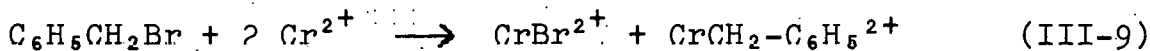
Trifluoromethylchromium(III) cation, CrCF_3^{2+} , was prepared by the method of Malik, *et al.* (52) wherein gaseous trifluoromethyl iodide reacts with Cr^{2+} in aqueous acid according to



A 20 ml solution 0.3 M in Cr^{2+} and 0.5 M in HClO_4 was bubbled with CF_3I for five minutes, and the capped bottle was then shaken vigorously for three hours at room temperature. The brown solution was then placed on a column of Dowex 50W-X8 cation exchange resin (15 x 1 cm, 100-200 mesh) in the hydrogen ion form. The pinkish-orange product was eluted with a solution that was 0.45 M in LiClO_4 and 0.05 M in HClO_4 . No green CrI^{2+} was observed on the column, presumably having been aquated during the synthesis. This procedure typically gave 50 ml of 2×10^{-2} M CrCF_3^{2+} , which is stable for weeks at room temperatures.

Aralkylchromium(III) complexes

Benzylchromium(III) cation, $\text{CrCH}_2\text{C}_6\text{H}_5^{2+}$, was prepared and purified by the method developed by Kochi and Davis (4) and modified by Chang and Espenson (48) wherein benzyl bromide reacts with Cr^{2+} in alcohol according to



Approximately 25 ml of ethanol or methanol was purged with nitrogen and cooled to 0°. To this was added 1.0 mmole

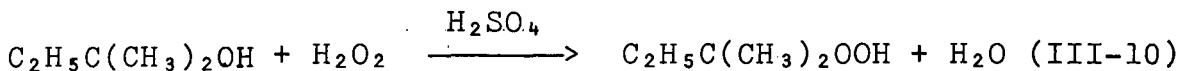
of neat benzyl bromide (0.1 ml) and 2.5 mmoles of Cr^{2+} (5 ml of 0.5 M), and the mixture was allowed to react for 10 minutes. The resulting green-brown solution was then placed on a column of Dowex 50W-X8 cation exchange resin (15 x 1 cm, 100-200 mesh) in the lithium form. The column was kept at 0° and was rendered air-free by prewashing with 300 ml of purged water. The CrBr^{2+} and excess Cr^{2+} were eluted with air-free 0.5 M LiClO_4 , and the yellow product $\text{CrCH}_2\text{C}_6\text{H}_5^{2+}$ was eluted with air-free 2.0 M LiClO_4 using slight nitrogen pressure to speed up the elution. This procedure typically yielded about 100 ml of 2×10^{-3} M $\text{CrCH}_2\text{C}_6\text{H}_5^{2+}$. The complex is sensitive to acid hydrolysis and oxygen decomposition, but the solution could be stored under nitrogen at -10° for up to a month.

The para-substituted benzylchromium(III) cations, $\text{CrCH}_2\text{C}_6\text{H}_4\text{-Z}^{2+}$, Z = CH_3 , Br, CF_3 , and CN, were all made and purified in exactly the same way as was $\text{CrCH}_2\text{C}_6\text{H}_5^{2+}$, substituting 1.0 mmole of the appropriate para-substituted benzyl bromide. The amounts of benzyl bromides used with 2.5 mmoles of Cr^{2+} were as follows: $\text{CH}_3\text{C}_6\text{H}_4\text{CH}_2\text{Br}$, 0.185 g; $\text{BrC}_6\text{H}_4\text{CH}_2\text{Br}$, 0.250 g; and $\text{NCC}_6\text{H}_4\text{CH}_2\text{Br}$, 0.240 g. The complex, $\text{CrCH}_2\text{C}_6\text{H}_4\text{CF}_3^{2+}$, had been synthesized eight months earlier and kept at -10°.¹

¹This complex was prepared by Ron Nohr using essentially the same method as described above.

Organic hydroperoxides

All the tertiary hydroperoxides, $R-C(CH_3)_2OOH$, except the tert-butyl compound ($R=CH_3$) which was obtained commercially, were made by modification of a literature method (53) wherein the corresponding tertiary alcohol reacts with H_2O_2 in the presence of H_2SO_4 as shown in equation III-10 for tert-amylhydroperoxide,



The detailed procedure varied for the different compounds as improvements in the method were discovered along the way.

For tert-amylhydroperoxide, $C_2H_5C(CH_3)_2OOH$, a mixture of H_2O (10.0 ml) and 11.2 ml of concentrated H_2SO_4 (0.2 mole) was cooled to 0° , and 23 ml of tert-amylalcohol (0.2 mole) was added dropwise with stirring over a period of about 30 minutes. Excess H_2O_2 (25 ml of 30% solution) was then added dropwise over a period of about 45 minutes, and the mixture was allowed to react at 0° with stirring for about 24 hours. The phases were then allowed to separate, the aqueous layer discarded, and the organic layer washed twice with H_2O . This crude material analyzed as 6.1 \underline{M} in hydroperoxide (the procedure for this analysis is described later), whereas neat $C_2H_5C(CH_3)_2OOH$ should be 8.6 \underline{M} based on an estimated density of 0.9 g ml^{-1} . This crude material was used in the preparation of $CrCH_2CH_3^{2+}$.

2-Methylpentyl-2-hydroperoxide, $\text{CH}_3\text{CH}_2\text{CH}_2\text{C}(\text{CH}_3)_2\text{OOH}$, was prepared in exactly the same way as the tert-amyl compound except on a 0.1 mole scale, and using 2-methyl-2-pentanol as the organic precursor. The crude product from this preparation analyzed as 6.5 M in peroxide compared to 7.6 M for neat $\text{CH}_3\text{CH}_2\text{CH}_2\text{C}(\text{CH}_3)_2\text{OOH}$ based on an estimated density of 0.9 g ml^{-1} , and this was used to prepare $\text{CrCH}_2\text{CH}_2\text{CH}_3^{2+}$.

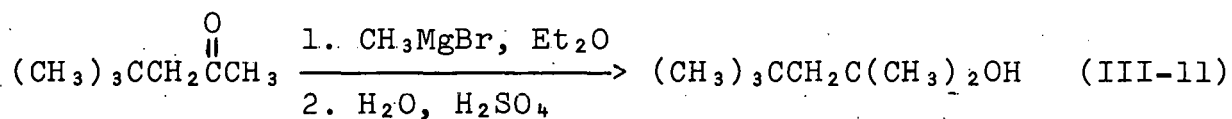
For the rest of the hydroperoxides, $\text{RC}(\text{CH}_3)_2\text{OOH}$, where $\text{R} = \text{CH}_2\text{C}(\text{CH}_3)_3$, $\text{CH}(\text{CH}_3)_2$, $\text{CH}(\text{CH}_3)\text{CH}_2\text{CH}_3$, and $\text{C}(\text{CH}_3)_3$, the yields were markedly improved by using 50% H_2O_2 instead of 30% and by adding the alcohol and H_2O_2 simultaneously rather than sequentially. (These changes could presumably be used profitably in the preceding preparations as well.)

The procedure for 2,4,4-trimethylpentyl-2-hydroperoxide, $\text{R} = \text{CH}_2\text{C}(\text{CH}_3)_3$, was as follows: a mixture of H_2O (3.1 ml) and 3.5 ml of concentrated H_2SO_4 (0.05 mole) was cooled to 0°. A 10.0 ml sample of 2,4,4-trimethyl-2-pentanol and about 6.0 ml of 50% H_2O_2 were then added simultaneously and dropwise over a period of about 45 minutes. The mixture was allowed to react for about 6 hours. The aqueous phase was separated from the organic phase by centrifugation, and the latter was washed twice with H_2O . This crude product was 5.1 M in hydroperoxide compared to 6.2 M estimated for the neat material, and was used to make neopentylchromium(III) ion.

The remaining hydroperoxides, $\text{RC}(\text{CH}_3)_2\text{OOH}$, ($\text{R} = \text{CH}(\text{CH}_3)_2$, $\text{CH}(\text{CH}_3)\text{C}_2\text{H}_5$, and $\text{C}(\text{CH}_3)_3$) were made by exactly the same

procedure using 0.06 mole of the appropriate alcohol. The crude products analyzed as 3.1 M, 3.6 M, and 3.3 M hydroperoxides for R = $\text{CH}(\text{CH}_3)_2$, $\text{CH}(\text{CH}_3)\text{C}_2\text{H}_5$, and $\text{C}(\text{CH}_3)_3$, respectively. These values are roughly half of those expected for the neat materials based on estimated densities of 0.9 g ml^{-1} .

All of the alcohols used in the hydroperoxide preparations were obtained commercially as neat liquids except 2,4,4-trimethyl-2-pentanol. This compound was synthesized by the method described by Williams (51) wherein the appropriate ketone reacts with methyl Grignard according to



To a clean, dry, three-necked flask fitted with a reflux condenser was added 12.2 g of magnesium turnings (0.5 mole) and 50 ml of dry ether. After cooling the mixture to 0°, 35 ml of CH_3Br (0.6 mole) was added slowly and allowed to react for one hour at reflux. After recooling to 0°, 50 ml of 4,4-dimethyl-2-pentanone (0.35 mole) was added dropwise over a period of about 30 minutes. This mixture was poured into 500 g of ice and 50 ml of concentrated H_2SO_4 . Most of the aqueous layer from this mixture was separated and discarded, and the organic layer plus about 50 ml of aqueous layer were distilled under vacuum at 20-25°. A heterogeneous

mixture of H_2O and $(CH_3)_3CH_2C(CH_3)_2OH$ was collected; the aqueous phase was discarded and the pure alcohol washed once with H_2O .

Mercury compounds

Solutions of mercuric perchlorate were prepared by boiling HgO powder in a slight excess of $HClO_4$. The solution was then filtered through high-retention filter paper to remove finely divided impurities.

Solutions of methylmercuric perchlorate, CH_3HgClO_4 , were prepared by reaction of CH_3HgCl with $AgClO_4$ in aqueous ethanol. A 1.89 g sample of CH_3HgCl (7.50 mmoles) was dissolved in 150 ml of absolute ethanol, and to this was added 1.40 g of $AgClO_4$ (6.75 mmoles) dissolved in 15 ml of H_2O . This mixture was allowed to react for about 3 hours with stirring to ensure complete reaction and coagulation of the $AgCl$ precipitate. The precipitate was removed by filtration through highly retentive filter paper. The filtrate was rotary evaporated to remove ethanol and diluted to 50 ml. This solution was shown by dithizone analysis (see below) to be 0.10 M in CH_3Hg^+ which is close to that predicted from the amount of $AgClO_4$ used in the synthesis. Also, a silver ion analysis showed the solution to be 4.4×10^{-4} M in Ag^+ .¹

¹This analysis was carried out by Dr. Fassel's group using atomic emission spectroscopy.

Solutions of benzylmercuric perchlorate, $C_6H_5CH_2HgClO_4$, were prepared in much the same way as CH_3HgClO_4 . A 0.593 g sample of $C_6H_5CH_2HgCl$ (1.81 mmoles) dissolved in 60 ml of absolute ethanol was mixed with 0.328 g of $AgClO_4$ (1.58 mmoles) and allowed to react with stirring for about 4 hours. The $AgCl$ precipitate was filtered and the ethanol from the filtrate was removed by rotary evaporation. A white solid, presumably unreacted $C_6H_5CH_2HgCl$, appeared upon evaporation and was removed by further filtration. The solution was analyzed for $C_6H_5CH_2Hg^+$ by Volhard titration and found to be 0.048 M in $C_6H_5CH_2Hg^+$. Analysis of the solution for silver ion showed it to be $9.2 \times 10^{-4} M$ in Ag^+ .

Benzylmercuric chloride was made using a literature procedure (54) by mixing equimolar amounts of dibenzylmercury and mercuric chloride in alcohol. A 0.276 g sample of $(C_6H_5-CH_2)_2Hg$ and 0.200 g of $HgCl_2$ were dissolved in 30 ml of absolute ethanol and allowed to react at room temperature for three hours. The product was crystallized by cooling to 0° for one hour, collected and air-dried. The white solid thus obtained had a melting point of 104-105° (lit. 104° (54)). This material was used to make solutions of benzylmercuric perchlorate.

Other materials

Chromium(II) perchlorate solutions were prepared by the standard method of reducing $Cr(ClO_4)_3$ (made by the reaction

of CrO_3 with H_2O_2 and HClO_4) with amalgamated zinc in dilute HClO_4 (see Part I, Experimental section).

Solid lithium perchlorate was made by neutralizing reagent grade Li_2CO_3 with HClO_4 , recrystallizing the product twice.

All other materials mentioned in Part III were reagent grade chemicals obtained commercially and used without further purification.

Methods

Analyses

The molar absorptivity of each organochromium complex was determined from the u.v.-visible spectrum of a freshly prepared solution which was then analyzed for total chromium by the standard chromate analysis (10). (An aliquot of the organochromium solution was added to a volumetric flask containing 2 ml of 6 M NaOH and 0.5 ml of 30% H_2O_2 . This solution was then boiled for 20-30 minutes, cooled, and diluted to the mark. The absorbance of this solution was then measured at λ 372 nm, ϵ 4830.) Subsequently, the concentration of a given organochromium(III) complex was determined spectrally based on the molar absorptivity.

Stock solutions of mercury(II) ion were analyzed by Volhard titration (55). An aliquot of the Hg^{2+} solution was titrated with standard NaSCN solution using iron(III) ion as the indicator.

Solutions of methylmercuric CH_3Hg^+ ion could not be obtained in greater than 0.1 M concentration, so the Volhard method was not satisfactory. A more sensitive analysis was therefore developed using dithizone reagent (diphenylthiocarbazone). This analysis is based on the mixed color method (56) wherein the absorbance at λ 618 nm of dithizone in CCl_4 solution is measured with and without prior extraction with the aqueous CH_3Hg^+ solution; the difference in absorbance is a direct measure of the $[\text{CH}_3\text{Hg}^+]$ in the aqueous phase. The extinction coefficient of dithizone at λ 618 nm was determined by extracting known amounts of Ag^+ ion with a CCl_4 solution of dithizone and measuring the absorbance at λ 618 nm; the value of ϵ is $3.40 \times 10^4 \text{ M}^{-1}\text{cm}^{-1}$.

An aliquot of dithizone solution was placed in a separatory funnel along with 1 M HClO_4 (1-5 ml) and an aliquot of the CH_3Hg^+ solution, the amount of CH_3Hg^+ being between 30% and 70% of the amount of dithizone. After vigorously shaking the separatory funnel for one minute, the absorbance of the CCl_4 phase was measured at λ 618 nm. The absorbance of the untreated dithizone solution was determined by repeating the above procedure using an equivalent amount of H_2O instead of the CH_3Hg^+ solution. The $[\text{CH}_3\text{Hg}^+]$ was computed from the difference in absorbance, ΔA , using the equation,

$$[\text{CH}_3\text{Hg}^+] = \frac{\Delta A \times V_{\text{Dz}}}{\epsilon_{\text{Dz}} \times b \times V_{\text{RHg}^+}} \quad (\text{III-12})$$

where V_{Dz} and V_{RHg^+} are the volume of the dithizone and CH_3Hg^+ solutions, respectively. In a typical analysis of 0.024 M CH_3Hg^+ (diluted 1:100) using a $5.7 \times 10^{-4} M$ dithizone solution, V_{Dz} was 9.80 ml, V_{RHg^+} was 1.95 ml, b was 0.5 cm, and ΔA was 0.82.

The alkylhydroperoxides, $RC(CH_3)_2OOH$, were determined by a modification of literature method (57) wherein $RC(CH_3)_2OOH$ is reduced by I^- in hot isopropanol/acetic acid solvent, and the I_3^- produced is titrated with standard $Na_2S_2O_3$.

To a 250 ml flask were added 40 ml of isopropanol, 2 ml of glacial acetic acid and an aliquot of $RC(CH_3)_2OOH$ (1-3 mmoles). This solution was heated to boiling and 1 to 2 grams of NaI added. The mixture was refluxed for 5 minutes and then cooled to room temperature. The I_3^- produced was titrated with standard $Na_2S_2O_3$ (0.1-0.2 M) to the disappearance of the yellow color of I_3^- . The concentration of $RC(CH_3)_2OOH$ in the aliquot was computed from the equation,

$$[RC(CH_3)_2OOH] = \frac{V_T \times \underline{M}_r}{V_A \times 2} \quad (III-13)$$

where V_T and V_A are the volumes of the titer and aliquot, respectively, and \underline{M}_r is the molarity of the $Na_2S_2O_3$ solution.

Lithium perchlorate solutions were analyzed by placing an aliquot of the solution on a column of Dowex 50W-X8 cation exchange resin in the hydrogen ion form, washing with H_2O , and

titrating the H^+ released with standard NaOH to the phenol-phthalein endpoint.

Spectra

The mercury(II) products of some of the reactions under study were identified by their nmr spectra. The organochromium complex, CrR^{2+} , was added to a slight excess of mercury(II) reactant. For the organomercury cation reactions, the H_2O -insoluble mercury product was extracted into $CHCl_3$ or CCl_4 . For the Hg^{2+} reactions, excess HCl was added to the reaction mixture to form H_2O -insoluble alkylmercuric chloride, which was extracted into $CHCl_3$ or CCl_4 . In both cases the solvent was evaporated, leaving the solid organomercury product, which was redissolved in 1 ml of an appropriate solvent, usually $CDCl_3$ or CCl_4 , and the nmr spectrum of the solution recorded using a Varian A60 nmr spectrometer.

All uv-visible spectra and absorbance data were recorded on a Cary 14 spectrophotometer equipped with a high-intensity tungsten lamp.

Stoichiometry

Two experiments were carried out to show that one mole of $Hg(II)$ reacts with one mole of CrR^{2+} . The experiments were carried out as follows: Into each of several 25 ml volumetric flasks was added a fixed amount of n-propylchromium stock solution (15.0 ml of $1.25 - 3.36 \times 10^{-3} \text{ M}$) in 50%

methanol/water and varying amounts of standard CH_3Hg^+ or Hg^{2+} solutions, also in 50% methanol/water. Immediately upon addition of these reagents and dilution to the mark for each flask, the absorbance of $\text{CrCH}_2\text{CH}_2\text{CH}_3^{2+}$ was measured at λ 393 nm ($\epsilon = 402 \text{ M}^{-1}\text{cm}^{-1}$ in 50% methanol/water). A plot of absorbance vs mole ratio, $\text{Hg}(\text{II})/\text{CrR}^{2+}$, was made. The point at which this plot breaks gives the value of the mole ratio which represents the number of moles of $\text{Hg}(\text{II})$ that reacts per mole of CrR^{2+} .

Kinetics

Kinetic runs on slow reactions ($t_{1,2} \geq 10 \text{ s}$) were done using a Cary 14 spectrophotometer equipped with a thermostatted cell compartment. All reagents except the CrR^{2+} complex were placed in an optical quartz cell and allowed to equilibrate to temperature for 20 minutes. An aliquot of the thermostatted CrR^{2+} stock solution was then added and the reaction monitored by the decay of the CrR^{2+} absorption. For reactions in which air-free conditions were required, the reaction cell was purged for 20 minutes prior to the addition of the CrR^{2+} complex.

Kinetic runs on faster reactions ($t_{1,2} \leq 20 \text{ s}$) were done on a Gibson-Durrum stopped-flow spectrophotometer having Kel-F components and equipped with a storage oscilloscope. In all experiments, the LiClO_4 used to maintain ionic strength was placed in the storage syringe containing the CrR^{2+} complex,

and HClO_4 was placed in the Hg(II) syringe. As in the Cary 14 runs, all reactions were monitored by the decay of the CrR^{2+} absorption. The raw data for a stopped-flow run consisted of a Polaroid photograph of the oscilloscope trace of voltage vs time.

For reactions of neopentylchromium(III) ion, the substrate was prepared in the storage reservoir of the stopped-flow instrument immediately prior to each run as described earlier, since this complex is unstable and could not be purified.

Pseudo-first-order conditions, with the Hg(II) reagent in excess, were used for all reactions except that of CrCH_3^{2+} with Hg^{2+} where second-order conditions were used. The pseudo-first-order rate constants, k_{obs} , were obtained either by the standard method or by the Swinbourne method. In the standard method, $\ln(A_t - A_\infty)$ is plotted against time according to

$$\ln(A_t - A_\infty) = \ln(A_0 - A_\infty) - k_{\text{obs}} t \quad (\text{III-14})$$

and the slope = $-k_{\text{obs}}$.

In the Swinbourne method, A_t is plotted against $A_{t+\tau}$ according to equation (III-15), where τ is a time interval corresponding to 0.5-l half life. The slope of the Swinbourne plot is $\exp(k_{\text{obs}}\tau)$ so that k_{obs} is $\ln(\text{slope})/\tau$.

$$A_t = A_\infty \{1 - \exp(k_{\text{obs}}\tau) + A_{t+\tau} \exp(k_{\text{obs}}\tau)\} \quad (\text{III-15})$$

The second-order rate constant was evaluated by dividing k_{obs} by $[Hg(II)]$, or equivalently from a plot of k_{obs} vs $[Hg(II)]$. In some cases the line does not pass through the origin, at $[Hg(II)] = 0$; the intercept in this case represents first-order rate constant for mercury-independent decomposition of the CrR^{2+} complex.

The reaction of $CrCH_3^{2+}$ with Hg^{2+} was too fast to study under first-order conditions, so the stopped-flow kinetic runs were done with Hg^{2+} in only two- or three-fold excess over $CrCH_3^{2+}$. The data were plotted according to the equation

$$\ln[Cr^{2+}]/[CrCH_3] = \ln[Cr^{2+}]_0/[CrCH_3]_0 + \{[Cr^{2+}]_0 - [CrCH_3]_0\} k_{Hg} t \quad (III-16)$$

The time at the beginning of the run, t_0 , was arbitrarily chosen from the stopped-flow trace and $[CrCH_3^{2+}]_0$ (concentration at t_0) was computed from the absorbance at t_0 . The initial concentration, $[CrCH_3^{2+}]_i$, was determined from the absorbance with the $CrCH_3^{2+}$ solution only in the observation chamber.¹ The difference between $[CrCH_3^{2+}]_i$ and $[CrCH_3^{2+}]_0$

¹The quantity $[CrCH_3^{2+}]_i$ is the theoretical concentration before any reaction with Hg^{2+} has occurred, and $[CrCH_3^{2+}]_0$ is the concentration after the reagents have been mixed and the decrease in absorbance for the run just begins. Since the reaction is so fast, $[CrCH_3^{2+}]_i$ is considerably higher than $[CrCH_3^{2+}]_0$ since some reaction occurs during mixing.

represents the amount of Hg^{2+} consumed before t_o is reached, and $[\text{Hg}^{2+}]_o$ is thus computed from this difference and $[\text{Hg}^{2+}]_i$, determined from dilution of the standard Hg^{2+} stock solution. Using these concentrations at t_o , $[\text{CrCH}_3^{2+}]$ and $[\text{Hg}^{2+}]$ for each point in the kinetic run were computed according to

$$[\text{CrCH}_3^{2+}] = \frac{A}{\epsilon b} \quad (\text{III-17})$$

and

$$[\text{Hg}^{2+}] = [\text{Hg}^{2+}]_o - [\text{CrCH}_3^{2+}]_o + [\text{CrCH}_3^{2+}] \quad (\text{III-18})$$

A plot of $[\text{Hg}^{2+}]/[\text{CrCH}_3^{2+}]$ vs time according to equation III-16 gives $\{[\text{Hg}^{2+}]_o - [\text{CrCH}_3^{2+}]_o\}k_{\text{Hg}}$ as the slope.

RESULTS

Characterization

Characterization of organochromium(III) complexes

Most of the organochromium complexes used in this study were characterized by comparison of the electronic spectrum with that of the known complex from the literature. A summary of the peak positions and extinction coefficients for all CrR^{2+} complexes is shown in Tables III-1 and III-2, along with data reported by other workers. The spectra of most of the CrR^{2+} ions are shown in Figures III-1 to III-8; the isopropyl- and neopentylchromium(III) ions are not shown since they were not obtained in pure form. The spectra of the para-substituted benzylchromium(III) ions are also not shown because significant decomposition of these complexes occurred in the ion exchange purification. The appearance of $p\text{-CH}_3$, $p\text{-Br}$, and $p\text{-CF}_3$ complexes are very similar to that of the parent benzylchromium(III) ion with the peak at λ 275-285 nm being the most intense. The spectrum of the $p\text{-CN}$ complex, however, differs in that the peak at λ 312 nm is more intense than that at λ 285 nm.

The discrepancies in ϵ values in Tables III-1 and III-2 are due to the fact that some decomposition of the CrR^{2+} invariably occurs in the purification procedure forming Cr^{3+} and nonabsorbing organic products. Since Cr^{3+} absorbs much

Table III-1. Spectral data for aliphatic and haloaliphatic CrR^{2+} complexes, λ given in nm, ϵ given in $\text{M}^{-1}\text{cm}^{-1}$

R	λ_1 (ε)	λ_2 (ε)	λ_3 (ε)	Ref.
CH_3	538 (12)	392 (246)	258 (2400)	25
	550 (12)	392 (243)	258 (2680)	47
	550 (96)	392 (196)	258 (2160)	49
CH_2CH_3	560 (8.5)	394 (390)	275 (2400)	- ^a
	562 (10)	394 (258)	275 (1445)	47
$\text{CH}_2\text{CH}_2\text{CH}_3$	550 (8.3)	393 (380)	276 (2650)	- ^a
	-	394 (250)	275 (1670)	47
$\text{CH}_2\text{C}(\text{CH}_3)_3$	-	405	283	- ^a
		387 (204)	285 (940)	47, 51
$\text{CH}(\text{CH}_3)_2$	557 (10)	399 (366)	290 (1800)	- ^{a,b}
$\text{CH}(\text{CH}_3)\text{C}_2\text{H}_5$	-	400 (370)	283 (1775)	- ^{a,b}
$\text{C}(\text{CH}_3)_3$	-	407	310	- ^{a,b}
CH_2Cl	517 (24)	393 (225)	260 (3560)	12
	517 (20)	391 (204)	262 (3470)	3
CH_2Br	520 (29)	397 (255)	266 (3280)	47
	520 (22)	397 (144)	267 (2630)	3
CF_3	490 (43.2)	380 (77.6)	220 (5500)	- ^a
	500 (40)	380 (67)	-	52

^aThis work.

^bNew complex original to this work.

Table III-2. Spectral data for aralkylchromium(III) complexes, $\text{CrCH}_2-\text{C}_6\text{H}_4-\text{Z}^{2+}$;
 λ given in nm, ϵ given in $\text{M}^{-1}\text{cm}^{-1}$

Z	λ_1 (ε)	λ_2 (ε)	λ_3 (ε)	λ_4 (ε)	Ref.
H	355 (1260)	297 (4070)	274 (4790)	240 (4300)	- ^a
	360 (2470)	297 (7920)	274 (8380)	243	⁴
	355 (2200)	297 (6970)	274 (7670)	-	- ^b
CH_3	360	300	276	-	- ^a
	362	301	277	-	- ^c
	364	302	278	240	⁴
Br	360	310	280	250	- ^a
	359	301	281	-	- ^c
	360	300	280	255	⁴
CF_3	355	298	280	245	- ^a
	354	298	280	-	- ^c
CN	sh 360	312	sh 285	260	- ^a
	-	312	sh 285	-	- ^c

^aThis work.

^bR. Nohr, unpublished results.

^cJ. Chang, unpublished results.

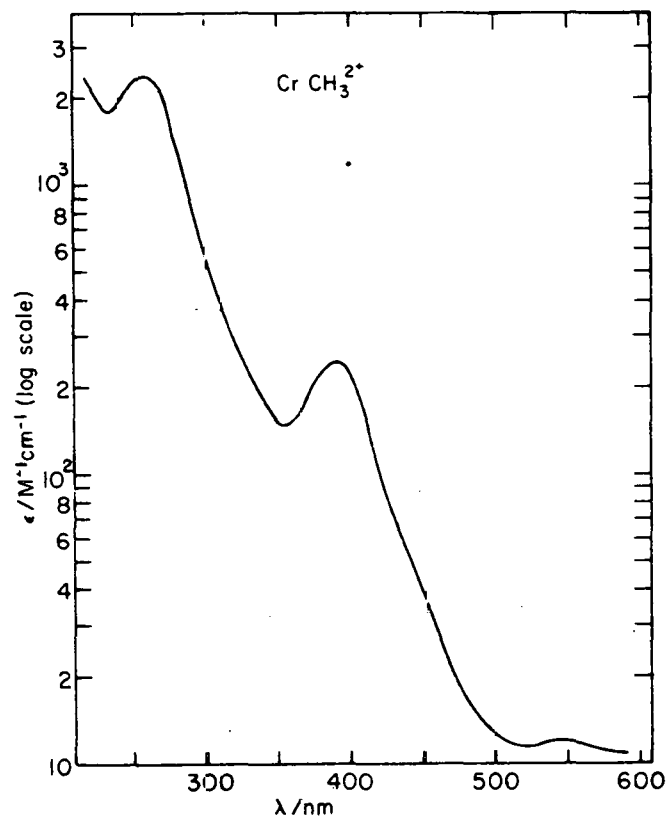


Figure III-1. Electronic spectrum of CrCH_3^{2+}

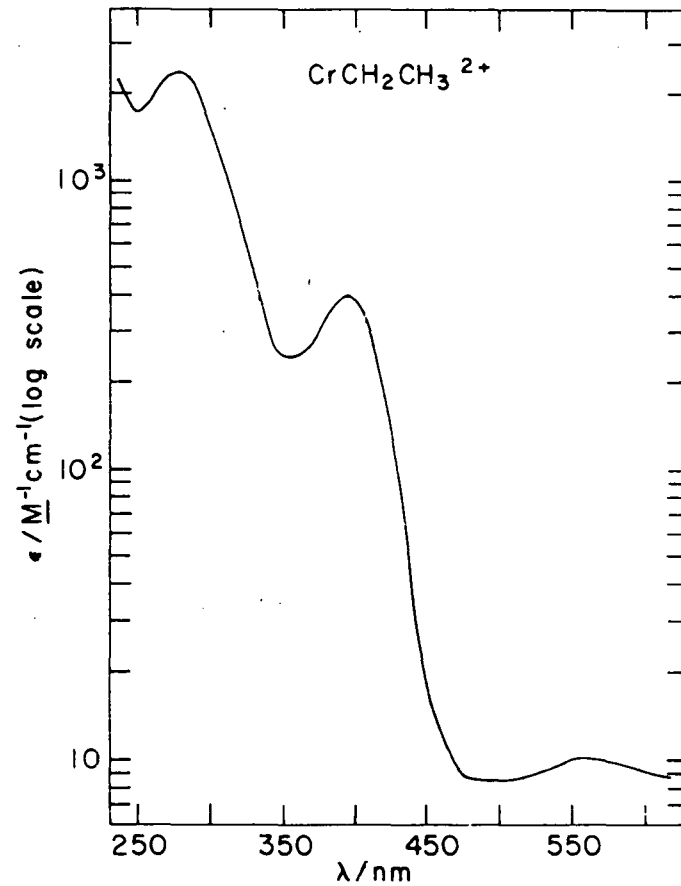


Figure III-2. Electronic spectrum of $\text{CrCH}_2\text{CH}_3^{2+}$

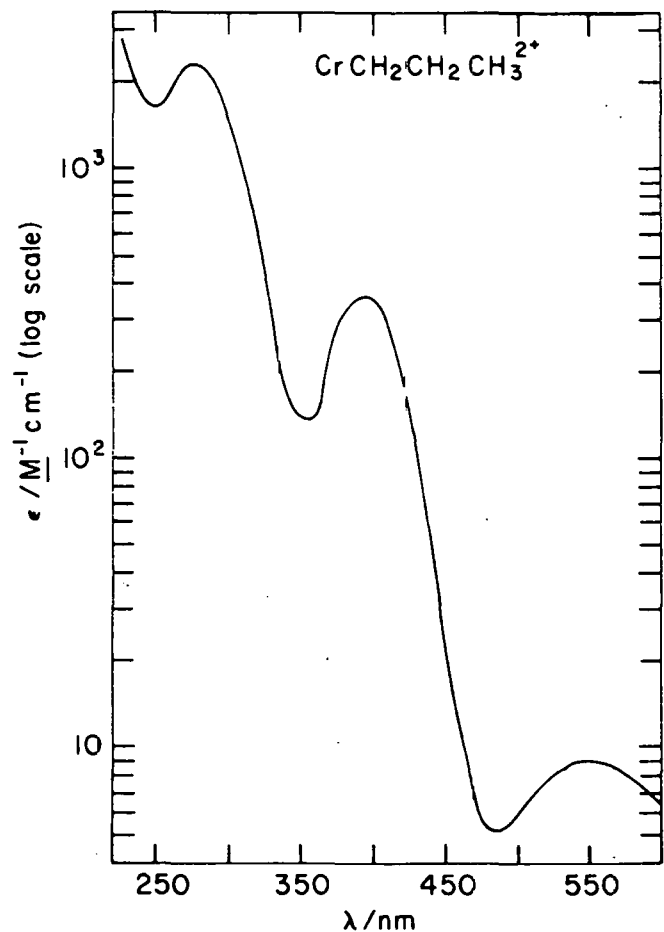


Figure III-3. Electronic spectrum of $\text{CrCH}_2\text{CH}_2\text{CH}_3^{2+}$

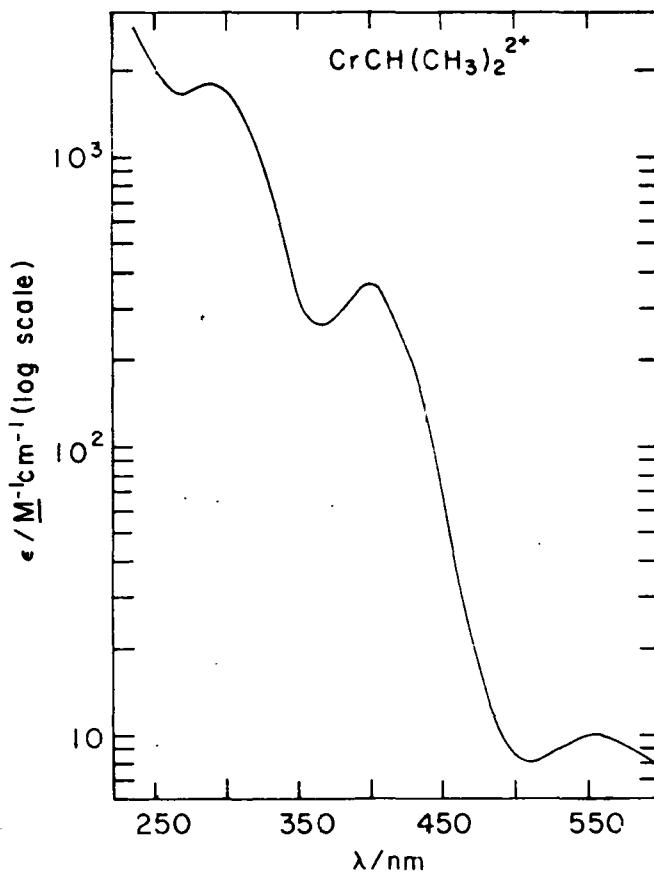


Figure III-4. Electronic spectrum of $\text{CrCH}(\text{CH}_3)_2^{2+}$

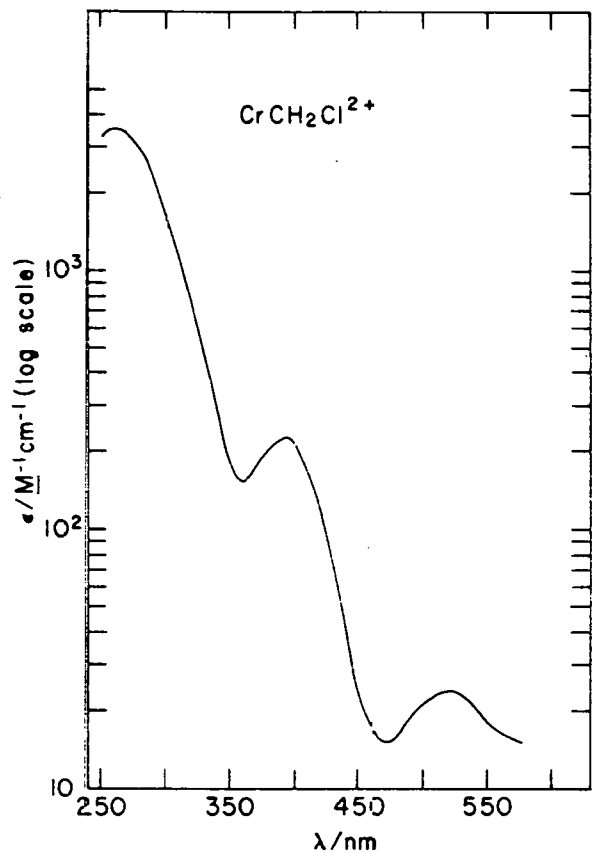


Figure III-5. Electronic spectrum of $\text{CrCH}_2\text{Cl}^{2+}$

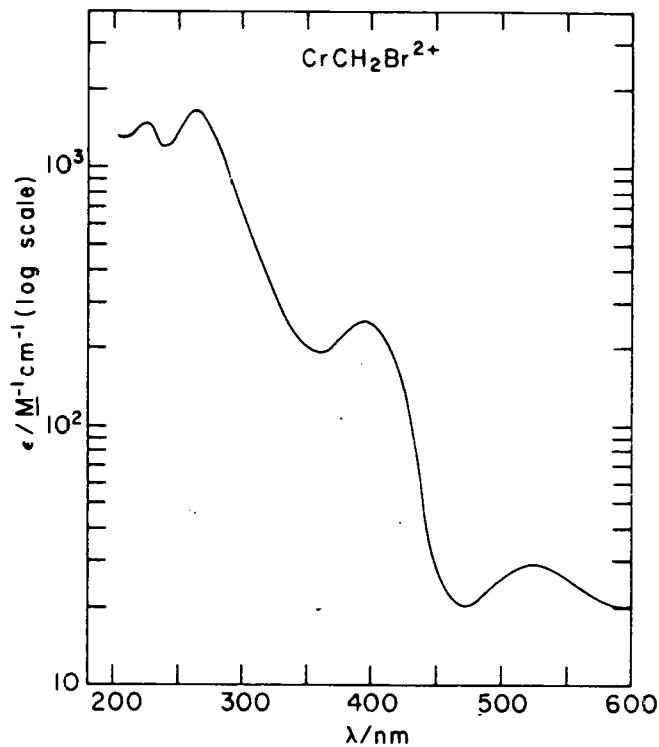


Figure III-6. Electronic spectrum of $\text{CrCH}_2\text{Br}^{2+}$

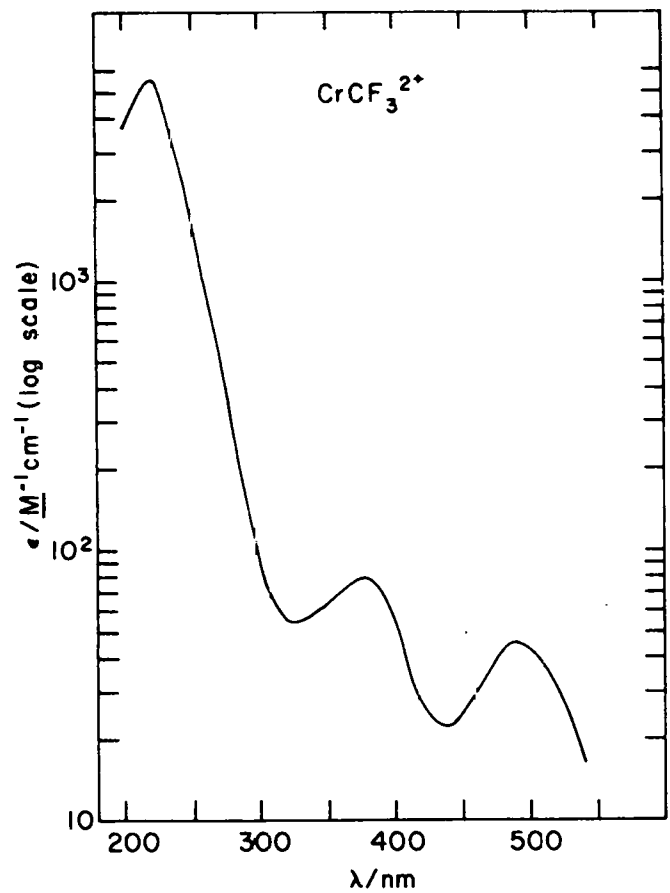


Figure III-7. Electronic spectrum of CrCF_3^{2+}

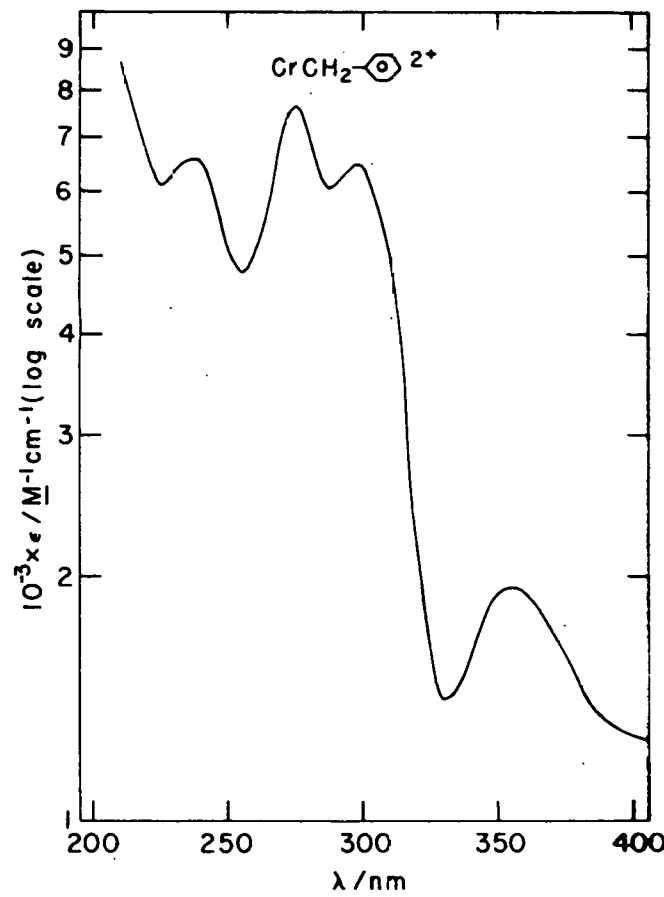


Figure III-8. Electronic spectrum of $\text{CrCH}_2\text{C}_6\text{H}_5^{2+}$

less than the CrR^{2+} ions below $\lambda 450$ nm where the spectral analyses were done, and since a total chromium analysis is used to obtain extinction coefficients, the ϵ values in Tables III-1 and III-2 are all lower than the true values. The highest value of ϵ for a given complex should therefore be regarded as a lower limit of the actual value. In estimating the concentration of a CrR^{2+} complex, the best ϵ value at the $\lambda 390-400$ nm peak or, for $\text{CrCH}_2\text{C}_6\text{H}_5^{2+}$, the peak at $\lambda 274$ nm was used.

Three of the entries in Table III-1 are new complexes original to this work: $\text{CrCH}(\text{CH}_3)_2^{2+}$, $\text{CrCH}(\text{CH}_3)\text{CH}_2\text{CH}_3^{2+}$, and $\text{CrC}(\text{CH}_3)_3^{2+}$. The identity of these species is assumed on the basis of the alkylhydroperoxides used in their synthesis. In the case of isopropylchromium(III) ion, further support for the identity of the complex comes from the fact that the product of its reaction with Hg^{2+} was shown to be $(\text{CH}_3)_2\text{CHHg}^+$ by its nmr spectrum (see below). Isopropyl-, sec-butyl-, and tert-butylchromium(III) ions are the first examples of secondary and tertiary organochromium complexes of this kind.

Nmr spectra of organomercury(II) products

The organomercury(II) products of seven of the reactions of CrR^{2+} complexes with Hg^{2+} , CH_3Hg^+ , or $\text{C}_6\text{H}_5\text{Hg}^+$ were determined by nmr experiments as described in the Experimental section. The results of these experiments are summarized in Table III-3. The identity of each mercury(II) compound in

Table III-3. Nmr data for organomercury products of reactions of CrR^{2+} with Hg(II); chemical shift (δ) referenced to TMS

Compound	Group	δ /ppm	Solvent	Comment	Ref.
$\text{CH}_3\text{CH}_2\text{HgCl}$	CH_2	1.81 - 2.22	CDCl_3	$J_{\text{H}^1-\text{Hg}^{199}} = \sim 220$ Hz	- ^a
		---	pyridine	$J_{\text{H}^1-\text{Hg}^{199}} = 116$ Hz	58
		1.97	CD_2Cl_2		59
	CH_3	1.18 - 1.53	CDCl_3	$J_{\text{H}^1-\text{Hg}^{199}} = \sim 290$ Hz	- ^a
		---	pyridine	$J_{\text{H}^1-\text{Hg}^{199}} = 296$ Hz	58
		1.35	CD_2Cl_2		59
$(\text{CH}_3)_3\text{CCH}_2\text{HgCl}$	CH_2	2.07	CCl_4		- ^a
		2.11	CCl_4		- ^b
		2.20	CDCl_3		60
	CH_3	1.07	CCl_4		- ^a
		1.11	CCl_4		- ^b
		1.08	CDCl_3		60
$(\text{CH}_3)_2\text{CHHgCl}$	CH	2.25 - 2.85	d^6 acetone	Ratio of Intensities = $\frac{1}{6.4}$	- ^a
	CH_3	1.50 (doublet)	d^6 acetone		- ^a
ClCH_2HgCl	CH_2	2.44	d^6 benzene	$J_{\text{H}^1-\text{Hg}^{199}} = 119$ Hz	- ^a
		2.54	d^6 benzene	$J_{\text{H}^1-\text{Hg}^{199}} = 119$ Hz	3

^aThis work.

^bAuthentic sample provided by Dr. R. Larock.

Table III-3. (Continued)

Compound	Group	δ /ppm	Solvent	Comment	Ref.
$C_6H_5CH_2HgCl$	CH_2	3.23	$CDCl_3$	$J_{H^1-Hg^{199}} = 253$ Hz	- ^a
		3.23	$CDCl_3$	$J_{H^1-Hg^{199}} = 253$ Hz	- ^c
$C_6H_5CH_2HgCH_3$	CH_2	2.30	$CDCl_3$		- ^a
		2.28	$CDCl_3$		54
	CH_3	0.38	$CDCl_3$		- ^a
		0.34	$CDCl_3$		54
$C_6H_5CH_2HgC_6H_5$	CH_2	2.45	$CDCl_3$		- ^a
		2.57	$CDCl_3$		54

^cAuthentic sample made by reaction of equimolar amounts of dibenzylmercury and mercuric chloride in ethanol.

Table III-3 was deduced in a different way from the nmr spectra, and a brief discussion of each compound follows.

The spectrum of $\text{CH}_3\text{CH}_2\text{HgCl}$ in CDCl_3 was determined, and proved to be complicated, consisting of two complex multiplets in the regions δ 1.81 - 2.22 ppm and δ 1.18 - 1.53 ppm. The precise values of the chemical shifts were not computed. The identity of $\text{CH}_3\text{CH}_2\text{HgCl}$ was deduced from the close similarity of this spectrum to that reported in the literature (58) using pyridine as solvent.

Neopentylmercuric chloride was confirmed by the similarity of chemical shifts in the product sample and an authentic sample. The concentration of $(\text{CH}_3)_3\text{CCH}_2\text{HgCl}$ was too low to allow integration of the two singlet peaks, but qualitatively the general appearance of the product and authentic spectra were the same.

The identity of isopropylmercuric chloride was deduced from the splitting pattern and the integration of the nmr spectrum. No authentic sample or literature spectra are available for comparison of chemical shifts. The pattern of an intense doublet and a symmetrical multiplet (seven peaks expected, five observed due to low concentration) with a ratio of 6.4:1 doublet:multiplet confirms the presence of the isopropyl group.

Chloromethylmercuric chloride and benzylmercuric chloride were identified by the values of the chemical shifts of the

methylene protons and by the values of $J_{H^1-Hg^{199}}$, the coupling constant between the methylene protons and the Hg^{199} nuclei.

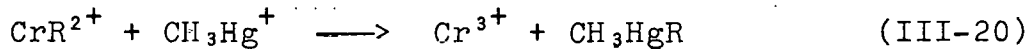
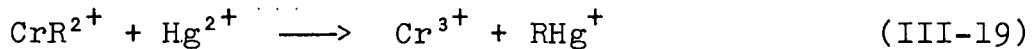
The product of the reaction of CH_3Hg^+ and $CrCH_2C_6H_5^{2+}$ was shown to be $C_6H_5CH_2HgCH_3$ by the values of the chemical shifts for the methyl and methylene protons. In this experiment, $(CH_3)_2Hg$ and $(C_6H_5CH_2)_2Hg$ were also present in the products as demonstrated by resonances at δ 0.27 ppm $((CH_3)_2Hg)$ and δ 2.41 ppm $((C_6H_5CH_2)_2Hg)$ (54). These products apparently result from a rapid exchange of alkyl groups. No exchange was observed when authentic samples of $(CH_3)_2Hg$ and $(C_6H_5CH_2)_2Hg$ were dissolved in $CDCl_3$, so it is concluded that the scrambling of alkyl groups in the organomercury product occurs in the aqueous phase as the reaction of CH_3Hg^+ and $CrCH_2C_6H_5^{2+}$ takes place.

Finally, the reaction of phenylmercuric ion, $C_6H_5Hg^+$, with $CrCH_2C_6H_5^{2+}$ was shown to give $C_6H_5CH_2HgC_6H_5$ by the value of the chemical shift for the methylene protons (54). No resonances for $(C_6H_5CH_2)_2Hg$ were observed in this experiment, so the rapid exchange of alkyl groups seen in the CH_3Hg^+ reaction apparently does not occur.

These results confirm that reactions of a given CrR^{2+} complex with $Hg(II)$ electrophiles give an organomercury product resulting from the transfer of the organic group from chromium to mercury. It is assumed that analogous reactions occur for all the CrR^{2+} complexes studied.

Characterization of reactions

The reactions of CrR^{2+} complexes with Hg^{2+} and CH_3Hg^+ are described by equations III-19 and III-20, respectively.



The characterization of the $\text{Hg}(\text{II})$ products was discussed in the previous section. The identity of Cr^{3+} as a product was established by its electronic spectrum (λ 574 nm, ϵ 13.3 M^{-1} cm^{-1} ; λ 408 nm, ϵ 15.8 $\text{M}^{-1}\text{cm}^{-1}$).

Evidence that the stoichiometry of the reactions is as written in equations III-19 and III-20 comes from spectrophotometric titrations on the reactions of n-propyl-chromium(III) ion with CH_3Hg^+ and Hg^{2+} as described in the Experimental section.

The titration curves for the two experiments are shown in Figures III-9 and III-10 for the CH_3Hg^+ and Hg^{2+} reactions, respectively. The mole ratio for the CH_3Hg^+ reaction is 0.91, indicating a stoichiometry of 1:1, as expected. The mole ratio for the Hg^{2+} reaction is 0.48, indicating a stoichiometry of 2:1, as expected when $[\text{Hg}^{2+}] \leq \frac{1}{2}[\text{CrR}^{2+}]$ since the RHg^+ produced initially further reacts with CrR^{2+} to give R_2Hg . Even though these experiments were carried out in 50% methanol/water (to keep the water-insoluble dialkylmercury from precipitating), the conclusion should hold for pure water

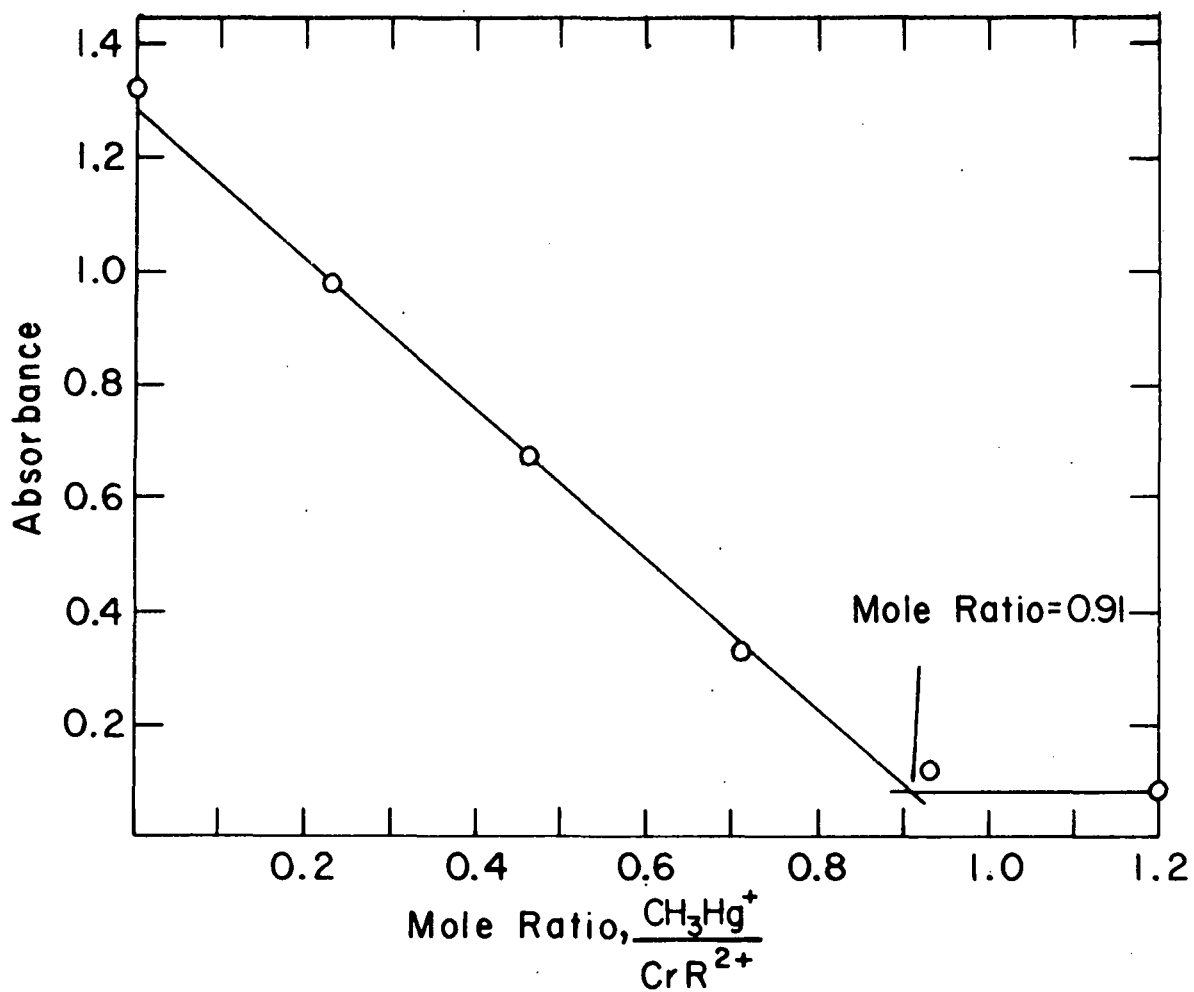


Figure III-9. Spectrophotometric titration for reaction of $\text{CrCH}_2\text{CH}_2\text{CH}_3^{2+}$ and CH_3Hg^+

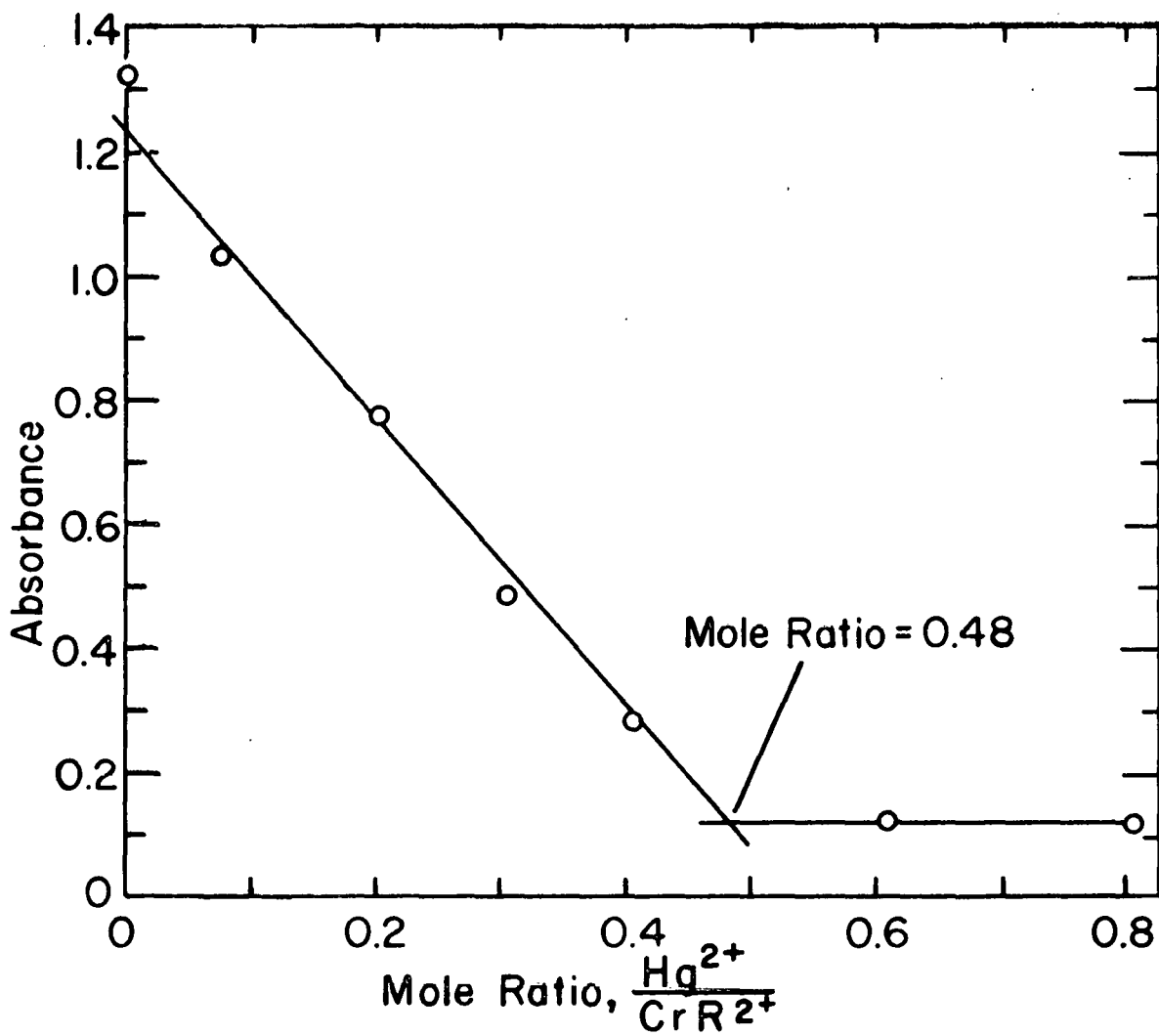


Figure III-10. Spectrophotometric titration for the reaction of $\text{CrCH}_2\text{CH}_2\text{CH}_3^{2+}$ and Hg^{2+}

as well. It is assumed that all the other CrR^{2+} complexes under study react in the same way with the Hg(II) reactants. This assumption seems well-founded in light of previous studies concerning reactions of CrR^{2+} complexes with Hg(II) and other electrophiles (see Introduction).

Kinetics

Preliminary experiments

Kinetics experiments were carried out for some prototype reactions represented in equations III-19 and III-20 in order to determine some general trends and kinetic features of these reactions. The organochromium(III) complexes used in these preliminary runs were CrCH_3^{2+} , $\text{CrCH}_2\text{C}_6\text{H}_5^{2+}$, and $\text{CrCH}_2\text{Cl}^{2+}$, and the Hg(II) reagents examined were $\text{Hg}^{2+}(\text{ClO}_4^-)_2$, CH_3Hg^+ (ClO_4^- and OAc^-), $\text{C}_6\text{H}_5\text{Hg}^+(\text{OAc}^-)$, and $\text{C}_6\text{H}_5\text{CH}_2\text{Hg}^+(\text{ClO}_4^-)$. The results of these experiments are described below.

All the reactions studied proved to be first-order in both $[\text{CrR}^{2+}]$ and $[\text{Hg(II)}]$. Most of the runs were done under pseudo-first-order conditions with the Hg(II) reagent in at least ten-fold excess. The first-order plots ($\ln|A_t - A_\infty|$ vs t) were all nicely linear confirming the first-order dependence on $[\text{CrR}^{2+}]$, and in the few cases where the $[\text{Hg(II)}]$ was varied, the quotient $k_{\text{obs}}/[\text{Hg(II)}]$ (k_{obs} is the pseudo-first-order rate constant) was constant demonstrating the first-order dependence on $[\text{Hg(II)}]$. In runs for the reaction of $\text{CH}_3\text{Hg}^{2+}(\text{OAc}^-)$ and CrCH_3^{2+} where second-order conditions were

used ($[\text{CH}_3\text{Hg}^{2+}] = [\text{CrCH}_3^{2+}] = 0.5 - 1.0 \times 10^{-5} \text{ M}$), the second-order plots (see Experimental section) were linear, consistent with the results of the pseudo-first-order experiments. These results along with those of the stoichiometry experiments indicate that the rate law for the reactions is

$$-\frac{d[\text{CrR}^{2+}]}{dt} = -\frac{d[\text{Hg(II)}]}{dt} = k[\text{CrR}^{2+}][\text{Hg(II)}] \quad (\text{III-21})$$

(Further support for this rate law is given later in the results of the systematic kinetic studies; in some cases, the above rate law does not strictly hold.)

In runs on the reaction of CH_3Hg^+ with $\text{CrCH}_2\text{C}_6\text{H}_5^{2+}$, ($[\text{CH}_3\text{Hg}^+] = 5 \times 10^{-4} \text{ M}$, $[\text{CrCH}_2\text{C}_6\text{H}_5^{2+}] = 4 \times 10^{-5} \text{ M}$, $[\text{H}^+] = 0.25 \text{ M}$, and $\mu = 0.50 \text{ M}$), it was found that the acetate salt of CH_3Hg^+ gave the same second-order rate constant as the perchlorate salt, $100 \text{ M}^{-1}\text{s}^{-1}$. This result implies that CH_3Hg^+ in acetate medium exists as the hydrated cation and not the acetate complex.¹ Since the CH_3HgOAc is commercially available, it was decided to use this as the source of CH_3Hg^+ ions in the systematic kinetic studies.

¹It is assumed that $\text{CH}_3\text{HgClO}_4$ is completely dissociated. If CH_3HgOAc were undissociated, one would expect it to react more slowly.

Another preliminary result was that for reactions of RHg^+ cations with CrCH_3^{2+} and $\text{CrCH}_2\text{C}_6\text{H}_5^{2+}$, the nature of R makes very little difference in the rate. In two kinetic runs on the reaction of CrCH_3^{2+} (1×10^{-4} M) with CH_3Hg^+ or $\text{C}_6\text{H}_5\text{Hg}^+$ (1.3×10^{-3} M) under identical conditions ($[\text{H}^+] = 0.25$ M, $\mu = 0.50$ M, $T = 25.0^\circ$) the second-order rate constants were 1.1×10^4 M⁻¹s⁻¹ and 1.6×10^4 M⁻¹s⁻¹, respectively. Likewise, for two runs on the reaction of $\text{CrCH}_2\text{C}_6\text{H}_5^{2+}$ (5×10^{-5} M) with the same two reagents, $[\text{CH}_3\text{Hg}^+] = 5.1 \times 10^{-4}$ M and $[\text{C}_6\text{H}_5\text{Hg}^+] = 1.1 \times 10^{-3}$ M ($[\text{H}^+] = 0.1$ M, $\mu = 0.1$ M, $T = 25.0^\circ$), the second-order rate constants were 65 and 40 M⁻¹s⁻¹, respectively. Finally, in two runs on the reaction of $\text{CrCH}_2\text{C}_6\text{H}_5^{2+}$ (2×10^{-4} M) with CH_3Hg^+ and $\text{C}_6\text{H}_5\text{CH}_2\text{Hg}^+$ (2.0×10^{-3} M), done in 2:1 solution of THF:H₂O ($[\text{H}^+] = 0.25$ M, $\mu = 0.50$ M, $T = 25.0^\circ$) the rate constants were 30 and 29 M⁻¹s⁻¹, respectively. The mixed solvent was used in this case to avoid precipitation of the water-insoluble diorganomercury product. The products of the $\text{C}_6\text{H}_5\text{Hg}^+$ reactions mentioned above were also insoluble in water, but it was possible to observe the reactions on the stopped-flow instrument before precipitation occurred.

In each of the above pairs of experiments, it can be seen that changing the R group in the mercuric species does not have much effect on the rate of its reaction with a given organochromium substrate. The rates of the Hg^{2+} reactions,

on the other hand, were systematically much higher than for RHg^+ reactions. It was therefore decided to use only Hg^{2+} and CH_3Hg^+ for the systematic kinetic studies, the later reactant being the most convenient of the three RHg^+ species to work with in terms of preparation and stability of stock solution, and solubility of organomercury products.

Another result from the preliminary experiments is that the rate of reactions of $\text{CrCH}_2\text{C}_6\text{H}_5^{2+}$ with either CH_3Hg^+ or Hg^{2+} is not affected by the presence of oxygen, even though benzylchromium(III) ion is known to react slowly with O_2 (4,24). Apparently, in this case the reaction of interest is so fast that the reaction with O_2 does not interfere. Later, it was found in one system that the reaction of the CrR^{2+} with O_2 did compete with the electrophilic reaction, and it was necessary to carry out the reactions under air-free conditions.

The dependence of the reactions on hydrogen ion concentration was investigated only cursorily in preliminary experiments since it was anticipated that runs at varying $[\text{H}^+]$ would be included in the systematic studies. The second-order rate constant for the reaction of CrCH_3^{2+} and Hg^{2+} was found to be approximately the same in $0.25 \text{ M} [\text{H}^+]$ ($\mu = 0.50 \text{ M}$) and in approximately $10^{-4} \text{ M} [\text{H}^+]$ ($\mu \approx 10^{-3} \text{ M}$). The reaction of $\text{CrCH}_2\text{C}_6\text{H}_5^{2+}$ with Hg^{2+} , however, was found to be approximately 250 times slower in $10^{-4} \text{ M} [\text{H}^+]$ ($\mu \approx 10^{-4} \text{ M}$) than in

0.25 M $[H^+]$. The reason for this disparity was not investigated but it may be related to the fact that mercuric ion exists predominantly as $HgOH^+$ at 10^{-4} M $[H^+]$ ($pK = 3.7$ (15, p. 32)). It was decided that the systematic kinetic studies be done at higher $[H^+]$ (0.1 - 0.5 M) using $LiClO_4$ to maintain ionic strength at 0.50 M.

Kinetics of Hg^{2+} reactions

Systematic kinetic studies were carried out on the reactions of Hg^{2+} and a wide range of CrR^{2+} complexes.

Pseudo-first-order conditions, with $[Hg^{2+}] \geq 10 [CrR^{2+}]$, were used in all cases except that of $CrCH_3^{2+}$ where second-order conditions were used. The Swinbourne method was used to calculate k_{obs} for all runs except those of $CrCH_2Br^{2+}$ and $CrCH_2C_6H_5^{2+}$ for which the standard method was used. Figures III-11 - III-13 show some typical first-order plots for the Hg^{2+} reactions. The linearity of all first-order plots confirms the first-order dependence on $[CrR^{2+}]$. The results of the experiments (except those for $CrCH(CH_3)_2^{2+}$) are shown in Tables III-4 - III-6.

The second-order rate constants, k_{Hg} , were all determined as the quotient, $k_{obs}/[Hg^{2+}]$ (except for $CrCH_3^{2+}$) and the reactions are shown to be first-order in $[Hg^{2+}]$ by the constancy of k_{Hg} with varying $[Hg^{2+}]$. Plots of k_{obs} vs $[Hg^{2+}]$, shown in Figures III-14 and III-15, which are linear and pass through the origin, further demonstrate that the reactions are

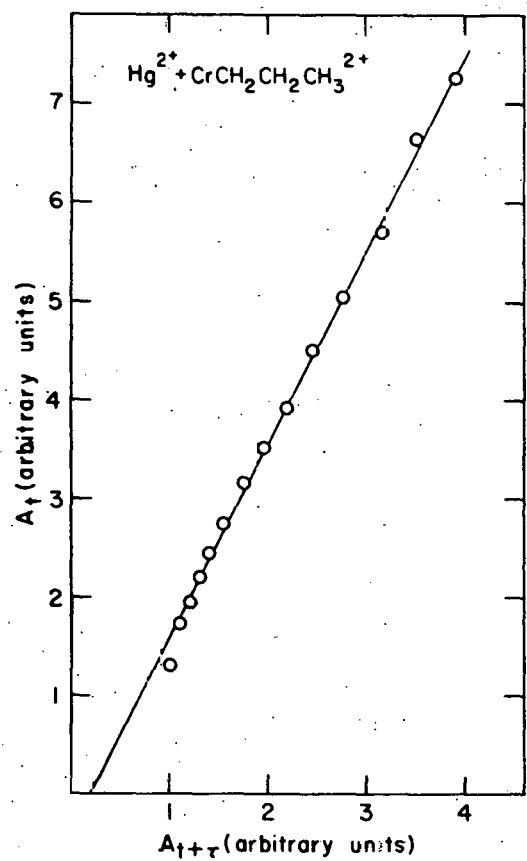


Figure III-11. Swinbourne rate plot for reaction of $\text{CrCH}_2\text{CH}_2\text{CH}_3^{2+}$ and Hg^{2+} , see Table III-4

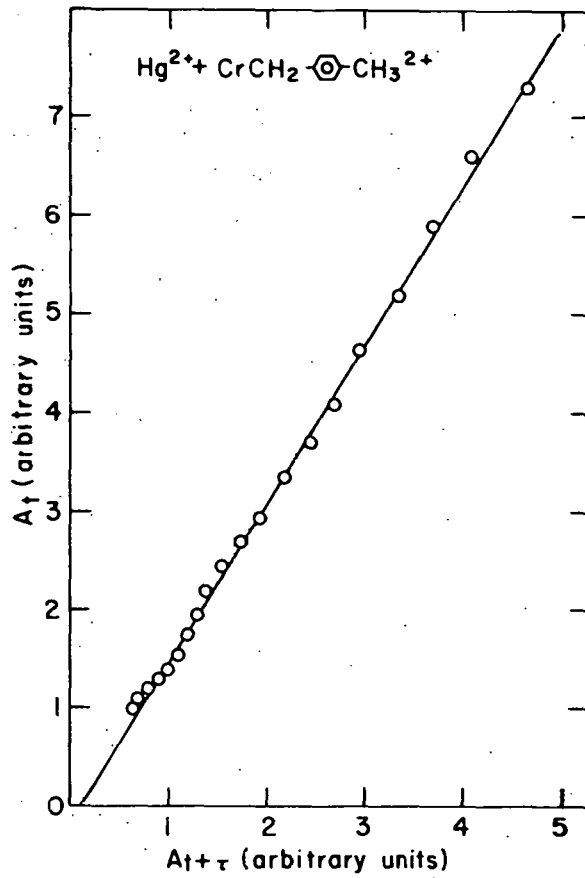


Figure III-12. Swinbourne rate plot for reaction of $\text{CrCH}_2\text{C}_6\text{H}_5^{2+}$ and Hg^{2+} , see Table III-6

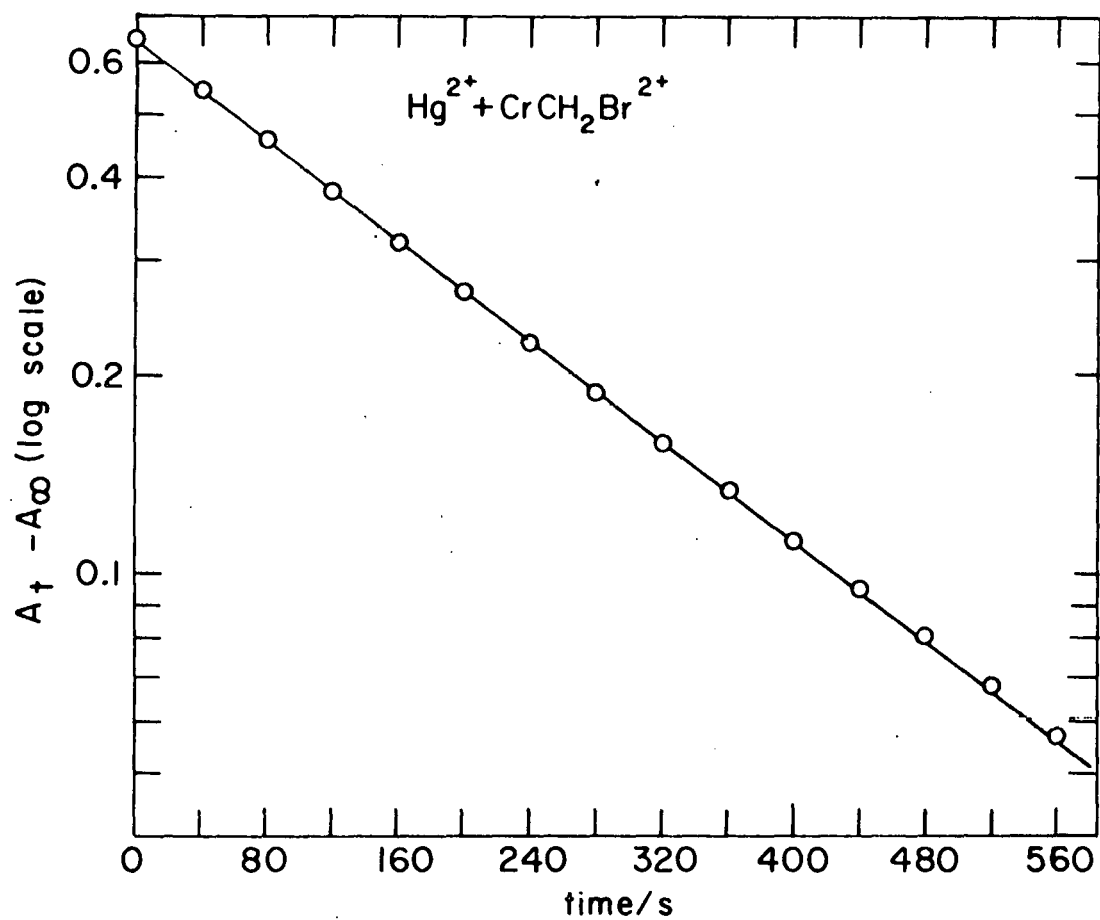


Figure III-13. Standard first-order rate plot for reaction of $\text{CrCH}_2\text{Br}^{2+}$ and Hg^{2+} , see Table III-5

Table III-4. Kinetic data for the reactions of Hg^{2+} with aliphatic CrR^{2+} complexes.
 Conditions: $[\text{H}^+] = 0.25 \text{ M}$, $\mu = 0.50 \text{ M}$, $T = 25.0^\circ$; runs done by
 stopped-flow method

R	$10^5 [\text{CrR}^{2+}] / \text{M}$	$10^4 [\text{Hg}^{2+}] / \text{M}$	λ / nm	$k_{\text{Hg}} / \text{M}^{-1} \text{s}^{-1}$	$\pm \bar{\delta} (\#)^a$	Comment
CH_3	3	0.53	258	1.1×10^7		
	3	0.53	258	0.96×10^7		
				$1.0 \pm 0.1 \times 10^7$		av k_{Hg} (25.0°)
C_2H_5	2	5.94	275	$1.36 \pm 0.08 \times 10^5$ (5)		
	3	5.94	275	$1.29 \pm 0.06 \times 10^5$ (4)		
	2	9.90	275	$1.50 \pm 0.07 \times 10^5$ (4)		
	3	5.94	275	$1.47 \pm 0.04 \times 10^5$ (3)		$[\text{H}^+] = 0.1 \text{ M}$
				$1.40 \pm 0.06 \times 10^5$		av k_{Hg} (25.0°)
$\text{CH}_2\text{CH}_2\text{CH}_3$	20	19.8	393	$3.39 \pm 0.06 \times 10^4$ (3)		
	3	1.98	275	$3.91 \pm 0.01 \times 10^4$ (2)		
	2.5	3.43	275	$3.50 \pm 0.02 \times 10^4$ (2)		
	3.6 ^b	5.02	275	$3.37 \pm 0.06 \times 10^4$ (2)		
	2.8	5.02	275	$3.36 \pm 0.04 \times 10^4$ (2)		$[\text{H}^+] = 0.10 \text{ M}$
	3.0	9.75	275	$3.16 \pm 0.02 \times 10^4$ (2)		$T = 17.7^\circ\text{C}$

^aFor each stopped-flow run, more than one trace was recorded and k computed;
 # denotes the number of traces per run and $\bar{\delta}$ is their average deviation.

^bThe first-order plot for this run is shown in Figure III-11.

Table III-4. (Continued).

R	$10^5 [\text{CrR}^{2+}] / \text{M}$	$10^4 [\text{Hg}^{2+}] / \text{M}$	λ / nm	$k_{\text{Hg}} / \text{M}^{-1} \text{s}^{-1} \pm \bar{\delta} (\#)$	Comment
$\text{CH}_2\text{CH}_2\text{CH}_3$	3.0	5.13	275	$3.00 \pm 0.03 \times 10^4$ (2)	$T = 17.7^\circ\text{C}$
	2.0	5.18	275	$4.10 \pm 0.18 \times 10^4$ (2)	$T = 29.9^\circ\text{C}$
	2.0	7.80	275	$4.06 \pm 0.21 \times 10^4$ (2)	$T = 29.9^\circ\text{C}$
				$3.50 \pm 0.17 \times 10^4$	$\text{av } k_{\text{Hg}} (25.0^\circ)$
$\text{CH}_2\text{C}(\text{CH}_3)_3$	~ 10	13.2	280	$4.7 \pm 0.1 \times 10^2$ (2)	
	~ 10	13.2	280	$5.1 \pm 0.1 \times 10^2$ (2)	Impure CrR^{2+} ^c
	~ 10	59.4	405	$4.8 \pm 0.3 \times 10^2$ (3)	
				$4.9 \pm 0.2 \times 10^2$	$\text{av } k_{\text{Hg}} (25.0^\circ)$

^cFor these runs, $\text{CrCH}_2\text{C}(\text{CH}_3)_3^{2+}$ was used without ion exchange purification as explained in the text.

Table III-5. Kinetic data for the reactions of Hg^{2+} with haloalkyl CrR^{2+} complexes.
 Conditions: $[\text{H}^+] = 0.25 \text{ M}$, $\mu = 0.50 \text{ M}$, $T = 25.0^\circ$; runs done on the
 Cary 14.

R	$10^3 [\text{CrR}^{2+}] / \text{M}$	$10^2 [\text{Hg}^{2+}] / \text{M}$	λ / nm	$k_{\text{Hg}} / \text{M}^{-1} \text{s}^{-1}$	Comment
CH ₂ Cl	1.9	2.12	390	0.579	
	1.9	3.22	390	0.583	
	1.9	3.22	390	0.596	
	1.9	3.22	390	0.569	$[\text{H}^+] = 0.135 \text{ M}$
	1.9	4.76	390	0.622	$[\text{H}^+] = 0.135 \text{ M}$
	1.9	3.22	390	0.365	$T = 17.3^\circ$
	1.9	3.22	390	0.348	$T = 17.3^\circ$
	1.9	3.22	390	0.746	$T = 29.4^\circ$
	1.9	3.22	390	0.714	$T = 29.4^\circ$
	1.9	3.22	390	1.04	$T = 36.0^\circ$
	1.9	3.22	390	1.01	$T = 36.0^\circ$
				0.590 ± 0.015	av k_{Hg} (25.0°)
CH ₂ Br	0.71	0.952	395	0.449	
	0.71	0.952	395	0.434	
	0.71 ^a	0.952	395	0.474	$[\text{H}^+] = 0.50 \text{ M}$
	0.71	3.81	395	0.514	$[\text{H}^+] = 0.50 \text{ M}$
				0.468 ± 0.026	av k_{Hg} (25.0°)

^aThe first-order plot for this run is shown in Figure III-13.

Table III-6. Kinetic data for the reactions of Hg^{2+} with para-substituted benzyl-chromium(III) ions, $\text{CrCH}_2-\text{C}_6\text{H}_4-\text{Z}^{2+}$. Conditions: $[\text{H}^+] = 0.25 \text{ M}$, $\mu = 0.50 \text{ M}$, $T = 25.0^\circ$; runs done by stopped-flow method

Z	$10^5 [\text{CrR}^{2+}] / \text{M}$	$10^4 [\text{Hg}^{2+}] / \text{M}$	λ / nm	$10^{-4} k_{\text{Hg}} / \text{M}^{-1} \text{s}^{-1} \pm \bar{\delta} (\#)$ ^a	Comment
H	5.8 ^b	6.03	355	4.79 ± 0.18	(3)
	6.8	6.53	355	4.93 ± 0.28	(2) $[\text{H}^+] = 0.10 \text{ M}$
	6.0	11.9	355	4.89 ± 0.22	(3)
				4.87 ± 0.22	av k_{Hg} (25.0°)
CH_3	2.6	2.64	301	4.82 ± 0.11	(3)
	5.4	5.94	301	5.34 ± 0.12	(3)
	6.2	5.94	301	5.51 ± 0.09	(3)
				5.22 ± 0.27	av k_{Hg} (25.0°)
Br	2	5.27	298	2.95 ± 0.06	(3)
	2	10.5	298	3.01 ± 0.09	(3)
				2.98 ± 0.07	av k_{Hg} (25.0°)
CF_3	4.3	5.02	298	2.11 ± 0.09	(3)
	5.3	10.6	298	2.09 ± 0.04	(3)
				2.10 ± 0.06	av k_{Hg} (25.0°)

^aFor each stopped-flow run more than one trace was recorded and k computed; # denotes the number of traces per run and $\bar{\delta}$ is their average deviation.

^bThe Swinbourne plot for this run is shown in Figure III-12.

Table III-6. (Continued)

Z	$10^5 [\text{CrR}^{2+}] / \text{M}$	$10^4 [\text{Hg}^{2+}] / \text{M}$	λ / nm	$10^{-4} k_{\text{Hg}} / \text{M}^{-1} \text{s}^{-1}$	$\pm \bar{\delta}$ (#)	Comment
CN	2.6	3.04	312	1.64 \pm 0.05	(3)	
	5.2	3.30	312	1.53 \pm 0.12	(3)	$[\text{H}^+] = 0.10 \text{ M}$
	5.2	6.60	312	1.74 \pm 0.02	(3)	
						av k_{Hg} (25.0°)

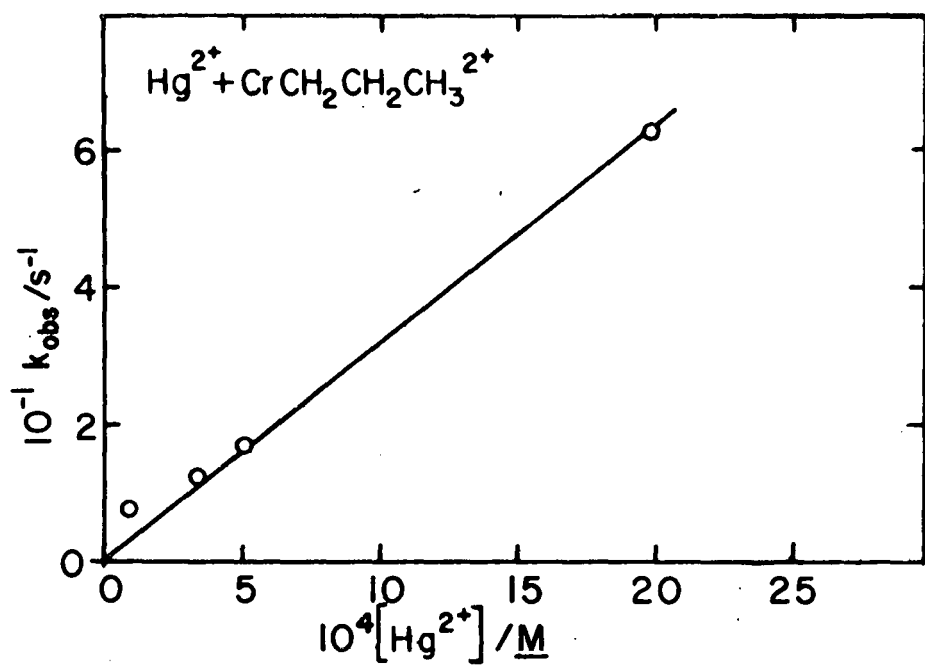


Figure III-14. Plot showing first-order dependence on $[Hg^{2+}]$ in reaction with $CrCH_2CH_2CH_3^{2+}$

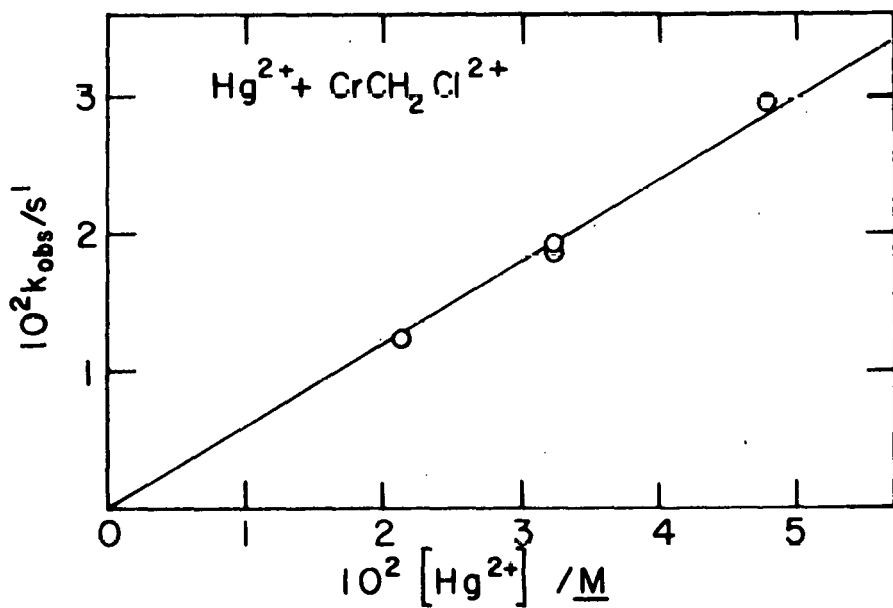


Figure III-15. Plot showing first-order dependence on $[\text{Hg}^{2+}]$ in reaction with $\text{CrCH}_2\text{Cl}^{2+}$

first-order in $[\text{Hg}^{2+}]$. It is assumed that those reactions on which only a few runs were done are also first-order in $[\text{Hg}^{2+}]$, and thus conform to the rate law given in equation III-21.

The reaction of CrCH_3^{2+} with Hg^{2+} (Table III-4) was studied under second-order conditions owing to its high rate. The details of computation of k_{Hg} are given in the Experimental section. Since the value of $[\text{CrCH}_3^{2+}]$ and $[\text{Hg}^{2+}]$ are rather uncertain (the ϵ value for CrCH_3^{2+} cannot be measured accurately) and since the kinetic runs were done at a fast sweep speed (2 ms/div), the k_{Hg} value of this reaction shown in Table III-4 should be regarded as a rough estimate.

For the reaction of $\text{CrCH}_2\text{C}(\text{CH}_3)_3^{2+}$ with Hg^{2+} (Table III-4) unpurified samples of the organochromium(III) complex were used, since the species decomposes so fast. The reaction mixtures for these runs therefore contained impurities not present in experiments on the other reactions. To determine how much error might be introduced because of this procedure, two runs were done on the reaction of $\text{CrCH}_2\text{CH}_2\text{CH}_3^{2+}$ with Hg^{2+} using impure samples of n-propylchromium(III) ion made in the same way as the neopentylchromium(III) species. The k_{Hg} value from these runs was $3.4 \times 10^4 \text{ M}^{-1}\text{s}^{-1}$ compared with $3.5 \times 10^4 \text{ M}^{-1}\text{s}^{-1}$ for the runs using pure $\text{CrCH}_2\text{CH}_2\text{CH}_3^{2+}$. It is concluded that the impurities present in the $\text{CrCH}_2\text{C}(\text{CH}_3)_3^{2+}$ runs do not interfere with the reaction with Hg^{2+} .

The kinetics experiments represented in Tables III-4 - III-6 for reactions of CrR^{2+} complexes not specifically

mentioned above were done in routine fashion according to the procedures described in the Experimental section. Included in Tables III-4 - III-6, along with the k_{Hg} of the individual runs, are average values of k_{Hg} at 25°.

The data for the $\text{CrCH}(\text{CH}_3)_2^{2+}$ reaction is shown in Table III-7. The plot of k_{obs} vs $[\text{Hg}^{2+}]$, shown in Figure III-16, in this case does not pass through the origin but has an intercept at $k_{\text{obs}} \approx 4 \times 10^{-4} \text{ s}^{-1}$. This result implies an $[\text{Hg}^{2+}]$ -independent term for the rate of consumption of $\text{CrCH}(\text{CH}_3)_2^{2+}$; the rate law thus becomes

$$-\frac{d[\text{CrR}^{2+}]}{dt} = k_{Hg}[\text{Hg}^{2+}][\text{CrR}^{2+}] + k_h[\text{CrR}^{2+}] \quad (\text{III-22})$$

This Hg^{2+} -independent term is due to hydrolysis of $\text{CrCH}(\text{CH}_3)_2^{2+}$, as independent experiments on the hydrolysis reaction gave a rate constant, k_h of $3 \times 10^{-4} \text{ s}^{-1}$ in the absence of oxygen. The hydrolysis in the presence of oxygen has a k_h of $\approx 3 \times 10^{-3} \text{ s}^{-1}$, and therefore the runs on the $\text{CrCH}(\text{CH}_3)_2^{2+}$ reaction with Hg^{2+} were done under air-free conditions. The slope of the line in Figure III-16 is $1.56 \pm 0.01 \text{ M}^{-1}\text{s}^{-1}$ which is the k_{Hg} value for this reaction.

In addition to the experiments represented in Tables III-4 - III-7, one run was attempted on the reaction of CrCF_3^{2+} and Hg^{2+} . With $[\text{CrCF}_3^{2+}] = 5.6 \times 10^{-3} \text{ M}$ and $[\text{Hg}^{2+}] = 0.37 \text{ M}$, no change in absorbance was observed at $\lambda 380 \text{ nm}$ after 24 hours. The upper limit on k_{Hg} is therefore $10^{-6} \text{ M}^{-1}\text{s}^{-1}$.

Table III-7. Kinetic data for the reaction of Hg^{2+} with $\text{CrCH}(\text{CH}_3)_2^{2+}$. Conditions: $[\text{H}^+] = 0.25 \text{ M}$, $\mu = 0.50 \text{ M}$, $\lambda = 290 \text{ nm}$, $T = 25.0^\circ$; runs done on Cary 14

$10^4 [\text{CrR}^{2+}] / \text{M}$	$10^3 [\text{Hg}^{2+}] / \text{M}$	$10^3 k_{\text{obs}} / \text{s}^{-1}$
1	0.952	1.81
1	1.94	3.40
1	3.50	5.78
1	6.32	10.2

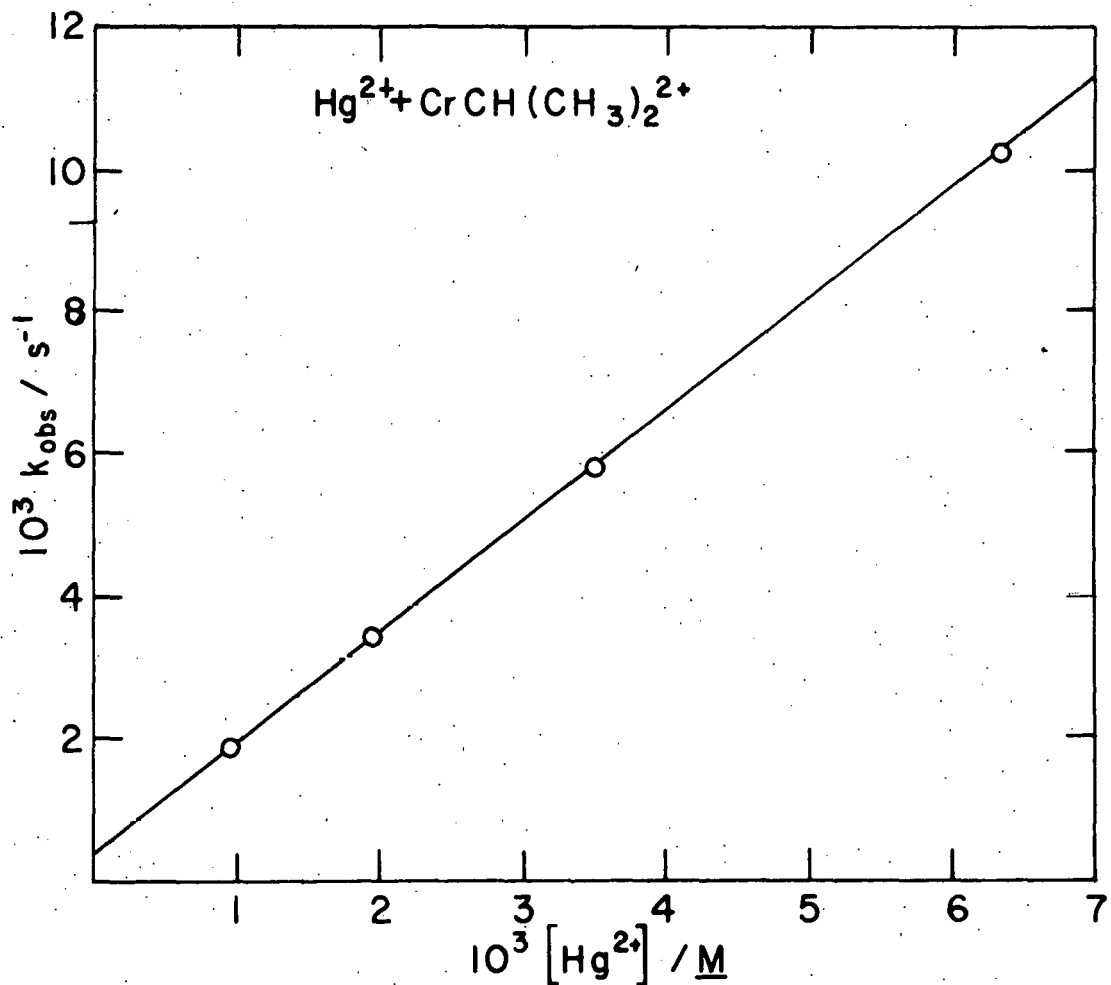


Figure III-16. Plot showing dependence on $[\text{Hg}^{2+}]$ in reaction with $\text{CrCH}(\text{CH}_3)_2^{2+}$, note nonlinear intercept

Finally, several of the reactions were studied as a function of $[H^+]$ between 0.1 and 0.5 M as shown in Tables III-4 - III-6 and in none of these was a significant difference in the second-order rate constant observed. This is true also for the $\text{CrCH}(\text{CH}_3)_2^{2+}$ reaction, since experiments done at $[H^+]$ of 0.10 M , 0.25 M , and 0.40 M in the presence of oxygen (not included in Table III-7) gave identical k_{obs} values. It is assumed that all reactions of Hg^{2+} with CrR^{2+} complexes are independent of $[H^+]$ between 0.10 M and 0.50 M .

Kinetics of CH_3Hg^+ reactions

Systematic kinetic studies were also carried out on the reactions of CH_3HgOAc with most of the CrR^{2+} complexes mentioned above for the Hg^{2+} reactions.

Pseudo-first-order conditions were used in all cases with $[\text{CH}_3\text{Hg}^+] \geq 10[\text{CrR}^{2+}]$, and Swinbourne method was used to calculate k_{obs} except for the $\text{CrCH}_2\text{C}_6\text{H}_5^{2+}$ reaction where the standard method was used. Some typical first-order plots are shown in Figures III-17 - III-19. The linearity of these plots (and those for all the other experiments) confirms the first-order dependence on $[\text{CrR}^{2+}]$.

The results of the experiments (except those for the $\text{CrCH}_2(\text{CH}_3)_3^{2+}$ reaction) are given in Tables III-8 and III-9. The second-order rate constants, k_{MeHg} , were computed as $k_{\text{obs}}/[\text{CH}_3\text{Hg}^+]$. The first-order dependence of the reactions

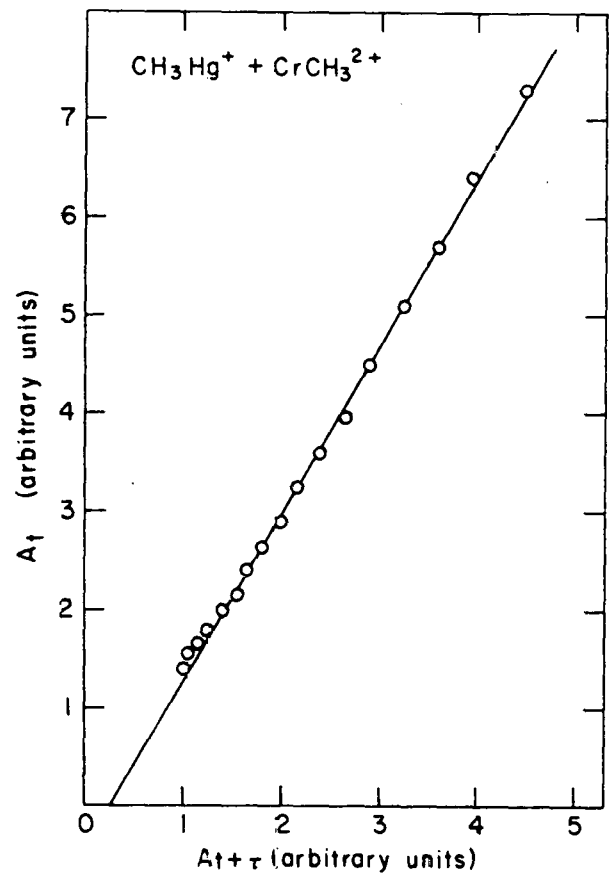


Figure III-17. Swinbourne rate plot for reaction of CrCH_3^{2+} and CH_3Hg^+ , see Table III-8

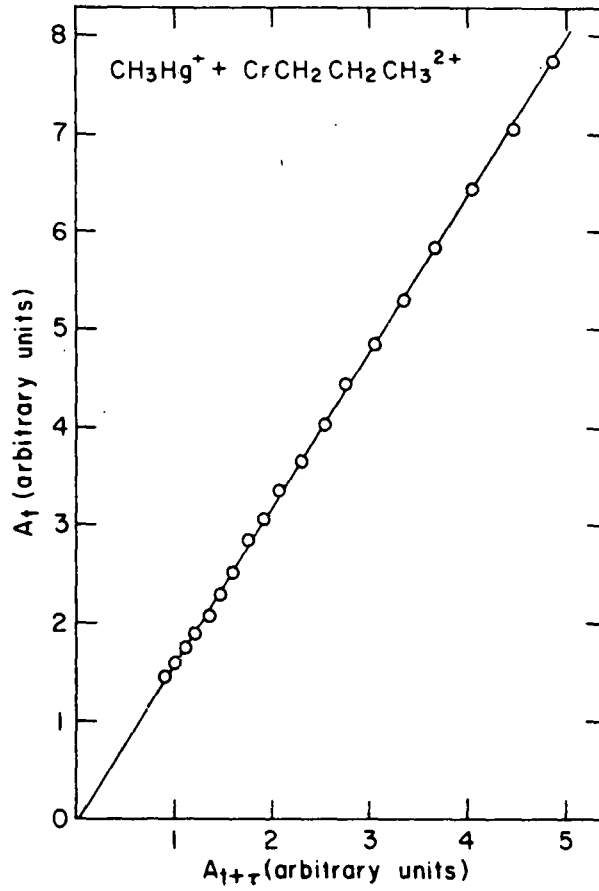


Figure III-18. Swinbourne rate plot for reaction of $\text{CrCH}_2\text{CH}_2\text{CH}_3^{2+}$ and CH_3Hg^+ , see Table III-8

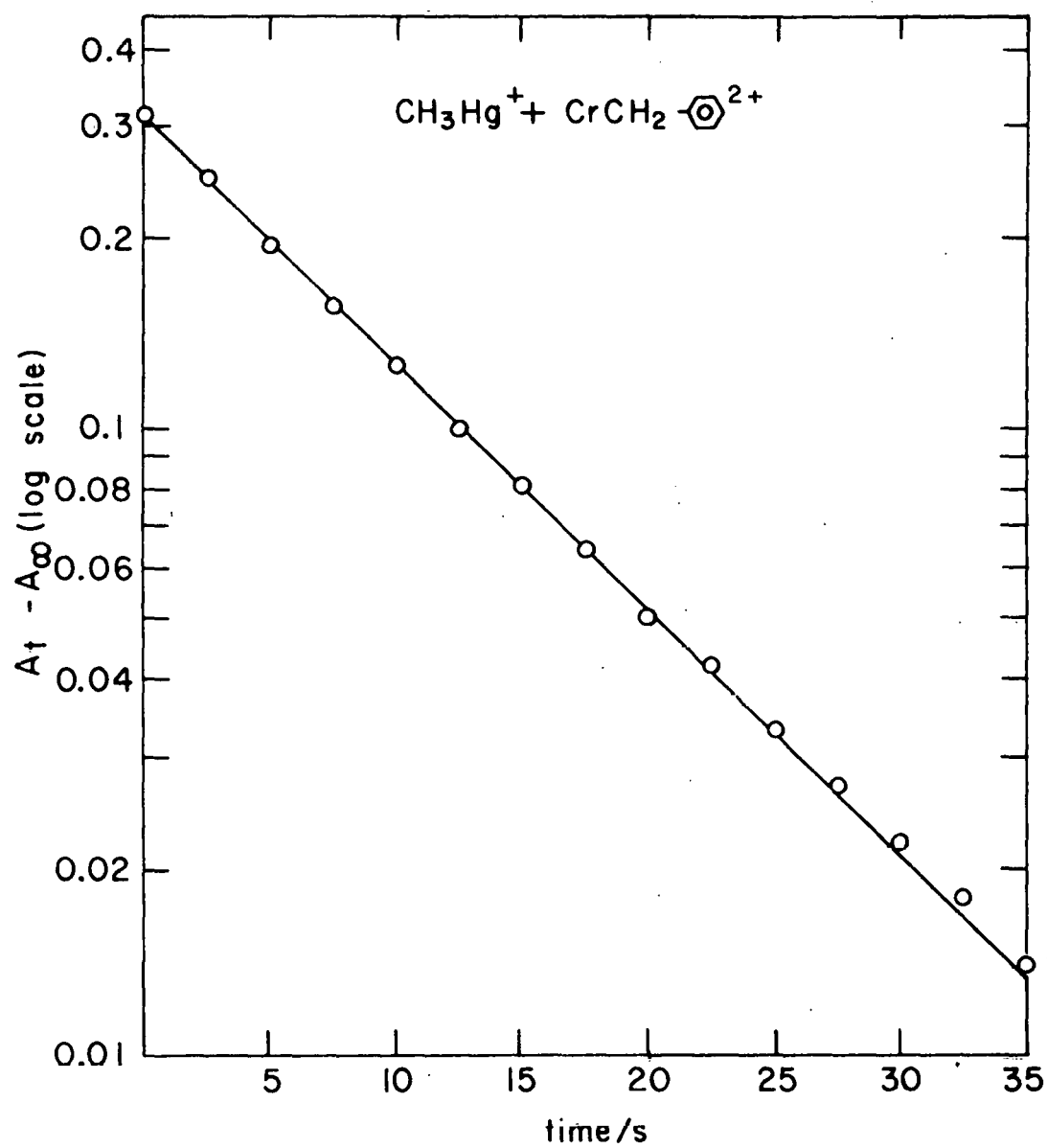


Figure III-19. Standard first-order rate plot for reaction of $\text{CrCH}_2\text{C}_6\text{H}_5^{2+}$ and CH_3Hg^+ , see Table III-9

Table III-8. Kinetic data for the reactions of $\text{CH}_3\text{Hg}^{2+}$ and aliphatic CrR^{2+} complexes. Conditions: $[\text{H}^+] = 0.25 \text{ M}$, $\mu = 0.50 \text{ M}$, $T = 25.0^\circ$; runs done by stopped-flow method

R	$10^5 [\text{CrR}^{2+}] / \text{M}$	$10^3 [\text{CH}_3\text{Hg}^{2+}] / \text{M}$	λ / nm	$k_{\text{MeHg}} / \text{M}^{-1} \text{s}^{-1} \pm \bar{\delta}$	(#) ^a	Comment
CH_3	3	1.06	258	$1.11 \pm 0.01 \times 10^4$	(3)	
	2	0.427	258	$1.14 \pm 0.06 \times 10^4$	(4)	
	2	0.627	258	$1.17 \pm 0.01 \times 10^4$	(3)	
	2	0.636	258	$1.64 \pm 0.09 \times 10^4$	(4)	$[\text{H}^+] = 0.10 \text{ M}$
	3	0.627	258	$1.53 \pm 0.09 \times 10^4$	(3)	$[\text{H}^+] = 0.10 \text{ M}$
	3 ^b	0.627	258	$1.06 \pm 0.02 \times 10^4$	(3)	$[\text{H}^+] = 0.40 \text{ M}$
	2	0.627	258	$3.16 \pm 0.26 \times 10^4$	(2)	$[\text{H}^+] = 0.02 \text{ M}$
CH_2CH_3	3	1.06	257	$1.97 \pm 0.03 \times 10^2$	(3)	
	2	1.59	275	$2.05 \pm 0.06 \times 10^2$	(3)	$[\text{H}^+] = 0.10 \text{ M}$
	3	2.12	275	$1.97 \pm 0.04 \times 10^2$	(3)	
				$1.99 \pm 0.04 \times 10^2$	av k_{MeHg}	(25.0°)
$\text{CH}_2\text{CH}_2\text{CH}_3$	6	0.976	275	$1.37 \pm 0.05 \times 10^2$	(3)	
	5	1.06	275	$1.16 \pm 0.01 \times 10^2$	(3)	
	17	1.99	393	$1.20 \pm 0.05 \times 10^2$	(2)	

^aFor each stopped-flow run more than one trace was recorded and k computed; # denotes the number of traces per run, and $\bar{\delta}$ is their average deviation.

^bThe Swinbourne plot for this run is shown in Figure III-17.

Table III-8. (Continued)

R	$10^5 [\text{CrR}^{2+}] / \text{M}$	$10^3 [\text{CH}_3\text{Hg}^+] / \text{M}$	λ / nm	$k_{\text{MeHg}} / \text{M}^{-1} \text{s}^{-1}$	$\pm \bar{\delta}$	(#)	Comment
$\text{CH}_2\text{CH}_2\text{CH}_3$	5 ^c	2.12	275	$1.16 \pm 0.03 \times 10^2$		(6)	
	5	2.12	275	$1.17 \pm 0.05 \times 10^2$		(4)	
	15	3.04	393	$1.23 \pm 0.14 \times 10^2$		(3)	
	17	4.10	393	$1.34 \pm 0.10 \times 10^2$		(2)	
	5	4.10	275	$1.14 \pm 0.02 \times 10^2$		(2)	$[\text{H}^+] = 0.10 \text{ M}$
	5	2.12	275	$0.78 \pm 0.01 \times 10^2$		(6)	$T = 15.1^\circ$
	5	2.12	275	$1.73 \pm 0.05 \times 10^2$		(5)	$T = 35.1^\circ$
	5	2.12	275	$2.35 \pm 0.05 \times 10^2$		(5)	$T = 41.4^\circ$
						$1.21 \pm 0.08 \times 10^2$	av k_{MeHg} (25.0°)

^cThe Swinbourne plot for this run is shown in Figure III-18.

Table III-9. Kinetic data for reactions of CH_3Hg^+ and para-substituted benzyl-chromium(III) complexes, $\text{CrCH}_2-\text{C}_6\text{H}_4-\text{Z}$. Conditions: $[\text{H}^+] = 0.25 \text{ M}$, $\mu = 0.50 \text{ M}$, $T = 25.0^\circ$; runs done on Cary 14 unless otherwise indicated

Z	$10^5 [\text{CrR}^{2+}] / \text{M}$	$10^4 [\text{CH}_3\text{Hg}^+] / \text{M}$	λ / nm	$k_{\text{MeHg}} / \text{M}^{-1} \text{s}^{-1}$	Comment
H	4.3	5.55	297	96	
	4.3	5.55	297	97	
	4.3	4.71	297	101	
	4.3	4.71	297	98	
	6	4.62	297	104	$[\text{H}^+] = 0.10 \text{ M}$
	6	4.62	297	106	$[\text{H}^+] = 0.10 \text{ M}$
	6	4.62	297	98	$[\text{H}^+] = 0.50 \text{ M}$
	6	4.62	297	97	$[\text{H}^+] = 0.50 \text{ M}$
	5.7	6.11	297	101	
	5.7	6.19	297	100	
5.7	6.19	297	102		
	10^a	9.80	355	100	
	10	9.80	355	98	

^aThe first-order plot for this run is shown in Figure III-19.

Table III-9. (Continued)

Z	$10^5 [\text{CrR}^{2+}] / \text{M}$	$10^4 [\text{CH}_3\text{Hg}^+] / \text{M}$	λ / nm	$k_{\text{MeHg}} / \text{M}^{-1} \text{s}^{-1}$	Comment
H	2	99.0	290	98 ± 4	(4) ^b
	2	99.0	290	96 ± 2	(3) ^b
				98 ± 1	av k_{MeHg} (25.0°)
CH_3	4.2	4.22	301	120	
	4.2	4.22	301	128	
	4.2	4.22	301	126	
	41	49.2	301	115 ± 4 121 ± 5	(2) ^b av k_{MeHg} (25.0°)
Br	3.6	10.3	298	59.4	
	3.6	10.3	298	56.7	
	3.6	10.3	298	54.2	
				56.8 ± 1.8	av k_{MeHg} (25.0°)
CF_3	7	10.3	298	35.7	
	7	10.3	298	33.5	
	7	10.3	298	34.9	
				34.7 ± 0.8	av k_{MeHg} (25.0°)

^bFor stopped-flow runs more than one trace was recorded and k_{MeHg} was computed for each. The k_{MeHg} values are given with average deviations and the number of traces per run.

Table III-9. (Continued)

Z	$10^5 [\text{CrR}^+]/\text{M}$	$10^4 [\text{CH}_3\text{Hg}^+]/\text{M}$	λ/nm	$k_{\text{MeHg}}/\text{M}^{-1}\text{s}^{-1}$	Comment
CN	7	8.0	312	23.7	
	7	8.03	312	24.4	
	11	17.2	312	24.1	
	11	17.2	312	23.0	
	11	17.2	312	24.1	
				23.9 ± 0.4	av k_{MeHg} (25.0°)

on $[\text{CH}_3\text{Hg}^+]$ is confirmed by the constancy of k_{MeHg} with varying methylmercuric ion concentration. Linear plots of k_{obs} vs $[\text{CH}_3\text{Hg}^+]$ for two of the reactions shown in Figures III-20 and III-21 further demonstrate this point. It is assumed that the reactions represented in Tables III-8 and III-9 for which only a few runs were done are also first-order in $[\text{CH}_3\text{Hg}^+]$ and thus conform to the rate law shown in equation III-21.

The results of the $\text{CrCH}_2\text{C}(\text{CH}_3)_3^{2+}$ reaction with CH_3Hg^+ are shown in Table III-10. In this case, the least-squares line of the plot of k_{obs} vs $[\text{CH}_3\text{Hg}^+]$ does not pass through the origin, as shown in Figure III-22; the intercept at $[\text{CH}_3\text{Hg}^+] = 0$ is $\sim 1 \times 10^{-2} \text{ s}^{-1}$. As in the reaction of Hg^{2+} and $\text{CrCH}(\text{CH}_3)_2^{2+}$ mentioned previously, this result indicates that hydrolysis of $\text{CrCH}_2\text{C}(\text{CH}_3)_3^{2+}$ interferes with the electrophilic reaction such that the rate law for the consumption of $\text{CrCH}_2\text{C}(\text{CH}_3)_3^{2+}$ complex is analogous to equation III-22. Independent experiments on the hydrolysis of $\text{CrCH}_2\text{C}(\text{CH}_3)_3^{2+}$ gave a rate constant, k_h , of $(4 \pm 1) \times 10^{-3} \text{ s}^{-1}$, and this number was insensitive to the presence of oxygen and hydrogen ion concentration. The disparity between the intercept in Figure III-22 and the directly-measured value of k_h may be due either to catalysis of the hydrolysis reaction by CH_3Hg^+ or simply to experimental error in the points in Figure III-22. The value of k_{MeHg} for this reaction,

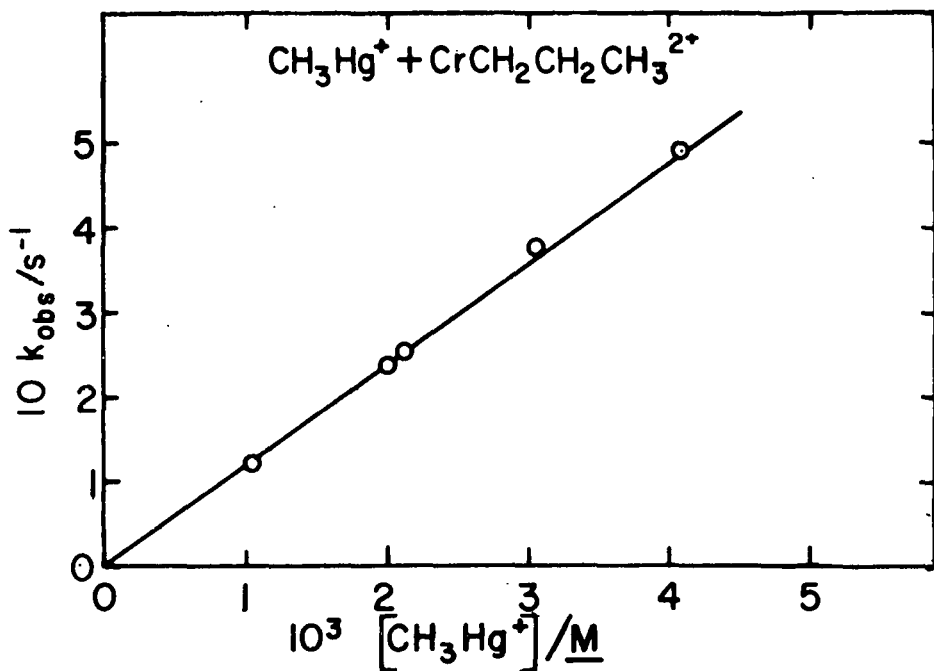


Figure III-20. Plot showing first order dependence on $[\text{CH}_3\text{Hg}^+]$ for reaction with $\text{CrCH}_2\text{CH}_2\text{CH}_3^{2+}$

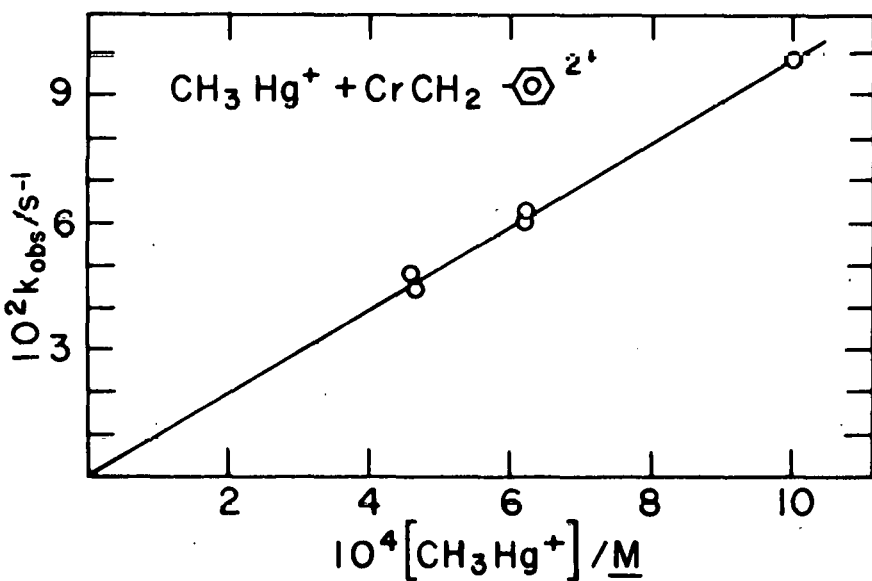


Figure III-21. Plot showing first-order dependence on $[\text{CH}_3\text{Hg}^+]$ for reaction with $\text{CrCH}_2\text{C}_6\text{H}_5^{2+}$

Table III-10. Kinetic data on reaction of $\text{CrCH}_2\text{C}(\text{CH}_3)_3^{2+}$ and CH_3Hg^+ . Conditions: $[\text{H}^+] = 0.25 \text{ M}$, $\mu = 0.50 \text{ M}$, $T = 25.0^\circ$, $[\text{CrR}^{2+}] = \sim 3 \times 10^{-4} \text{ M}$

$10^3 [\text{CH}_3\text{Hg}^+]$	$10^2 k_{\text{obs}} / \text{s}^{-1} \pm \bar{\delta}$	(#) ^a	λ/nm	Comment
1.78	2.25 ± 0.05	(2)	405	
2.21	2.17 ± 0.10	(2)	280	
2.41	2.12	(1)	280	$[\text{H}^+] = 0.10 \text{ M}$
2.41	2.55	(1)	280	$[\text{H}^+] = 0.40 \text{ M}$
4.82	4.47	(1)	280	
4.82	4.26	(1)	260	
5.00	3.62	(1)	405	
8.34	5.68	(1)	405	

^aRuns carried out by stopped-flow method. In this case only 1 or 2 traces per run could be obtained since the reaction is slow and decomposition is significant. In runs where two traces were obtained, δ is the average deviation.

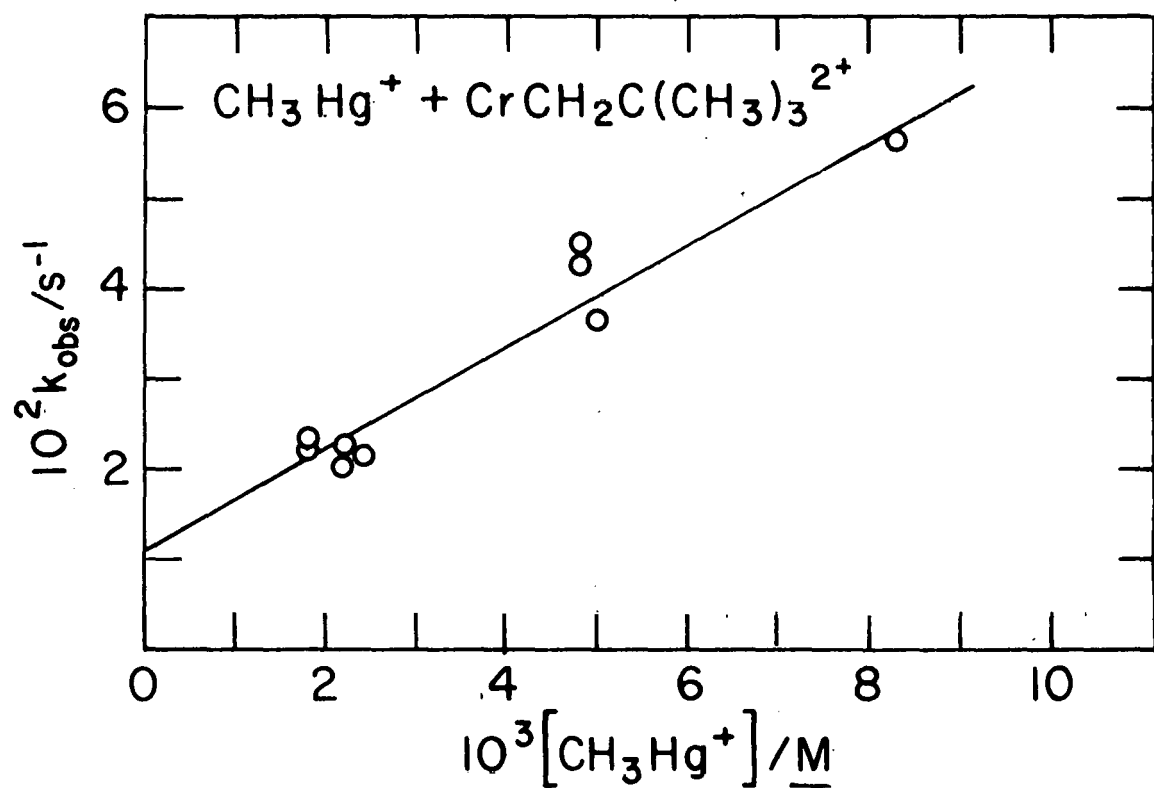


Figure III-22. Plot showing dependence on $[\text{CH}_3\text{Hg}^+]$ for reaction with $\text{CrCH}_2\text{C}(\text{CH}_3)_3^{2+}$, note non-zero intercept

computed as the least-squares slope of the line in Figure III-22, is $5.8 \pm 0.6 \text{ M}^{-1}\text{s}^{-1}$.

The experiments on the reaction of $\text{CrCH}_2\text{C}(\text{CH}_3)_3^{2+}$ with CH_3Hg^+ (Table III-8) were done using unpurified samples of $\text{CrCH}_2\text{C}(\text{CH}_3)_3^{2+}$. One kinetic run was done on the reaction of $\text{CrCH}_2\text{CH}_2\text{CH}_3^{2+}$ and CH_3Hg^+ to check the validity of the procedure. The value of k_{MeHg} measured in this experiment was $97 \text{ M}^{-1}\text{s}^{-1}$ compared with $121 \pm 8 \text{ M}^{-1}\text{s}^{-1}$ for runs using pure $\text{CrCH}_2\text{CH}_2\text{CH}_3^{2+}$. The agreement of these numbers is not so good as in the reaction of Hg^{2+} and $\text{CrCH}_2\text{CH}_2\text{CH}_3^{2+}$ (see above); so the value of k_{MeHg} for the $\text{CrCH}_2\text{C}(\text{CH}_3)_3^{2+}$ reaction given above should be regarded as a rough estimate of the true value. It may be that, whereas the impurities present in reaction solutions are innocuous to the fast Hg^{2+} reaction, they interfere with the slower CH_3Hg^+ reactions. This rationale may also help explain the large scatter in Figure III-22.

The reaction of CH_3Hg^+ and $\text{CrCH}_2\text{Cl}^{2+}$ was very slow and only two crude experiments were done in which temperature was not controlled. In a run carried out at $\lambda 268 \text{ nm}$ with $[\text{CrCH}_2\text{Cl}^{2+}] = 8 \times 10^{-5} \text{ M}$, and $[\text{CH}_3\text{Hg}^+] = 1.9 \times 10^{-2} \text{ M}$ ($[\text{H}^+] = 0.25 \text{ M}$, $\mu = 0.50 \text{ M}$, $T = \text{room temperature}$) the value of k_{MeHg} was $5.8 \times 10^{-4} \text{ M}^{-1}\text{s}^{-1}$. In a similar run at $\lambda 390 \text{ nm}$ with $[\text{CrCH}_2\text{Cl}^{2+}] = 2.0 \times 10^{-3} \text{ M}$ and $[\text{CH}_3\text{Hg}^+] = 1.4 \times 10^{-2} \text{ M}$, the value of k_{MeHg} was $8.5 \times 10^{-4} \text{ M}^{-1}\text{s}^{-1}$. The average value

of $6 \times 10^{-4} \text{ M}^{-1}\text{s}^{-1}$ should be regarded as a rough estimate of k_{MeHg} for this reaction. The reactions of CH_3Hg^+ with $\text{CrCH}_2\text{Br}^{2+}$ and $\text{CrCH}(\text{CH}_3)_2^{2+}$ were expected to be just as slow and no kinetic runs were done at all.

As in the case of the Hg^{2+} reactions, the reactions of CH_3Hg^+ and CrR^{2+} complexes (with one exception) are insensitive to $[\text{H}^+]$ between 0.10 M and 0.50 M , as shown in Tables III-8 and III-9. The reaction of CrCH_3^{2+} does show a mild $[\text{H}^+]$ dependence (Table III-8) which takes the form of $k_{\text{MeHg}} = a + b/[\text{H}^+]$ as shown by a plot of k_{MeHg} vs $[\text{H}^+]^{-1}$ in Figure III-23. The origin of this $[\text{H}^+]$ dependence was not investigated further, and we have no explanation for it. Since the k_{MeHg} value to be compared to those of the other reactions should be the $[\text{H}^+]$ -independent term, the intercept at $[\text{H}^+]^{-1} = 0$ in Figure III-23, $1 \times 10^4 \text{ M}^{-1}\text{s}^{-1}$, is taken as the k_{MeHg} for the reaction of CrCH_3^{2+} and CH_3Hg^+ .

Activation parameters and Hammett correlations

The reactions of $\text{CrCH}_2\text{CH}_2\text{CH}_3^{2+}$ with Hg^{2+} and CH_3Hg^+ and that of $\text{CrCH}_2\text{Cl}^{2+}$ with Hg^{2+} were studied as a function of temperature to determine activation parameters. These data are included in Tables III-4, III-5, and III-8. The values of ΔH^\ddagger and ΔS^\ddagger for the three reactions were computed according to the Eyring equation (61),

$$\ln \frac{k}{T} = \ln \frac{R}{N_h} + \frac{\Delta S^\ddagger}{R} - \frac{\Delta H^\ddagger}{RT} \quad (\text{III-23})$$

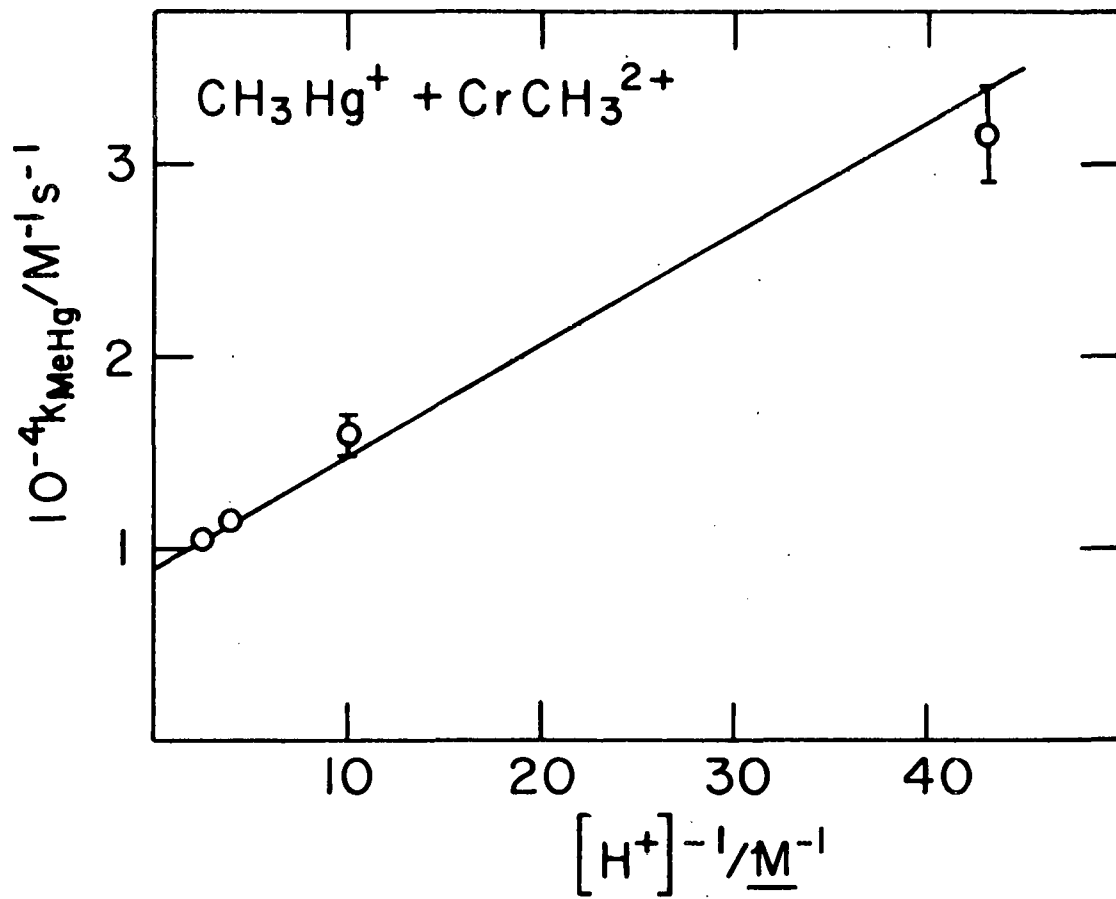


Figure III-23. Plot of k_{MeHg} vs $[H^+]^{-1}$ for reaction of CrCH_3^{2+} and CH_3Hg^+

where R in this instance is the gas constant, N is Avogadro's number, and h is Planck's constant. The computations were carried out using a program which calculates the slope of a plot of $\ln k/T$ vs $1/T$ by the method of least-squares.

The Eyring plots for the three reactions are shown in Figures III-24 - III-26 with the experimental points used in the calculations. For the reaction of $\text{CrCH}_2\text{CH}_2\text{CH}_3^{2+}$ and Hg^{2+} , ΔH^\ddagger and ΔS^\ddagger are 13.8 ± 3.3 kJ/mole and -111 ± 11 J/K mole, respectively; for $\text{CrCH}_2\text{Cl}^{2+}$ and Hg^{2+} , ΔH^\ddagger and ΔS^\ddagger are 39.8 ± 0.8 kJ/mole and -116 ± 3 J/K mole, respectively; and for $\text{CrCH}_2\text{CH}_2\text{CH}_3^{2+}$ and CH_3Hg^+ , ΔH^\ddagger and ΔS^\ddagger are 28.6 ± 2.4 kJ/mole and -109 ± 8 J/K mole, respectively. These data will be discussed in a later section.

The second-order rate constants for the reactions of the para-substituted benzylchromium(III) ions with Hg^{2+} and CH_3Hg^+ (Tables III-6 and III-9) were used to determine whether the substituent effect follows the Hammett equation,¹

$$\log k = \log k_0 + \rho\sigma \quad (\text{III-24})$$

Table III-11 summarizes the second-order-rate constants for the reactions and shows the Hammett sigma values for the

¹The theory of the Hammett relation and definitions of terms are described in detail in reference 62.

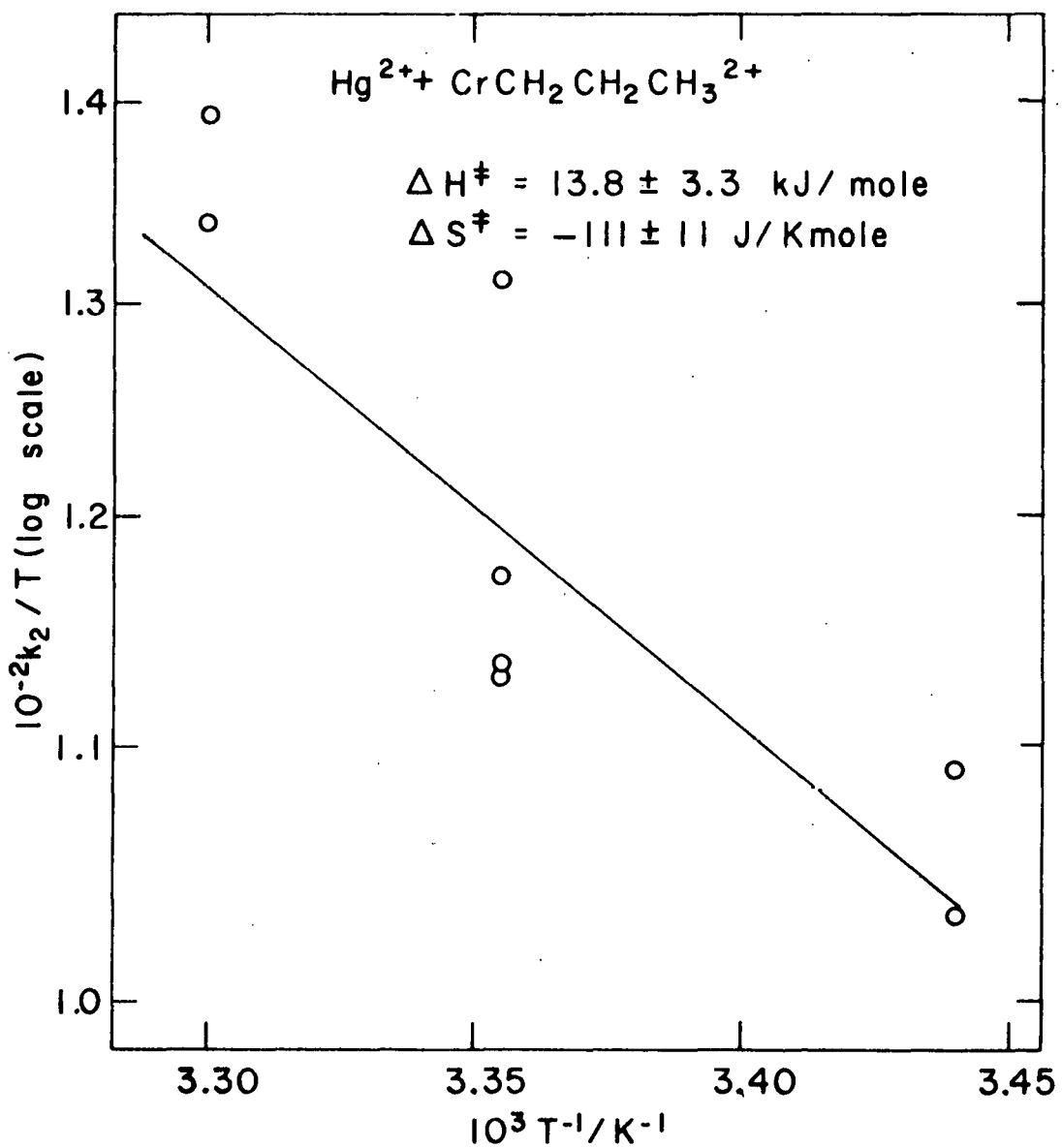


Figure III-24. Eyring plot for reaction $\text{CrCH}_2\text{CH}_2\text{CH}_3^{2+}$ and Hg^{2+}

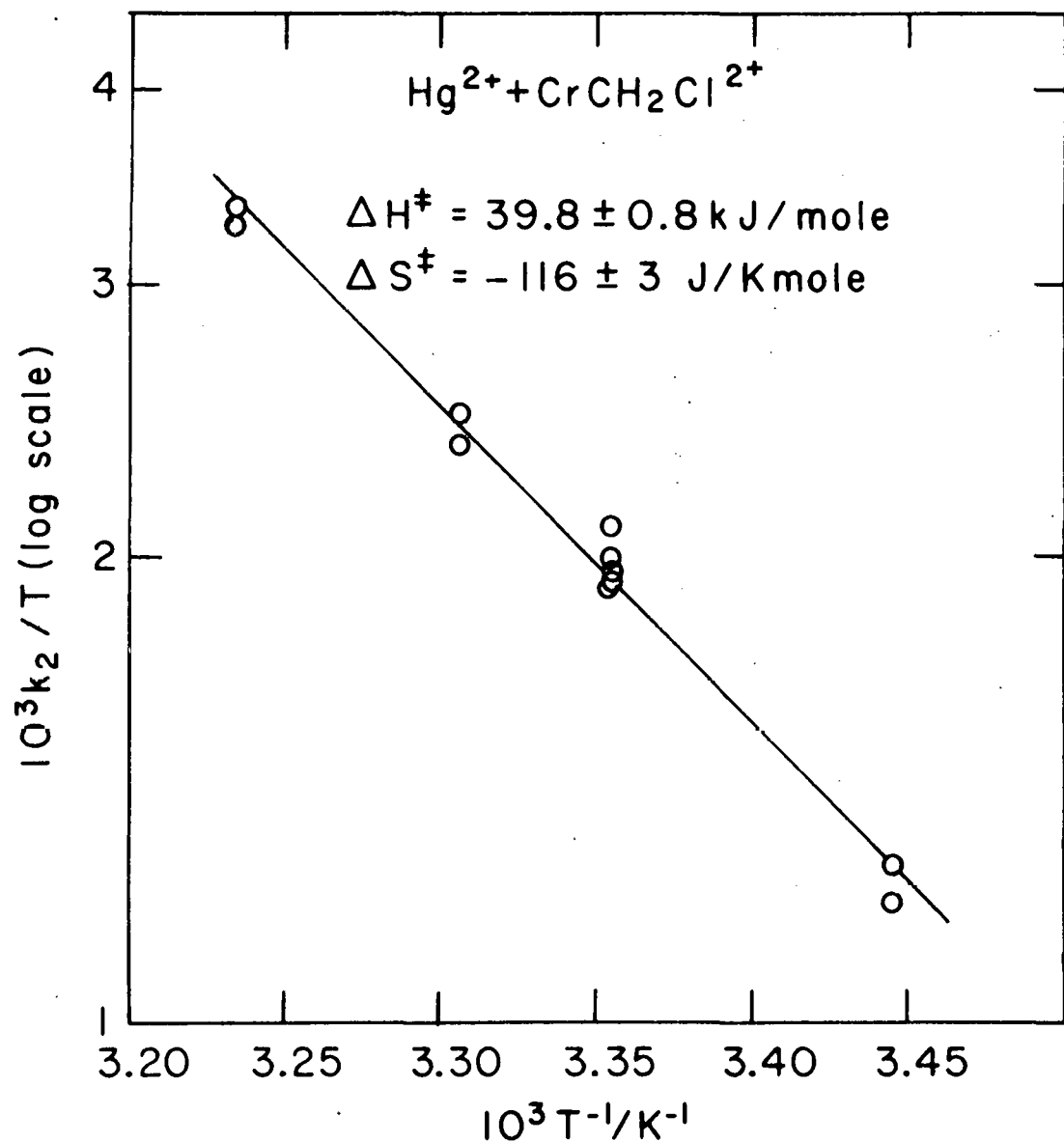


Figure III-25. Eyring plot for reaction of $\text{CrCH}_2\text{Cl}^{2+}$ and Hg^{2+}

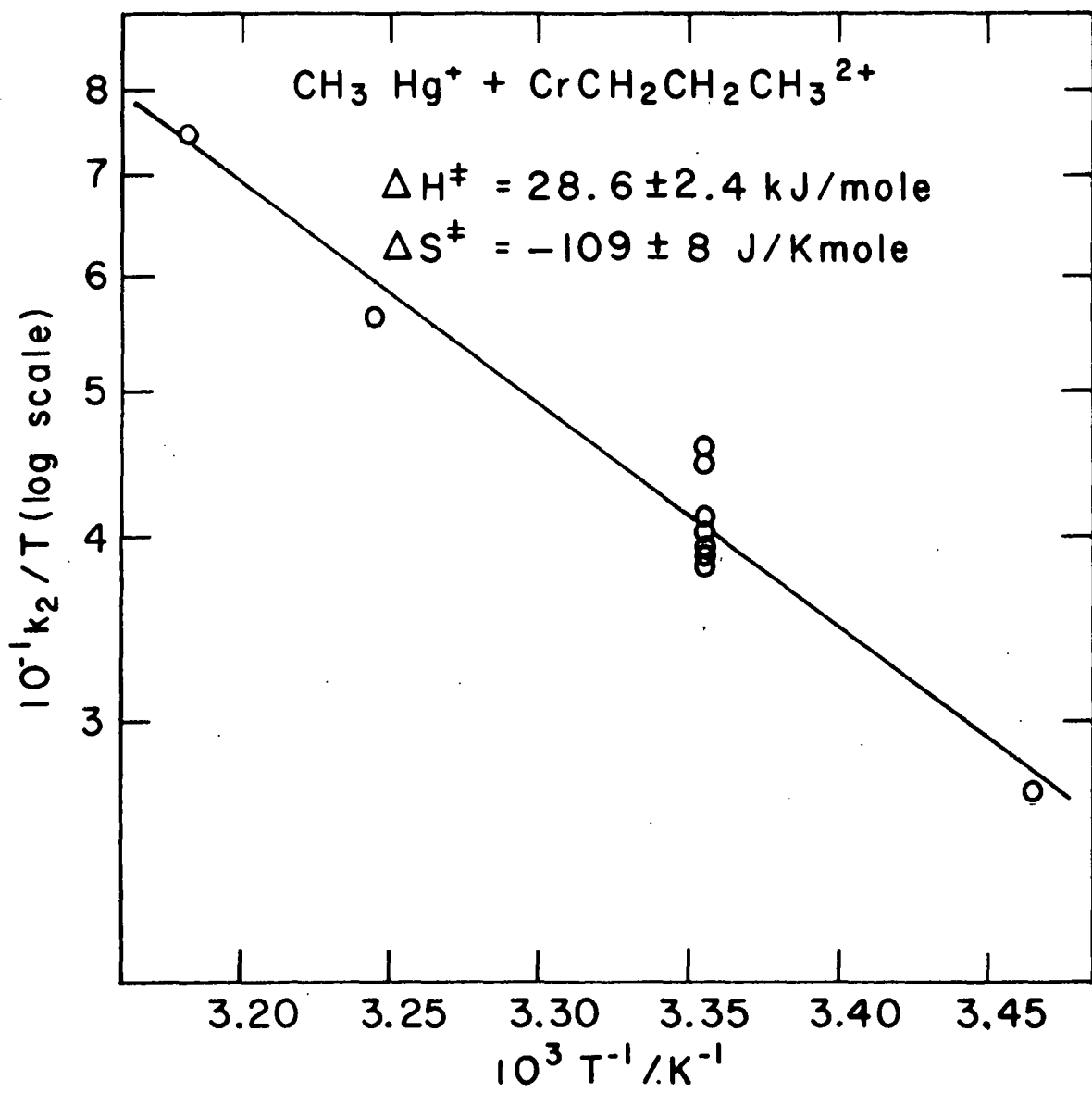


Figure III-26. Eyring plot for reaction of $\text{CrCH}_2\text{CH}_2\text{CH}_3^{2+}$ and CH_3Hg^+

Table III-11. Summary of second-order rate constants for reaction of Hg^{2+} and CH_3Hg^+ with para-substituted benzylchromium(III) ions, $\text{CrCH}_2\text{C}_6\text{H}_5-\text{Z}$ and Hammett σ values for the various substituents

Z	σ	$10^{-4} k_{\text{Hg}} / \text{M}^{-1} \text{s}^{-1}$	$k_{\text{MeHg}} / \text{M}^{-1} \text{s}^{-1}$
Me	-0.17	5.22	121
H	0	4.87	99.5
Br	0.23	2.98	56.8
CF_3	0.54	2.10	34.7
CN	0.66	1.65	23.9

various substituents. The plots of $\log k$ vs σ are shown in Figures III-27 and III-28. The slopes of these plots were computed using a linear least-squares computer program. The value of ρ for the Hg^{2+} reactions is -0.62 with a standard deviation of 0.05 and a correlation coefficient of -0.984. For the CH_3Hg^+ reactions $\rho = -0.85$ with a standard deviation of 0.05 and correlation coefficient of 0.989. The correlation is quite good and both reactions follow equation III-24 well. The significance of these results will be discussed in the next section.

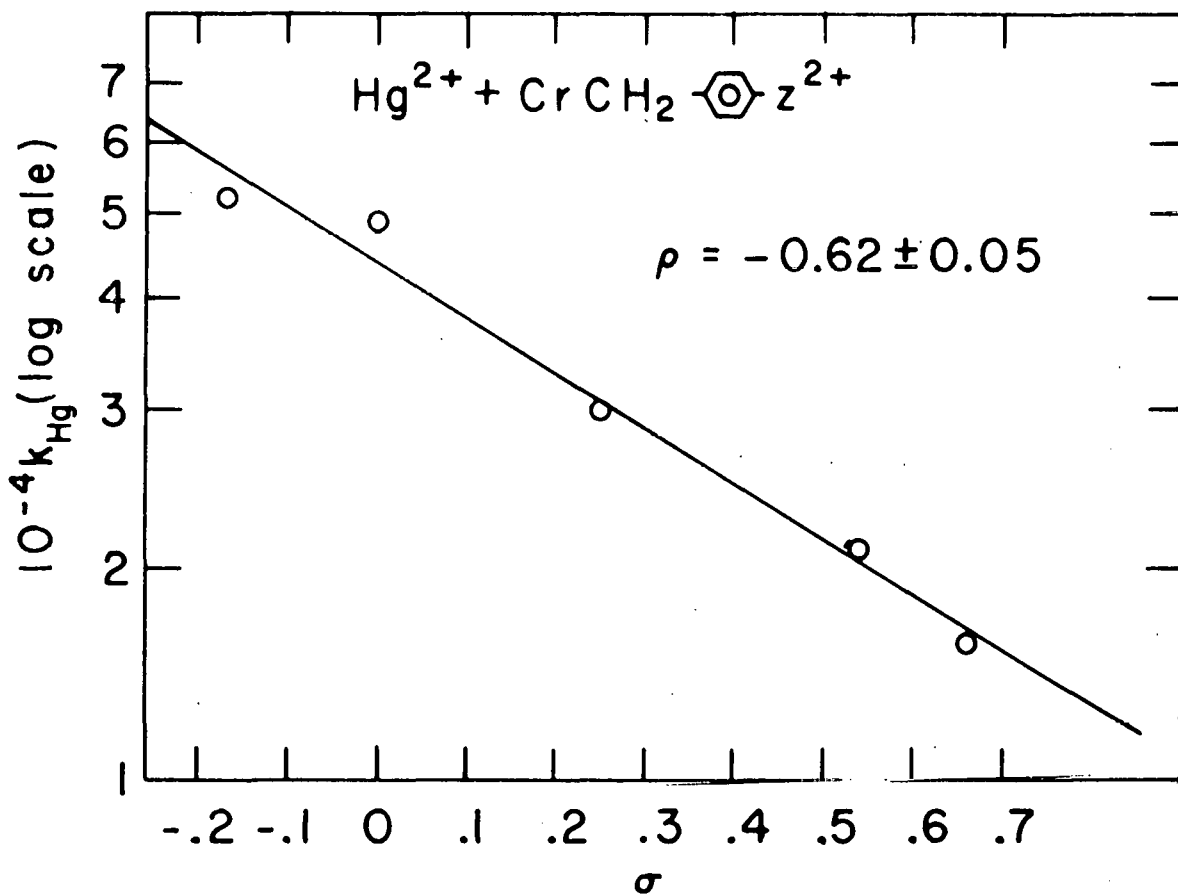


Figure III-27. Hammett plot for reactions of para-substituted benzylchromium(III) ions with Hg^{2+}

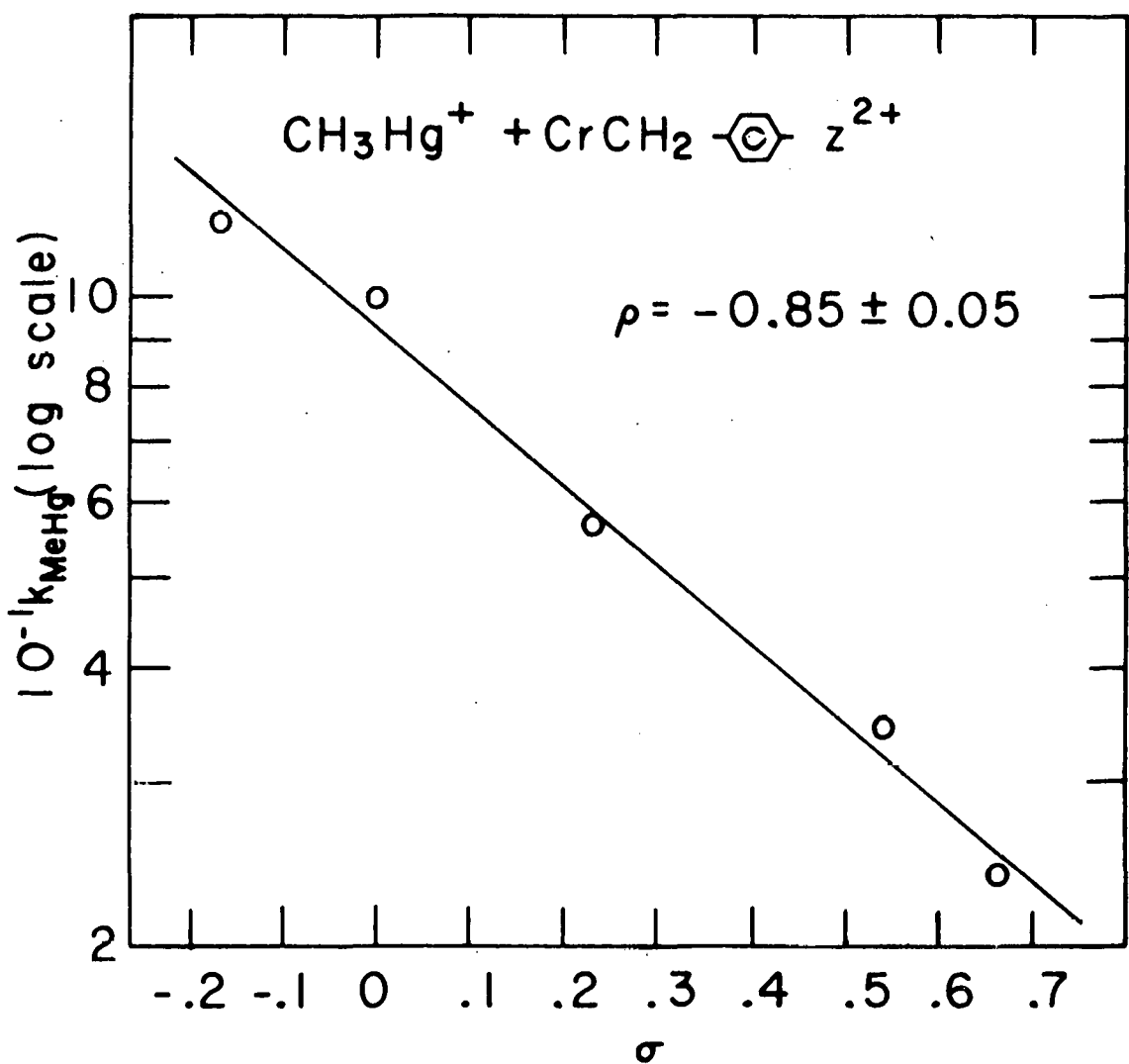


Figure III-28. Hammett plot for the reactions of para-substituted benzylchromium(III) ions with CH_3Hg^+

DISCUSSION

The rate law for all the reactions of CrR^{2+} complexes with the $\text{Hg}(\text{II})$ electrophiles under study is as written in equation III-21. In two cases, the reaction of Hg^{2+} with $\text{CrCH}(\text{CH}_3)_2^{2+}$ and that of CH_3Hg^+ and $\text{CrCH}_2\text{C}(\text{CH}_3)_3^{2+}$, a mercury-independent term was observed for the rate of disappearance of CrR^{2+} (equation III-22), but this was shown to be hydrolysis of the organochromium(III) species. It should be stressed, however, that hydrolysis is a side reaction of CrR^{2+} and is independent of the $\text{Hg}(\text{II})$ reaction. The conclusion, therefore, is that all the reactions under study are second-order, consistent with S_E^2 mechanisms. In only one instance was the second-order rate constant dependent on $[\text{H}^+]$ between 0.10 and 0.50 M , that of the reaction of CH_3Hg^+ and CrCH_3^{2+} . As stated above, the cause of this $[\text{H}^+]$ dependence is not known.

The rates of the Hg^{2+} reactions are systematically faster than those of the organomercuric ions; this result is expected since Hg^{2+} is a much stronger electrophile than RHg^+ . It is assumed, therefore, that in the reactions of Hg^{2+} with CrR^{2+} no dialkylmercurial, R_2Hg , can form, even though some RHg^+ is present after reaction has begun. Not only is Hg^{2+} a better electrophile, but in the kinetic runs, $[\text{Hg}^{2+}]$, being in pseudo-first-order excess, is always much greater than $[\text{RHg}^+]$.¹

¹In the stoichiometry experiment, $[\text{Hg}^{2+}]$ was always lower than $[\text{CrR}^{2+}]$ so that R_2Hg would result from the reaction of RHg^+ with excess CrR^{2+} .

The rates for the reactions of the various organomercuric ions, CH_3Hg^+ , $\text{C}_6\text{H}_5\text{Hg}^+$, and $\text{C}_6\text{H}_5\text{CH}_2\text{Hg}^+$, are all about the same. This result is not surprising since the organic group attached to mercury is presumably remote from the reaction site and is therefore not expected to have an appreciable steric effect. One might expect a small electronic effect from the organic substituent, since the electrophilicity of the Hg(II) species should depend on electron density at the metal, but the above result indicates that this effect is negligible for the electrophiles studied.

A summary of the second-order rate constants for the reactions of CrR^{2+} complexes with Hg^{2+} and CH_3Hg^+ is shown in Table III-12, along with those for the Br_2 reactions and those for some other electrophilic reactions. Some important trends embodied in these data are discussed below.

It is clear that the reactions are sensitive to a profound electronic effect wherein electron-withdrawing substituents lower the rate. This is especially pronounced for $-\text{CF}_3$, for which no reaction with Hg^{2+} was seen at all. A particularly apt comparison is that of the $\text{CrCH}_2\text{CH}_3^{2+}$ and $\text{CrCH}_2\text{Cl}^{2+}$ reactions. Here, the steric bulk of the methyl group and the chlorine atom are about the same, but the rates of electrophilic cleavage are different by factors of $\sim 10^5$ for the Hg(II) reactions. This large electronic effect is also evident in the Br_2 reactions.

Table III-12. Summary of second-order rate constants for the reactions of CrR^{2+} with Hg^{2+} , CH_3Hg^+ , and Br_2 and for reactions of other organometallic complexes with Hg^{2+} ; k 's given in $\text{M}^{-1}\text{s}^{-1}$ at 25°

Substrate	k_{Hg}	k_{MeHg}	k_{Br_2} ^a
CrCH_3^{2+}	$\sim 1 \times 10^7$	1×10^4	2.1×10^6
$\text{CrCH}_2\text{CH}_3^{2+}$	1.5×10^5	2.0×10^2	5.1×10^5
$\text{CrCH}_2\text{CH}_2\text{CH}_3^{2+}$	3.5×10^4	1.2×10^2	6.2×10^5
$\text{CrCH}_2\text{C}(\text{CH}_3)_3$	4.9×10^2	5.8	1.0×10^4
$\text{CrCH}(\text{CH}_3)_2^{2+}$	1.6		---
$\text{CrCH}_2\text{Cl}^{2+}$	0.59	$\sim 6 \times 10^{-4}$	1.1
$\text{CrCH}_2\text{Br}^{2+}$	0.47	---	0.35
CrCF_3^{2+}	$< 10^{-6}$	---	---
$\text{CrCH}_2-\text{C}_6\text{H}_5^{2+}$	4.9×10^4	100	8.3×10^5
$\text{CrCH}_2-\text{C}_6\text{H}_5\text{CH}_3^{2+}$	5.2×10^4	121	---
$\text{CrCH}_2-\text{C}_6\text{H}_5\text{Br}^{2+}$	3.0×10^4	57	2.3×10^5
$\text{CrCH}_2-\text{C}_6\text{H}_5\text{CF}_3^{2+}$	2.1×10^4	35	1.5×10^5
$\text{CrCH}_2-\text{C}_6\text{H}_5\text{CN}^{2+}$	1.6×10^4	24	9.6×10^4
$\text{CrCH}_2-\text{C}_6\text{H}_5\text{NH}^{3+b}$	5×10^2	---	---
$\text{CrCH}_2-\text{C}_6\text{H}_5\text{NH}^{3+b}$	2×10^2	---	---
$\text{CrCH}_2-\text{C}_6\text{H}_5\text{NH}^{3+b}$	3×10^1	---	---
$\text{CH}_3\text{Co}(\text{dmgh})_2\text{OH}^{\text{C}}$	65	---	---

^aData from reference 47 and 48.

^bData from reference 45.

^cData from reference 34.

It is interesting in this regard that the rates of the reactions of $\text{CrCH}_2\text{Cl}^{2+}$ and $\text{CrCH}_2\text{Br}^{2+}$ differ only slightly, even though chlorine is somewhat more electronegative than bromine. Apparently, the greater size of the Br atom counterbalances the electronic effect. The fact that electron-withdrawing substituents slow down the reaction is consistent with the S_E^2 mechanism, since the greater the electron density on the carbon undergoing substitution, the more facile should be the electrophilic attack.

A more subtle but more quantitative manifestation of the electronic effect is seen in the rate differences for the reactions of the para-substituted benzylchromium(III) ions. The Hammett ρ values for the Hg^{2+} and CH_3Hg^+ reactions are -0.62 ± 0.05 and -0.85 ± 0.05 , respectively. The negative ρ 's are a result of the fact that electron-withdrawing substituents retard the reactions. In addition, the values of ρ are approximately the same as those found for other reactions considered to go by S_E^2 (open) mechanism, for example, $\text{CrR}^{2+} + \text{I}_2$, $\rho = -0.82$ (48); $\text{CrR}^{2+} + \text{Br}_2$, $\rho = -1.29$ (48); and $\text{RCO(dmgH)}_2\text{OH}_2 + \text{Hg}^{2+}$, $\rho = -1.2$ (35).

Another implication of the negative ρ value is that the important rate process is bond-making in the transition state rather than bond-breaking. A negative ρ indicates that positive charge builds up on the reacting carbon atom (62). If bond-breaking were important in the transition state,

negative charge would develop on the reacting carbon and the expected ρ would be positive.

We can conclude from the rate law and the electronic effects that the reactions go through an S_E^2 (open) mechanism. This conclusion is consistent with the work of Johnson and coworkers on the reactions of 2-, 3-, and 4-pyridinomethyl-chromium(III) cations with various halo-substituted mercury(II) species (44-46). It is also consistent with the results of Espenson and coworkers on the reactions of CrR^{2+} complexes with halogens (47, 48).

In addition to the electronic effect on the reaction of CrR^{2+} with $Hg(II)$, there is also a strong steric effect. As the steric congestion around the α -carbon in the CrR^{2+} complex is increased, the rate of electrophilic attack decreases. This is especially pronounced in going from primary R groups such as ethyl to the secondary R group, isopropyl, where the rate constant for the Hg^{2+} reaction goes down by 10^5 . Table III-13 shows this trend in terms of relative rates with the k for $R = CH_3$ equated to 100 for each reaction series.

The rate trends for the Hg^{2+} and CH_3Hg^+ reactions do not parallel each other exactly, the steric effect for the Hg^{2+} reactions being more pronounced than for the CH_3Hg^+ reactions. This result is somewhat surprising since the only obvious difference between these two species is their electrophilic

Table III-13. Rate trends for S_N^2 reactions, values of k_R/k_{CH_3} , for aliphatic R groups

Reaction	R					Stereochemistry	Ref.
	CH ₃	C ₂ H ₅	n-C ₃ H ₇	neo-C ₅ H ₁₁	iso-C ₃ H ₇		
CrR ²⁺ + Hg ²⁺ ^a	100	1.5	0.35	4.9×10^{-3}	1.6×10^{-5}		
CrR ²⁺ + CH ₃ Hg ⁺ ^a	100	2.0	1.2	0.058	---		
CrR ²⁺ + Br ₂ ^a	100	24	30	0.47	---		46
RCO(dmgH) ₂ OH ₂ + Hg ²⁺ ^a	100	0.19	0.14	0.014	$<1 \times 10^{-5}$	Inversion	33, 35
RSn(neoC ₅ H ₁₁) ₃ + Br ₂ ^b	100	14	4.1	0.058	0.75	Inversion	63
RHgBr + HgBr ₂ ^c	100	42	---	33	---	Retention	64, 65
HCl + R ₂ Hg ^d	100	595	320	---	350	Retention	64 ^e
S _N ²	100	30	1.3	3×10^{-5}	8×10^{-2}	Inversion	64 ^e

^aIn H₂O, T = 25°, k's given in Table III-12.

^bIn CH₃OH, T = 45°, k(CH₃) = 16.6 M⁻¹s⁻¹.

^cIn C₂H₅OH, T = 100°, k(CH₃) = 12.8 M⁻¹s⁻¹.

^dIn DMSO, T = 50°, k(CH₃) = 1.3 x 10⁻⁴ M⁻¹s⁻¹.

^eThe data was taken from reference 64 although this is not the original source.

strengths. If the methyl group in CH_3Hg^+ were to exert an appreciable steric effect itself, one would expect the CH_3Hg^+ reaction to have the more pronounced drop in rate as the steric hindrance of R increases.

The cause of the observed trend is likely due to the differences in solvation of the two $\text{Hg}(\text{II})$ species. The Hg^{2+} , having a higher charge, is undoubtedly more highly solvated than CH_3Hg^+ which also has the hydrophobic methyl group attached to it. With more water molecules tightly bound to Hg^{2+} , its effective size is bigger than CH_3Hg^+ , and the steric crowding at the reaction center would affect the rate more, even though Hg^{2+} is the stronger electrophile. This rationale is consistent with the even smaller steric effect in the Br_2 reactions, since the uncharged Br_2 molecule should be solvated even less than CH_3Hg^+ .

Also shown in Table III-13 are the rate trends for the same aliphatic R series in reactions for which the mechanism and stereochemistry are known with certainty. In each case, the mechanism is S_{E}^2 (open) (except, of course, the S_{N}^2 reaction). We would like to infer the stereochemistry of the CrR^{2+} reactions with $\text{Hg}(\text{II})$ electrophiles from the comparison of the rate trends.

The parallel is not very good between any of the reactions of known stereochemistry and the CrR^{2+} reactions, but the comparison with those that go with inversion is better than

with the retention reactions. It is clear that for the inversion reactions, there is a much more pronounced steric effect than for retention, a trend that holds for the CrR^{2+} reactions. This comparison makes it very tempting to conclude that the reactions of CrR^{2+} with Hg^{2+} and CH_3Hg^+ go with inversion of configuration (transition state I, see Introduction). This conclusion should be treated with caution, however, since there are very few examples of inversion for electrophilic reactions of mercury(II) species (31, p. 111, 66 and 67).

A summary of the activation parameters from Figures III-24 - III-26 is shown in Table III-14, along with those measured by Williams and Espenson (47) for the CrR^{2+} reactions with Br_2 . In the Hg(II) reactions, the change in rate between aliphatic- and halo-alkyl CrR^{2+} reactions and between Hg^{2+} and CH_3Hg^+ reactions comes from the difference in ΔH^\ddagger , with ΔS^\ddagger being about the same for all three reactions. For the Br_2 reactions, however, the difference in rate between aliphatic- and halo-alkyl CrR^{2+} comes from the difference in ΔS^\ddagger . At first thought, this may appear to be anomalous in view of the assumed similarity in mechanism (i.e., both $\text{S}_{\text{E}}2$ (open) with inversion), but there are significant differences as well. In the Hg(II) reactions, a cation simply replaces another cation bonded to carbon (equation III-19 and III-20). In the Br_2 reaction (equation III-5) a neutral molecule approaches

Table III-14. Summary of activation parameters for reactions of CrR^{2+} complexes

Reaction	$k/\text{M}^{-1}\text{s}^{-1}$ at 25°	$\Delta H^\ddagger/\text{kJ mol}^{-1}$	$\Delta S^\ddagger/\text{J K}^{-1}\text{mol}^{-1}$
$\text{CrCH}_2\text{CH}_2\text{CH}_3^{2+} + \text{Hg}^{2+}$	$(3.50 \pm 0.15)10^4$	13.8 ± 3.3	-111 ± 11
$\text{CrCH}_2\text{Cl}^{2+} + \text{Hg}^{2+}$	0.595 ± 0.015	39.8 ± 0.8	-116 ± 3
$\text{CrCH}_2\text{CH}_2\text{CH}_3^{2+} + \text{CH}_3\text{Hg}^+$	$(1.21 \pm 0.08)10^2$	28.6 ± 2.4	-109 ± 8
$\text{CrCH}_2\text{CH}_3^{2+} + \text{Br}_2$	$(4.9 \pm 0.5)10^5$	44.7 ± 3.3	$+15 \pm 11$
$\text{CrCH}_2\text{Cl}^{2+} + \text{Br}_2$	1.06 ± 0.06	33.0 ± 1.7	-134 ± 6

the carbon atom of the CrR^{2+} complex and becomes highly polarized in the transition state which then breaks up into a cation (Cr^{3+}), another neutral molecule (RBr), and an anion (Br^-). The charge distribution, bonding, and solvation in the transition states for these two reactions are no doubt very different and it is therefore not surprising that the activation parameters show different trends.

BIBLIOGRAPHY

1. F. A. L. Anet and E. L. LeBlanc, J. Amer. Chem. Soc., 79, 2649 (1957).
2. F. A. L. Anet, Can. J. Chem., 37, 58 (1959).
3. D. Dodd and M. D. Johnson, J. Chem. Soc. (A), 34 (1968).
4. J. K. Kochi and D. D. Davis, J. Amer. Chem. Soc., 86, 5264 (1964).
5. R. G. Coombes, M. D. Johnson, and N. Winterton, J. Chem. Soc., 7029 (1965).
6. L. E. Castro and W. C. Kray, J. Amer. Chem. Soc., 88, 4447 (1966).
7. R. S. Nohr and L. O. Spreer, J. Amer. Chem. Soc., 96, 2618 (1974).
8. J. H. Espenson and J. P. Birk, Inorg. Chem., 4, 527 (1965).
9. H. Diehl, H. Clark, and H. H. Willard, Inorg. Syn., 1, 186 (1939).
10. G. W. Haupt, J. Res. Nat'l Bur. Stand., 48, 414 (1952).
11. B. A. Zabin and H. Taube, Inorg. Chem., 3, 963 (1964).
12. W. R. Bushey, Ph.D. Thesis, Iowa State University (1972).
13. D. L. Ball and E. L. King, J. Amer. Chem. Soc., 80, 1091 (1958).
14. A. Anderson and N. A. Bonner, J. Amer. Chem. Soc., 76, 3826 (1954).
15. F. Basolo and R. G. Pearson, "Mechanisms of Inorganic Reactions", 2nd ed., John Wiley and Sons, New York, N.Y., 1967, Ch. 3.
16. R. G. Coombes and M. D. Johnson, J. Chem. Soc. (A), 177, (1966).
17. A. R. Schmidt and T. D. Swaddle, J. Chem. Soc. (A), 1927, (1970).

18. H. Cohen and D. Meyerstein, J. Chem. Soc., Chem. Commun., 320 (1972).
19. R. L. Bixler and C. Niemann, J. Org. Chem., 23, 575 (1958).
20. J. H. Endicott and H. Taube, Inorg. Chem., 4, 437 (1965).
21. G. Friedlander and J. Kennedy, "Nuclear and Radiochemistry", John Wiley and Sons, Inc., New York, N.Y., 1955, Ch. 11.
22. K. U. Ingold in "Free Radicals", J. K. Kochi, Ed., John Wiley and Sons, Inc., New York, N.Y., 1973, pp. 40-56.
23. J. K. Kochi and D. Buchanan, J. Amer. Chem. Soc., 87, 853 (1965).
24. R. S. Nohr and J. H. Espenson, J. Amer. Chem. Soc., 97, 3392 (1975).
25. J. H. Espenson and J. S. Shveima, J. Amer. Chem. Soc., 95, 4468 (1973).
26. J. H. Espenson and T. D. Sellers, J. Amer. Chem. Soc., 96, 94 (1974).
27. R. H. Prince and M. G. Seagal, Nature, 249, 247 (1974).
28. A. van den Bergen and B. O. West, Chem. Commun., 52 (1971).
29. J. Z. Chrzastowski, C. J. Cooksey, M. D. Johnson, B. L. Lockman, and P. N. Steggles, J. Amer. Chem. Soc., 97, 934 (1975).
30. K. U. Ingold and B. P. Roberts, "Free-Radical Substitution Reactions", Wiley-Interscience, New York, N.Y., 1971, pp. 72-90.
31. M. H. Abraham in "Comprehensive Chemical Kinetics", Vol. 12, C. H. Bamford and C. F. H. Tipper, Eds., Elsevier, Amsterdam, 1973.
32. F. R. Jensen and B. Rickborn, "Electrophilic Substitution of Organomercurials", McGraw-Hill, New York, N.Y., 1968.
33. L. J. Dizikes and A. Wojcicki, J. Amer. Chem. Soc., 97, 2540 (1975).

34. A. Adin and J. H. Espenson, Chem. Commun., 653 (1971).
35. P. Abley, E. R. Dockal, and J. Halpern, J. Amer. Chem. Soc., 95, 3166 (1973).
36. H. L. Fritz, J. H. Espenson, D. A. Williams, and G. A. Molander, J. Amer. Chem. Soc., 96, 2378 (1974).
37. M. Tada and H. Ogawa, Tetrahedron Lett., 2639 (1973).
38. G. Tazluer, R. Dreos, G. Costa, and M. Green, J. Organomet. Chem., 81, 107 (1974).
39. R. Dreos, G. Tazluer, N. Marish, and G. Costa, J. Organomet. Chem., 93, 227 (1975).
40. J. H. Espenson, W. R. Bushey, and M. E. Chmielewski, Inorg. Chem., 14, 1302 (1975).
41. J.-Y. Kim, J. Imura, T. Ukita, and T. Kwan, Bull. Chem. Soc. Japan, 44, 300 (1971).
42. G. N. Schrauzer, J. H. Weber, T. M. Beckham, and R. K. Y. Ho, Tetrahedron Lett., 275 (1975).
43. R. E. DiSimone, M. W. Penley, L. Charbonneau, S. G. Smith, J. M. Wood, H. A. O. Hill, J. M. Pratt, S. Risdale, and R. J. P. Williams, Biochim. Biophys. Acta, 304, 851 (1973).
44. R. G. Coombes and M. D. Johnson, J. Chem. Soc. (A), 1805 (1966).
45. D. Dodd, M. D. Johnson, and D. Vamplew, J. Chem. Soc. (B), 1841 (1971).
46. R. G. Coombes, M. D. Johnson, and D. Vamplew, J. Chem. Soc. (A), 2297 (1968).
47. J. H. Espenson and D. A. Williams, J. Amer. Chem. Soc., 96, 1008 (1974).
48. J. C. Chang and J. H. Espenson, Chem. Commun., 233 (1974).
49. M. Ardon, K. Woolmington, and A. Pernick, Inorg. Chem., 10, 2812 (1971).
50. W. Schmidt, J. H. Swinehart, and H. Taube, J. Amer. Chem. Soc., 93, 1117 (1971).

51. D. A. Williams, M.S. Thesis, Iowa State University (1972).
52. S. H. Malik, W. Schmidt, and L. O. Spreer, Inorg. Chem., 13, 2986 (1974).
53. N. A. Milas and D. M. Surgenor, J. Amer. Chem. Soc., 68, 205 (1946).
54. M. D. Rausch and J. R. Van Wazer, Inorg. Chem., 3, 761 (1964).
55. R. B. Fischer and D. G. Peters, "Quantitative Chemical Analysis", 3rd ed., W. D. Saunders Co., Philadelphia, 1968, p. 384.
56. E. B. Sandell, "Colorimetric Determination of Traces of Metals", 3rd ed., Interscience Publ. Inc., New York, N.Y., 1959, pp. 163-176, 621-640.
57. C. D. Wagner, R. H. Smith, and E. D. Peter, Anal. Chem., 19, 976 (1947).
58. J. V. Hatton, W. G. Schneider, and W. Siebrand, J. Chem. Phys., 39, 1330 (1963).
59. D. F. Evans and J. P. Maher, J. Chem. Soc., 1525 (1962).
60. G. Singh and G. S. Reddy, J. Organomet. Chem., 42, 267 (1972).
61. J. F. Bunnett in "Technique of Organic Chemistry", Vol. VIII-Part I, 2nd ed., A. Weissberger, Ed., Interscience Publishers, Inc., New York, N.Y., 1961, p. 200.
62. J. S. Shorter, "Correlation Analysis in Organic Chemistry", Clarendon Press, Oxford, 1973.
63. F. R. Jensen and D. D. Davis, J. Amer. Chem. Soc., 93, 4048 (1971).
64. E. D. Hughes and H. C. Volger, J. Chem. Soc., 2359 (1961).
65. E. C. Hughes, C. K. Ingold, F. G. Thorpe, and H. C. Volger, J. Chem. Soc., 1133 (1961).
66. M. H. Abraham and P. L. Grellier, J. Chem. Soc., Perkin II, 1132 (1973).
67. F. R. Jensen, V. Madan, and D. H. Buchanan, J. Amer. Chem. Soc., 93, 5283 (1971).

ACKNOWLEDGEMENTS

I would like to thank Professor James H. Espenson without whose guidance and encouragement this work would not have been possible. Dr. W. S. Trahanovsky provided informative discussion. I would also like to thank Ms. Sue Musselman for an excellent job of typing the final draft of this thesis. Finally, I am deeply indebted to my wife, Diana, who provided tolerance, sympathy, and love throughout this work and who typed the rough draft.